
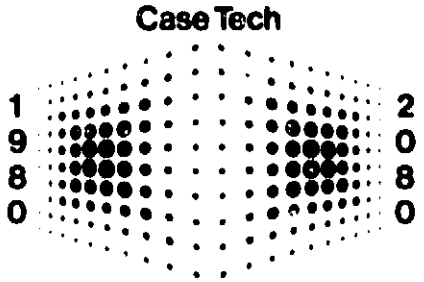


# ELECTROMAGNETIC WAVES AND WAVE PROPAGATION REPORT



Department of Electrical Engineering
and
Applied Physics
Case Institute of Technology
Case Western Reserve University
University Circle
Cleveland, Ohio 44106

# PERTURBATION-ITERATION THEORY FOR ANALYZING MICROWAVE STRIPLINES

by

BRIAN E. KRETCH

REPORT WGR-85-5 SEPTEMBER 1985

The research reported on in this report was supported by NASA-Lewis Research Center, Cleveland, Ohio, under Grant NCC 3-29.

# PERTURBATION-ITERATION THEORY FOR ANALYZING MICROWAVE STRIPLINES

by

BRIAN EDWARD KRETCH

Submitted in partial fulfillment of the
Requirements for the Degree of
Master of Science

Thesis Advisor: R. E. Collin

Department of Electrical Engineering & Applied Physics
Case Western Reserve University
August 1985

PERTURBATION-ITERATION THEORY

FOR ANALYSING MICROWAVE STRIPLINES

ABSTRACT

by

BRIAN EDWARD KRETCH

A perturbation-iteration technique is presented for determining the propagation constant and characteristic impedance of an unshielded microstrip transmission line. The method converges to the correct solution with a few iterations at each frequency and is equivalent to a full wave analysis. The perturbation-iteration method gives a direct solution for the propagation constant without having to find the roots of a transcendental dispersion equation.

The theory is presented in detail along with numerical results for the effective dielectric constant and characteristic impedance for a wide range of substrate dielectric constants, stripline dimensions, and frequencies.

## ACKNOWLEDGEMENTS

I would like to express my deepest thanks and appreciation to my advisor, Dr. Robert E. Collin, for his help, guidance, assistance, and above all, patience during my tenure as a student at Case.

I would like to thank Mr. Philip A. Legge and Dr. Paul C. Claspy for the opportunity to pursue a Master's Degree at Case.

I would like to thank Ms. Victoria Gilbert for typing this Thesis.

I would like to thank my family and friends for their love and support while I pursued my Master's Degree.

The work of this thesis was supported by NASA-Lewis Research Center, Cleveland, Ohio under Grant NCC 3-29.

Dedication

to

Walter Allan Kretch

Case Institute of Technology

1943

and

Edward Dennis Kretch

Case School of Applied Science

1913

TABLE OF CONTENTS

# CHAPTER I

# INTRODUCTION

## 1.1 Introduction

The analysis of infinite, straight, unshielded microwave striplines is an area of great importance in microwave field theory. Microwave striplines are used extensively in high frequency communication networks for radar and satellite systems. Figure 1.1 shows the cross section of typical unshielded and shielded microstrip lines and also the related slot line. The effectiveness of their use in circuits is contingent on how well the designer can understand the striplines to know their properties and characteristics. There has been a great deal of previous research in the area of modeling and analysis of microwave striplines that encompasses three basic approaches: 1) static or quasi-TEM analysis, 2) dispersion modeling, and 3) fullwave analysis.

Wave propagation along a microwave stripline is similar to pure TEM propagation. The differences arise due to the presence of the ground plane and the dielectric substrate. At low frequencies, these deviations are negligable so that the waves can be analyzed as pure TEM waves. This is the foundation of the static or quasi-TEM analysis. As the frequency increases, the frequency effects become more predominant and the analysis must also include these effects. This is the basis of the fullwave analysis. Models of the microwave stripline can also be developed to simplify the evaluation of high frequency properties. Such is the method used

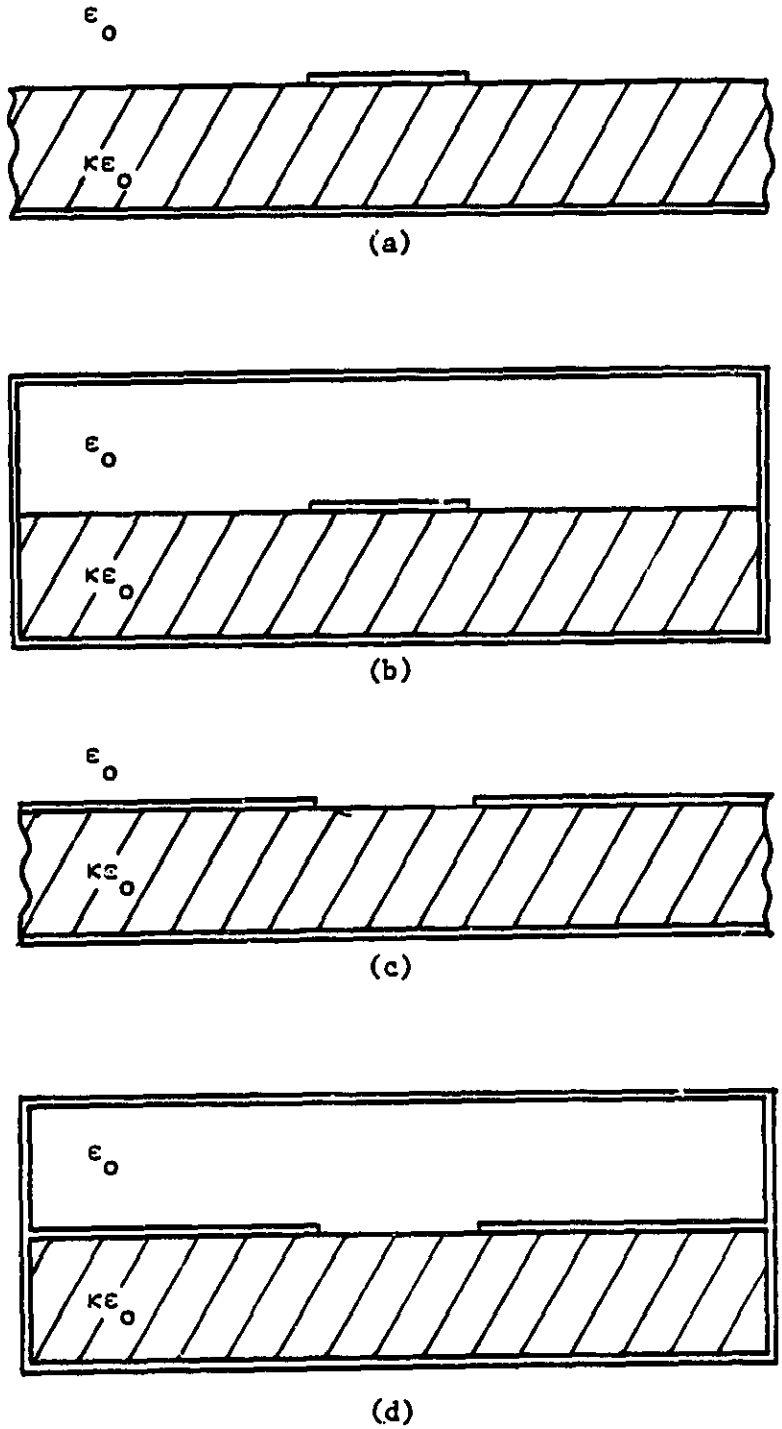


Figure 1.1 (a) Unshielded Microstrip Line, (b) Shielded Microstrip Line, (c) Slot Line, (d) Shielded Slot Line.

in dispersion models.

The different approaches for analyzing the microwave stripline all utilize the same basic boundary conditions. These boundary conditions all emanate from Maxwell's Equations:

$$\nabla \times \vec{E} = -j\omega\vec{B}$$
$$\nabla \times \vec{H} = j\omega\vec{D} + \vec{J}$$
$$\nabla \cdot \vec{D} = \rho$$
$$\nabla \cdot \vec{B} = 0 \qquad (1.1)$$

The media will be assumed to be isotropic which permits the following relations:

$$\vec{D} = \kappa\varepsilon_o\vec{E}$$
$$\vec{B} = \mu_o\vec{H} \qquad (1.2)$$

The boundary conditions will thus encompass the following:

$E_x, E_z, H_y = 0$ at $y = 0$ and on the microstrip

$E_x, E_z, H_x, H_z$ are continuous across the air-dielectric interface

$$H_x^+ - H_x^- = -J_z$$
$$H_z^+ - H_z^- = J_x$$
$$E_y^+ - E_y^- = \rho/\varepsilon_o \qquad (1.3)$$

where $J_x$ and $J_z$ are the components of the total current density and $\rho$ is the total charge density on the microstrip.

In Sec. 1.2 - 1.4, a brief review of past work on microwave stripline propagation will be presented. This review will be brief with further references provided so that a more complete understanding of them may be acquired if desired.

## 1.2 Quasi-TEM Analysis

The first type of analysis examined will be the static, or quasi-TEM analysis. As previously mentioned, the wave propagation at low frequencies (up to 1GHz) can be approximated by a pure TEM wave. The foundation of this analysis is based on the previously stated boundary conditions and contingent on a few basic assumptions. Since the frequency, $\omega$, is assumed to be small and approach zero, the terms $j\omega\vec{D}$ and $j\omega\vec{B}$ in Maxwell's equations (1-2) may be assumed to equal zero. In a different sense, this assumption states that as $\omega$ approaches zero, the wavelength $\lambda$ approaches infinity. This assumption introduces negligible error into the stripline analysis at sufficiently low frequencies. Thus, at any location along the microstrip but not on the strip,

$$\nabla \times \vec{E} = -j\omega\mu_o \vec{H} \approx 0$$

$$\nabla \times \vec{H} = j\omega\vec{D} \approx 0$$

On the strip, the condition still demands that

$$\nabla \times \vec{H} = j\omega\vec{D} + \vec{J} \approx \vec{J}$$

Using the relationship

$$\vec{B} = \nabla \times \vec{A}$$

along with the Lorentz condition

$$\nabla \cdot \vec{A} = -j\omega\mu_o\epsilon_o\kappa\Phi$$

the following two relationships can be developed:

$$\nabla_t^2 \vec{A} = -\mu_o \vec{J}$$

$$\nabla_t^2 \Phi = -\rho/\epsilon_o$$

These assumptions and equations form the basis by which different quasi-static analyses are developed and employed.

The essential quantities to be solved for in the quasi-TEM analysis are the characteristic impedance $Z_c$ and the propagation constant $\beta$. These entities are obtained by first determining two static capacitances per unit length along the stripline. The first capacitance $C_a$ is found by replacing the substrate by air while maintaining the same configuration. The second capacitance $C_o$ is defined as that of the stripline with the substrate present. With these two quantities, the values of $Z_c$ and $\beta$ may be solved for by using the following equations:

$$Z = (1/c)\sqrt{1/C_a\ C_o} \tag{1.4a}$$

$$\beta = k_o \sqrt{C_o/C_a} \tag{1.4b}$$

where

$c$ = Speed of light

$k_o = \omega/c$

An alternative approach to solving for $Z_c$ and $\beta$ is to determine the static inductance per unit length of the microstrip $L_o$ using the relationship

$L_o I_o = A_z$ on the microstrip

where

$I_o$ = total z-directed current

$A_z$ = z-directed vector potential

and leading to the solutions

$$\beta = \omega\sqrt{L_o C_o}$$

$$Z_c = \sqrt{\frac{L_o}{C_o}}$$

From the solution for the propagation constant $\beta$, an effective dielectric constant $\kappa_{eff}$ may be obtained. This is given by

$$\kappa_{eff} = \left(\frac{\beta}{k_o}\right)^2$$

The significance of $\kappa_{eff}$ is to have a simple direct relationship between the quasi-TEM wave with a dielectric and the quasi-TEM wave

with a dielectric having an effective dielectric constant $\kappa_{eff}$. This permits easy calculations of $\beta$ at various frequencies.

There are many techniques used for solving for $Z_c$ and $\beta$ along the infinite line. The following summarizes the more prominent methods and lists references for further research if desired.

The first method is the Conformal Transformation Method [1-3] This method solves for $C_o$ and $C_a$ using a conformal transformation. The difficulty with this method is that the microstrip structure cannot be conformally mapped into a different form which is easily analyzed. Approximations would have to be incorporated into the analysis which would decrease the accuracy of the method. The second type of static analysis is the Variational Method [4-5] In this method, a stationary expression for the capacitance in terms of charge distribution is formed. The charge distribution is represented by a functional form containing one or more variational parameters. The best approximation to the capacitance is then obtained by choosing the variational parameters so as to make the expression for the capacitance stationary. For a given accuracy, the computations are of the same order of complexity as that of other methods. The third method of analysis is the Relaxation Method [6]. This technique divides the cross section of the stripline into a grid, assuming values of potentials at all points, and then modifying these values, or "relaxing" them, by using a finite difference approximation to Laplace's equation for the potential field. The final method is termed the Integral Equation

Method [ 7 ]. This technique uses a Green's Function to formulate an integral equation to solve for the charge density. The capacitances are then determined from the charge density and potential, which has been presumed to have assigned a constant value on the conducting strip. These methods are the main ones employed in solving for the unknown $Z_c$ and $\beta$ under static conditions.

## 1.3 Dispersion Models

The second type of analysis of the straight, infinite, unshielded microwave stripline is developing and applying dispersion models. The static analysis is useful in that it is an easy approach for studying the waves at low frequencies. Its principal deficiency, though, results from its failure to account for the non-TEM nature of the waves at higher frequencies. In particular, $\beta$ is not a linear function of $\omega$ so the stripline is dispersive. Also, the characteristic impedance increases slowly with frequency. At sufficiently high frequencies, other modes begin to propagate. Consequently, various ad hoc dispersion models have been developed which help to analyze the striplines and take into account these non-TEM characteristics. Furthermore, they help to present direct relationships for $Z_c$ and $\kappa_{eff}$ in accordance with a specific frequency. These models can thus contribute to a better understanding of the wave propagation along the stripline over a more diverse range of frequencies.

The first type of dispersion model is the Coupled TEM and TM modes Model [ 8 ]. This model developes a direct equation for $\kappa_{eff}$

based on the assumption that the non-TEM characteristics can be attributed to the lowest order surface wave $TM_0$ mode. Empirical Relations [ 9 ] have also been developed, based on various theoretical and experimental studies of wave dispersion which yield a direct equation for the wave phase velocity. The Dielectric-loaded Ridged Waveguide Model [10] and the Planar Waveguide Model [11] alter the configuration of the microwave stripline structure for ease of direct mathematical computation of $\kappa_{eff}$ and $Z_c$ while maintaining the same dispersion characteristics as that of the stripline. The final dispersion model is the Coupled Transmission Model [12]. This model describes the stripline in terms of coupled TEM and TE modes using coupled transmission lines and basic circuit analysis to solve for $\kappa_{eff}$ and $Z_c$. The consequences of using dispersion models will be to cause the stripline to be easier to mathematically analyze while sacrificing some accuracy in the results. The various approximate dispersion models are useful in many engineering applications but generally are not sufficiently accurate in critical applications where the exact values of $Z_c$ and $\beta$ are needed.

## 1.4 Full Wave Analysis

The final and most accurate microstrip analysis is the Fullwave Analysis [13-17]. This method makes no quasi-static assumptions while analyzing the microstrip configuration exactly as given with no conversion to analytically simpler, but less accurate, dispersion models. The fullwave analysis employs an integral equation method in either

the space or Fourier transform domain and is solved using the method of moments. These different techniques are initially based on equivalent representations of the waves along the microstrip. The analysis then assumes that the propagating wave is composed of hybrid TE and TM modes along the line due to two separate scalar potentials. The individual wave entities due to separate modes are converted to the Fourier Transform Domain (FTD) where they can be evaluated. By applying the correct boundary conditions in conjunction with one of the aforementioned methods of analysis, the waves can be solved for along a stripline. The boundary conditions used are those given in Sec. 1.1 with no assumptions made concerning the waves or stripline. The spatial domain solution applies the boundary conditions using a Green's function integral in the space domain. The unknown current is expanded in terms of a suitably chosen set of basis functions. This will result in computation of the amplitudes of the longitudinal and transverse currents using the method of moments. The FTD solution uses a Green's function applied in the FTD to solve for the current amplitudes. This is done using Galerkin's Method along with an infinite weighted set of current density basis functions. The fullwave analysis can thus be used to examine the wave nature of the stripline with extreme accuracy with one important consequence: the analysis is very complicated with a great deal of numerical analysis required. The propagation constant $\beta$ comes from the dispersion equation that is obtained and since this dispersion equation is a complicated transcendental equation, finding its roots

is quite complex. The dispersion equation gives the propagation constant of higher modes as well as that of the quasi-TEM mode. This important factor must be taken into account when choosing a technique for stripline analysis.

## 1.5 Perturbation-Iteration Method

The methods for analyzing the infinite straight, unshielded microwave stripline that have been previously developed each have their usefullness as well as their deficiences. The quasi-TEM analysis is adequate for analyzing the microstrip at low frequencies in a simple manner but is not sufficiently accurate at high frequencies. The dispersion model permits the analysis to be done with mathematical ease while sacrificing accuracy due to the approximations inherent to the models. The fullwave analysis is very accurate at all ranges of frequencies but is extremely cumbersome in computations. A new technique has been developed to analyze the waves along the stripline which offers greater simplicity than existing fullwave analysis. This method, the Perturbation-Iteration Method, initially solves for the field components at quasi-TEM frequency values. As the frequency increases, the entities are found using frequency dependent Green's functions and an iteration method to successively yield greater accuracy. At each iteration level the value of $\beta$ as the previously determined one is used to formulate the new frequency dependent Green's functions at the new frequency. The iteration is then carried out to yield a new more accurate $\beta$ and a field solution that satisfies the field equations

at higher frequencies. The effective frequency range is theoretically infinite which makes this technique attractive and useful. The most important feature that distinguishes this method from the full wave analysis described above is that $\beta$ is found explicitly instead of being determined from a complex dispersion equation. The pertinent equations and techniques of the Perturbation-Iteration Method will be developed for the complete analysis of the waves along the stripline in this thesis. The theory is developed in Chap. 2 along with the required Green's functions. Chapter 3 presents extensive numerical and graphical results for the propagation constant $\beta$ as a function of dielectric constant of the substrate, width to height ratio of the stripline, and frequency. The corresponding results for characteristic impedance are also presented. The final chapter is the concluding one and contains suggestions for further work and a brief discussion of a perturbation method that was initially developed but abandoned in favor of the Perturbation-Iteration Method.

# CHAPTER 2

# PERTURBATION-ITERATION METHOD THEORY

## 2.1 Introduction

The Perturbation-Iteration Method used for analyzing the infinite, straight, unshielded, microwave stripline is a straightforward approach which utilizes two static Green's functions, three frequency dependent Green's functions, and Fourier representations of the quantities associated with the microstrip structure. As the theory is developed, certain assumptions and approximations are made to help carry out the procedure in a much easier and faster fashion. The stripline structure is displayed again in Fig. 2.1 with an important assumption applied to it: ground plane sidewalls are put on both sides of the microstrip structure to allow for Fourier representation of the fields along the stripline. The validity of inserting the side walls is based on the assumption that all of the fields decay to approximately zero at a reasonable distance from the microstrip. The stripline is oriented to allow for propagation of the fields in the $+z$ direction with a propagation constant $\beta$. The dielectric substrate is considered to be uniform, linear, isotropic and possess a dielectric constant $\kappa$. The thickness of the stripline is taken to be infinitely thin and therefore neglected. For certain calculations, the stripline is assumed to be just above the dielectric substrate in the air-filled region at a

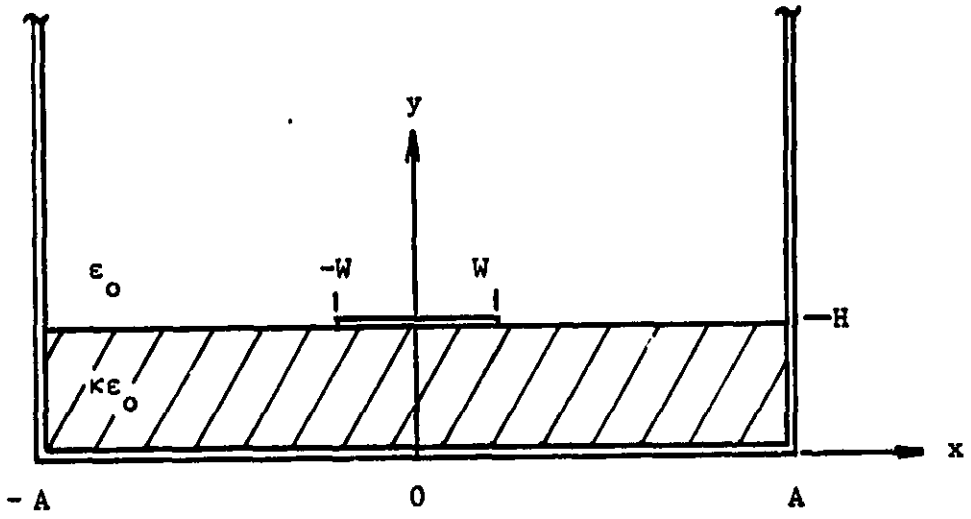


Figure 2.1 Unshielded Microstrip Line with Ground Plane Side Walls.

height of $y = H^+$.

The basic approach of the Perturbation-Iteration Method begins with a static analysis of the fields by letting $\omega = 0$. This yields a static charge density $\rho$ and $+z$ directed current density $J_z$ being determined and used to solve for $\beta$ and the characteristic impedance $Z_c$. The next step is to increase the frequency by a small increment allowing $\beta$ to be approximated from the static analysis. New values of $\rho$ and $J_z$ are subsequently determined which are used to solve for new $\beta$ and $Z_c$ at the given frequency and which are more accurate than the previously approximate values. This scheme may be repeated while maintaining $\omega$ constant which improves the values of $\beta$ and $Z_c$ or by increasing $\omega$ to yield new values of $\beta$ and $Z_c$ so as to cover a broader range of frequencies. At any one frequency, three or four iterations are usually sufficient to give values for $\beta$ and $Z_c$ that are essentially the exact converged values.

Before the mathematical theory is developed, an enumeration procedure is established to clarify the interpretation of the various field quantities. This theory involves a continuously iterating process which must be monitored so that proper field entity values of particular iterative levels are operated on correctly. The various field entities, such as $\vec{E}$, $\vec{H}$, $\vec{A}$, $\vec{J}$, $\Phi$, and $\rho$, all contain a subscript to signify the level of iteration being referred to. As an

example, $\Phi$ has an iterating enumeration of $\Phi_o$, $\Phi_1$, $\Phi_2$, etc. The three Green's functions also contain an iterating enumeration that is signified by a superscript while being separately designated by a subscript. Thus, the first Green's function has an iterating enumeration of $G_1^o$, $G_1^1$, $G_1^2$, etc. and similarly for the second Green's function. The third Green's function iterates similarly except it begins with the 1 level iteration. The o level iteration in all of the quatities are referred to as the static values since at this iteration, the frequency always equals zero. Additionally, $G_1^o$ and $G_2^o$ are static functions while at further iterations, they become frequency dependent functions. The propagation constant $\beta$ has an iterating enumeration of $\beta_1$, $\beta_2$, $\beta_3$, etc. There is no $\beta_o$ since there is no wave propagation on the stripline at $\omega = 0$. The characteristic impedance $Z_c$ has an iterating enumeration of $Z_{c_o}$, $Z_{c_1}$, $Z_{c_2}$, etc. The frequency and frequency dependent variable (wave number)

$$k_o = \omega\sqrt{\mu_o\varepsilon_o}$$

also have an iterating enumeration. The frequency iterates in the manner $\omega_1$, $\omega_2$, $\omega_3$, etc. while $k_o$ iterates in the fashion $k_{o,1}$ $k_{o,2}$ $k_{o,3}$, etc. Since the stripline is specified using cartesian coordinates, the subscripts x, y, and z are added to signify particular components of vector quantities. As an example, $A_{1y}$ signifies the y-component of the

vector potential $\vec{A}$ in the 1 level iteration. Many of the quantities are expressed by using Fourier series representation. Each particular Fourier component is assigned a subscript n to mean the nth component. Examples of this notation are $J_{ozn}$ and $G^1_{2n}$. $J_{ozn}$ denotes the nth Fourier component of the static z directed current density while $G^1_{2n}$ denotes the nth Fourier component of the second Green's function in the 1 level iteration. Any Fourier components of derivatives will be designated as, for example, $\frac{\partial A_{1yn}}{\partial y}$. Two frequency dependent parameters which are defined later in the theoretical development also sequentially iterated. They are displayed and iterate in the fashion $\omega_{1n,1}$, $\omega_{1n,2}$, $\omega_{1n,3}$, etc. and $\omega_{2n,1}$, $\omega_{2n,2}$, $\omega_{2n,3}$, etc. Certain values which are determined are not exact values but are rather relative values which are subsequently correctly scaled. They are designated using a subscript "r" as, for example, $A_{oz,r}$. Where current and charge densities are used to calculate the total currents and charges, respectively, the subscript "T" is used to denote a total quantity. Thus, $I_{1T}$ means the total 1 level current. The del operator is also modified in certain situations to $\nabla_t$ to mean the operation is carried out with respect to the transverse components only. In this thesis, it is always the x and y components which are transverse. The basic field equations initially are developed in the general case with no iterative subscripts. The iterating

enumeration subsequently is applied to these equations while developing the proper Green's functions and wave solutions to use in the Perturbation-Iteration Method.

A modification to the calculations is employed which facilitates an easier and faster analysis. With reference to Fig. 2.1, all dimensions of the microstrip structure are measured relative to one-half of the width W of the stripline. Therefore, the microstrip is considered 2 units wide, the side ground walls extend from -a to a where $a = \frac{A}{W}$ and the height of the dielectric substrate equals $\alpha$ where $\alpha = \frac{H}{W}$. For certain calculations, the stripline is then located at a height $y = \alpha^+$. This modification permits this analysis to apply to any size structure with proper scaling applied to the dimensions of it.

## 2.2 The Field Equations

The analysis begins with the formulation of the field equations. Since the fields are assumed to be propagating down the stripline in the +z direction, they may be represented as

$$\vec{A} = \vec{A}(x, y)e^{-j\beta z} \qquad \vec{E} = \vec{E}(x, y)e^{-j\beta z} \qquad \rho = \rho(x, y)e^{-j\beta z}$$

$$\Phi = \Phi(x, y)e^{-j\beta z} \qquad \vec{H} = \vec{H}(x, y)e^{-j\beta z} \qquad \vec{J} = \vec{J}(x, y)e^{-j\beta z}$$

The field equations are developed by employing Maxwell's equations

$$\nabla \times \vec{E} = -\frac{\partial \vec{B}}{\partial t} = -j\omega\mu_o \vec{H}$$

$$\nabla \times \vec{H} = \frac{\partial \vec{D}}{\partial t} + \vec{J} = j\omega\varepsilon_o\kappa(y)\vec{E} + \vec{J}$$

$$\nabla \cdot \vec{B} = \mu_o \nabla\cdot\vec{H} = 0$$

$$\nabla \cdot \vec{D} = \varepsilon_o \nabla\cdot(\kappa(y)\ \vec{E}) = \rho$$

We let

$$\nabla \times \vec{H} = \frac{1}{\mu_o}\ \nabla \times \nabla \times \vec{A} = \frac{1}{\mu_o}\ (\nabla\nabla\cdot\vec{A} - \nabla^2\vec{A}) = j\omega\varepsilon_o\kappa(y)\vec{E} + \vec{J} \qquad (2.1)$$

Using the Lorentz condition:

$$\nabla \cdot \vec{A} = -j\omega\mu_o\varepsilon_o\kappa(y)\ \phi$$

$$\nabla\nabla \cdot \vec{A} = -j\omega\mu_o\varepsilon_o\nabla(\kappa(y)\phi) = -j\omega\mu_o\varepsilon_o[\ \kappa(y)\nabla\phi + \phi\nabla\kappa(y)\ ]$$

and combining with (2.1) results in

$$-j\omega\varepsilon_o[\kappa(y)\nabla\phi + \phi\nabla\kappa(y)] - \frac{1}{\mu_o}\nabla^2\vec{A} = j\omega\varepsilon_o\kappa(y)\vec{E} + \vec{J} \qquad (2.2)$$

Combining (2.2) with $\vec{E} = -j\omega\vec{A} - \nabla\phi$ gives

$$-j\omega\varepsilon_o\kappa(y)\nabla\phi\ \ -j\omega\varepsilon_o\ \phi\nabla\kappa(y) - \frac{1}{\mu_o}\ \nabla^2\vec{A} = \vec{J} + \ \omega^2\varepsilon_o\kappa(y)\vec{A} - j\omega\varepsilon_o\kappa(y)\nabla\phi$$

which can be written as

$$\nabla^2\vec{A} = \nabla_t^2\vec{A} + \nabla_z^2\vec{A} = \nabla_t^2\vec{A} - \beta^2\vec{A} = -\mu_o\vec{J} - \omega^2\mu_o\varepsilon_o\kappa(y)\vec{A} - j\omega\mu_o\varepsilon_o\phi\nabla\kappa(y)$$

Letting $k_o^2 = \omega^2 \mu_o \varepsilon_o$ gives the final equation for $\vec{A}$ :

$$\nabla_t^2 \vec{A} + (\kappa(y)\, k_o^2 - \beta^2)\, \vec{A} = -\mu_o \vec{J} - j\omega\mu_o\varepsilon_o \phi \nabla\kappa(y) \qquad (2.3a)$$

The $y$ component of this equation is

$$\nabla_t^2 A_y + (\kappa(y) k_o^2 - \beta^2) A_y = -j\omega\mu_o\varepsilon_o (1-\kappa)\phi(\alpha)\delta(y-\alpha) \qquad (2.3b)$$

Note that $\nabla\kappa(y) = \vec{a}_y (1-\kappa)\, \delta(y-\alpha)$ since $\kappa(y)$ undergoes a step change from $\kappa$ to $1$ as $y$ crosses the point $y = \alpha$. In order that the second derivative term $\frac{\partial^2 A_y}{\partial y^2}$ yields a delta function term, $A_y$ must be continuous at $y = \alpha$ and $\frac{\partial A_y}{\partial y}$ must have a discontinuity of strength $j\omega\mu_o\varepsilon_o(1-\kappa)\,\phi$ at $y = \alpha$.

A similar equation for $\Phi$ is developed. We begin with

$$\nabla \cdot \vec{D} = \rho$$

$$\nabla \cdot (\kappa(y)\vec{E}) = \frac{\rho}{\varepsilon_o}$$

Substituting in $\vec{E} = -j\omega\vec{A} - \nabla\Phi$ yields

$$\kappa(y)\nabla\cdot(-j\omega\vec{A} - \nabla\Phi) = \frac{\rho}{\varepsilon_o} - \vec{E}\cdot\nabla\kappa(y)$$

By using the Lorentz condition we obtain

$$\nabla_t^2 \phi - (\kappa(y) k_o^2 - \beta^2)\, \phi = \frac{-\rho}{\kappa(y)\varepsilon_o} + \frac{\vec{E}\cdot\nabla\kappa(y)}{\kappa(y)}$$

$$\nabla_t^2\phi - (\kappa(y)k_o^2 - \beta^2)\phi = \frac{E_y(1-\kappa)\delta(y-\alpha)}{\kappa(y)}$$

Since the stripline is assumed to be at $y = \alpha^+$, the source term $\frac{\rho}{\kappa(y)\varepsilon_o} = \frac{\rho}{\varepsilon_o}$. The term $\frac{E_y(1-\kappa)\,\delta(y-\alpha)}{\kappa(y)}$ equals zero at all points $y \neq \alpha$ since $\delta(y-\alpha) = 0$ at these points. This term may be eliminated from the partial differential equation through use of an appropriate boundary condition on $\partial\phi/\partial y$ at $y = \alpha$, as we demonstrate below. We can replace $\vec{E}\cdot\nabla\kappa(y)$ by

$$E_y \frac{\partial\kappa(y)}{\partial y} = -(j\omega A_y + \frac{\partial\phi}{\partial y}) \frac{\partial\kappa(y)}{\partial y}$$

and rewrite the equation for $\phi$ in the form

$$\kappa(y)\left[\frac{\partial^2\phi}{\partial y^2} + \frac{\partial^2\phi}{\partial x^2} + \frac{\partial^2\phi}{\partial z^2}\right] + \frac{\partial\phi}{\partial y}\frac{\partial\kappa(y)}{\partial y} + \kappa^2(y)k_o^2\,\phi$$

$$= \frac{\partial}{\partial y}\kappa(y)\frac{\partial\phi}{\partial y} + \kappa(y)\left[\frac{\partial^2\phi}{\partial x^2} + \frac{\partial^2\phi}{\partial y^2}\right] + \kappa^2(y)k_c^2\,\phi$$

$$= -\frac{\rho}{\varepsilon_o} + j\omega A_y(\kappa-1)\,\delta(y-\alpha)$$

since $A_y$ is continuous at $y = \alpha$. If we integrate this equation once with respect to $y$ about a vanishing small interval centered on $y = \alpha$ and take note of the fact that $\rho$ is assumed to be just above the interface we obtain

$$\int_{\alpha_-}^{\alpha_+} \frac{\partial}{\partial y}\left[\kappa(y)\,\frac{\partial \phi}{\partial y}\right]dy = \kappa(y)\,\frac{\partial \phi}{\partial y}\Bigg|_{\alpha_-}^{\alpha_+}$$

$$= \frac{\partial \phi}{\partial y}\Bigg|_{\alpha_+} - \kappa\,\frac{\partial \phi}{\partial y}\Bigg|_{\alpha_-} = j\omega(\kappa-1)\,A_y(\alpha)$$

This is the required boundary condition on $\frac{\partial \phi}{\partial y}$ at the interface. In each region $y<\alpha$ and $y>\alpha$ we note that $\nabla\kappa(y)=0$. Hence we can solve for $\phi$ in each region and properly join the two solutions using the above boundary conditions. Thus the equation for $\phi$ that is used is

$$\nabla_t^2 \phi + (\kappa(y)k_o^2 - \beta^2)\phi = -\frac{\rho}{\varepsilon_o} \tag{2.4a}$$

along with the boundary conditions that $\phi$ is continuous across the air-dielectric interface and

$$\frac{\partial \phi}{\partial y}\Bigg|_{\alpha_+} - \kappa\,\frac{\partial \phi}{\partial y}\Bigg|_{\alpha_-} = j\omega(\kappa-1)\,A_y(\alpha) \tag{2.4b}$$

In the lowest order solution $A_y$ is zero so $\kappa(y)\,\frac{\partial \phi}{\partial y}$ is made continuous at $y=\alpha$.

## 2.3 Zero Order Solution

The Perturbation-Iteration Method commences with the evaluation of the static field entities and Green's functions. In the static analysis, $\omega = 0$ and therefore $\beta = 0$. Thus, the wave equations reduce to Poisson's equations and are

$$\nabla_t^2 \vec{A}_o = -\mu_o \vec{J}_o(\kappa)\delta(y-\alpha^+) \tag{2.5}$$

$$\nabla_t^2 \phi_o = -\frac{\rho(x)}{\varepsilon_o}\delta(y-\alpha^+) \tag{2.6}$$

At the static level there is only a D.C. charge and current on the microstrip. This translates into the following condition:

$$\vec{J}_o = J_{oz}\vec{a}_z$$

Therefore (2.5) reduces to a scalar Poisson equation

$$\nabla_t^2 A_{oz} = -\mu_o J_{oz}(x)\delta(y-\alpha^+) \tag{2.7}$$

The two static Green's function, $G_1^o$ and $G_2^o$, are now developed to facilitate the solutions of the equations (2.7) and (2.6), respectively. These functions will be developed using Fourier series analysis. Only the odd harmonics are required since the solution must be even about $x = 0$.

The Green's function $G_1^o$ is found first and is used to solve for $J_{oz}$ in the integral equation:

$$2\int_0^1 G_1^o(x,x',y,y')\, J_{oz}(x',y')\, dx' = \frac{A_{oz}}{\mu_o} = 1 \qquad (2.8a)$$

obtained by setting $A_{oz}$ equal to $\mu_o$ on the strip. This value of $A_{oz}$ is shown later to be a relative value that can be correctly scaled to yield the true value of $J_{oz}$. Since relative values are used, the above is rewritten as

$$2\int_0^1 G_1^o\, J_{oz,r}\, dx' = \frac{A_{oz,r}}{\mu_o} = 1 \qquad (2.8b)$$

$G_1^o$ is chosen to satisfy the equation

$$\nabla_t^2 G_1^o = -\delta(x-x')\delta(y-y') \qquad (2.9)$$

with boundary conditions

$G_1^o$, $\frac{\partial G_1^o}{\partial y}$ are continuous at $y = \alpha$

$G_1^o$ is continuous at $y = y'$

$G_1^o = 0$ at $y = 0, \infty$

$G_1^o = 0$ at $x = a, -a$

Assume that the solution is:

$$G_1^o = \begin{cases} \sum_{n=1,3..}^{\infty} a_n \sinh\omega_n y \cos\omega_n x & y \leq y' \\ \sum_{n=1,3..}^{\infty} b_n e^{-\omega_n y} \cos\omega_n x & y \geq y' \end{cases}$$

$$\omega_n = \frac{n\pi}{2a}$$

In solving for $G_1^o$, the following Fourier series representation, which is employed throughout the entire analysis, is used:

$$\sum_{n=1,3..}^{\infty} A_n \cos\omega_n x = \delta(x-x')$$

$$A_n = -\frac{\cos\omega_n x'}{a}$$

Equation (2.9) is integrated across the discontinuity $y'$, taking Fourier components only, to give

$$\frac{\partial G_{1n}^o}{\partial y}\Bigg|_{y'_-}^{y'_+} = \frac{\cos\omega_n x'}{a}$$

Finally, by satisfying the boundary condition of $G_1^o$ being continuous at $y'$, employing the above, and taking only the Fourier components, the Fourier coefficients are solved for:

$$a_n \sin\omega_n y' = b_n e^{-\omega_n y'}$$

$$-\omega_n b_n e^{-\omega_n y'} - \omega_n a_n \cosh\omega_n y' = -\frac{\cos\omega_n x'}{a}$$

Thus,

$$a_n = \frac{e^{-\omega_n y'} \cos\omega_n x'}{\omega_n a}, \quad b_n = \frac{\sinh\omega_n y' \cos\omega_n x'}{\omega_n a}$$

Since the source points of $A_{oz,r}$ are on the stripline, the conversion $y' = \alpha$ will be made. Hence $G_1^o$ is given by

$$G_1^o = \begin{cases} \displaystyle\sum_{n=1,3..}^{\infty} \frac{e^{-\omega_n \alpha} \cos\omega_n x'}{\omega_n a} \sinh\omega_n y \cos\omega_n x & y \leq \alpha \\ \displaystyle\sum_{n=1,3..}^{\infty} \frac{\sinh\omega_n \alpha \cos\omega_n x'}{\omega_n a} e^{-\omega_n y} \cos\omega_n x & y \geq \alpha \end{cases} \tag{2.10}$$

$$\omega_n = \frac{n\pi}{2a}$$

The Green's function $G_2^o$ is solved for in order to solve the equation

$$2\int_0^1 G_2^o(x,x',y,y')\rho_o(x',y')\,dx' = \varepsilon_o \phi_o = 1 \tag{2.11}$$

where $\phi_o$ is set equal to $\frac{1}{\varepsilon_o}$ on the microstrip. In the same manner as $A_{oz}$, this value of $\phi_o$ is nominal and is used later to properly scale $A_{oz,r}$ and $J_{oz,r}$.

$G_2^o$ must satisfy the equation

$$\nabla_t^2 G_2^o = -\delta(x-x')\delta(y-y')$$

with boundary conditions

$G_2^o$, $\kappa(y) \frac{\partial G_2^o}{\partial y}$ are continuous at $y = \alpha$

$G_2^o$ is continuous at $y'$

$G_2^o = 0$ at $y = 0, \infty$

$G_2^o = 0$ at $x = a, -a$

Assume that the solution is:

$$G_2^o = \begin{cases} \sum_{n=1,3..}^{\infty} a_n \sinh\omega_n y \cos\omega_n x & o \leq y \leq \alpha \\ \sum_{n=1,3..}^{\infty} (b_n e^{-\omega_n y} + c_n e^{\omega_n y}) \cos\omega_n x & \alpha \leq y \leq y' \\ \sum_{n=1,3..}^{\infty} d_n e^{-\omega_n y} \cos\omega_n x & y' \leq y \end{cases}$$

$$\omega_n = \frac{n\pi}{2a}$$

As shown before,

$$\frac{\partial G_{2n}^{o}}{\partial y}\Bigg|_{y'_-}^{y'_+} = -\frac{\cos\omega_n x'}{a}$$

The boundary conditions of continuity of $G_2^o$ and $\kappa(y)\frac{\partial G_2^o}{\partial y}$ at $y = \alpha$, continuity of $G_2^o$ at $y = y'$, using the above, and taking only Fourier components yields the following equations:

$$a_n \sinh\omega_n\alpha = b_n e^{-\omega_n\alpha} + c_n e^{\omega_n\alpha}$$

$$\kappa\omega_n a_n \cosh\omega_n\alpha = -\omega_n b_n e^{-\omega_n\alpha} + \omega_n c_n e^{\omega_n\alpha}$$

$$b_n e^{-\omega_n y'} + c_n e^{\omega_n y'} = d_n e^{-\omega_n y'}$$

$$\omega_n d_n e^{-\omega_n y'} + \omega_n b_n e^{-\omega_n y'} - \omega_n c_n e^{\omega_n y'} = -\frac{\cos\omega_n x'}{a}$$

Once again, by assuming that the source points are on the microstrip and setting $y' = \alpha$, the final solution becomes

$$G_2^o = \begin{cases} \displaystyle\sum_{n=1,3..}^{\infty} \frac{\cos\omega_n x' \sinh\omega_n y}{\omega_n a(\sinh\omega_n\alpha + \kappa\cosh\omega_n\alpha)} \cos\omega_n x & 0 \le y \le \alpha \\ \displaystyle\sum_{n=1,3..}^{\infty} \frac{\cos\omega_n x' \sinh\omega_n\alpha e^{\omega_n\alpha} e^{-\omega_n y}}{\omega_n a(\sinh\omega_n\alpha + \kappa\cosh\omega_n\alpha)} \cos\omega_n x & \alpha \le y \end{cases} \qquad (2.12)$$

$$\omega_n = \frac{n\pi}{2a}$$

The numerical solutions for $\rho_o$ and $J_{oz,r}$ are next performed. To accomplish this task, (2.8) and (2.11) are utilized with the respective Green's functions $G_1^o$ and $G_2^o$. Since the potentials are being fixed and measured on the microstrip, the observation points of $G_1^o$ and $G_2^o$ are at $y = \alpha$. As previously indicated, $A_{oz,r}$ is fixed to the constant value of $\frac{1}{\mu_o}$ and $\Phi_o$ is fixed to the constant value of $\varepsilon_o$. These values are nominal and permit easier calculations of $J_{oz,r}$ and $\rho_o$. They basically represent the level of excitation on the microstrip and can obviously be varied to any values. The values of $A_{oz,r}$ and $J_{oz,r}$ are properly scaled at a later point. As is also shown, the amplitudes of both potentials are independent of $\beta$ and $Z_c$. The first source to be determined is $J_{oz,r}$. The process begins with (2.8)

$$2\int_0^1 G_1^o \, J_{oz,r} \, dx' = \frac{A_{oz,r}}{\mu_o} = 1$$

$$2\int_0^{.1} \sum_{n=1,3..}^{\infty} \frac{\cos\omega_n x' \, \sinh\omega_n \alpha \, e^{-\omega_n \alpha}}{\omega_n a} \cos\omega_n x \; J_{oz,r} \, dx' \qquad (2.13)$$

$G_1^o$ is simplified and approximated to permit an easier evaluation. We rewrite the expression for $G_1^o$ as follows:

$$G_1^o = \sum_{n=1,3..}^{\infty} \frac{\cos\omega_n x' \sinh\omega_n \alpha \; e^{-\omega_n \alpha}}{\omega_n a} \cos\omega_n x$$

$$= \sum_{n=1,3..}^{\infty} \frac{\cos\omega_n x' (1-e^{-2\omega_n \alpha})}{\omega_n a} \cos\omega_n x$$

$$= \sum_{n=1,3..}^{\infty} \frac{1}{2\pi n} [\cos\omega_n (x-x') + \cos\omega_n (x+x')][1-e^{-2\omega_n \alpha}]$$

By applying the identity [ ]

$$\mathrm{Re} \sum_{n=1,3..}^{\infty} \frac{e^{jnu}}{n} = \frac{1}{2} \mathrm{Re}\left[\ln \frac{1 + e^{ju}}{1 - e^{ju}}\right] = -\frac{1}{2} \ln\left|\tan \frac{u}{2}\right|$$

to $G_1^o$, the result is

$$G_1^o = -\frac{1}{4\pi} \ln[\tan \frac{\pi}{4a}|x-x'| \tan \frac{\pi}{4a}|x+x'|]$$

$$-\frac{1}{8\pi} \ln\left\{\left[\frac{\cosh \frac{\pi\alpha}{a} + \cos \frac{\pi}{2a}(x-x')}{\cosh \frac{\pi\alpha}{a} - \cos \frac{\pi}{2a}(x-x')}\right]\left[\frac{\cosh \frac{\pi\alpha}{a} + \cos \frac{\pi}{2a}(x+x')}{\cosh \frac{\pi\alpha}{a} - \cos \frac{\pi}{2a}(x+x')}\right]\right\}$$

$$= G_{1a}^o + G_{1b}^o$$

The series identity

$$\ln|\tan u| = \ln|x| + \frac{x^2}{3} + \frac{7x^4}{90} + \ldots$$

is applied to $G_{1a}$, the dominant terms are retained, and the

result is

$$G_{1a}^{o} = -\frac{1}{2\pi} \ln \frac{\pi}{4a} - \frac{1}{4\pi} \ln|(x^2-x'^2)| - \frac{\pi}{96a^2}(x^2+x'^2)$$

$$- \frac{7}{180\pi}\left(\frac{\pi}{4a}\right)^4 (x^4+6x^2x'^2+x'^4)$$

The series identities

$$\cosh x = 1 + \frac{x^2}{2!} + \frac{x^4}{4!} + \ldots$$

$$\cos x = 1 - \frac{x^2}{2!} + \frac{x^4}{4!} + \ldots$$

are applied to $G_{1b}^{o}$, the dominant terms are retained, and the result is

$$G_{1b}^{o} = \frac{1}{2\pi} \ln \frac{\pi}{4a} + \frac{1}{8\pi} \ln\left\{[(2\alpha)^2 + (x-x')^2][(2\alpha)^2 + (x+x')^2]\right\}$$

$$+ \frac{1}{72\pi}\left(\frac{\pi}{4a}\right)^4 [(x-x')^4 + (x+x')^4]$$

$$+ \left[\frac{2}{3\pi}\left(\frac{\pi}{8a}\right)^2 - \frac{2}{9\pi}\left(\frac{\pi}{4a}\right)^4 (2\alpha)^2\right](x^2+x'^2)$$

$$- \frac{2}{3\pi}\left(\frac{\pi}{8a}\right)^2 (2\alpha)^2 + \frac{1}{36\pi}\left(\frac{\pi}{4a}\right)^4 (2\alpha)^4$$

On the stripline, $\frac{x}{a}$ and $\frac{\alpha}{a}$ are very small provided a is chosen to be greater than or equal to 10. The two functions $G_{1a}^{o}$ and $G_{1b}^{o}$ are recombined and, after employing the fact

that terms containing $(\frac{\pi}{4a})^4$ are negligibly small and thus discarded, the final result is:

$$G_1^o = -\frac{1}{4\pi}\left\{ \ln\left|x^2 - x'^2\right| - \frac{1}{2}\ln\left\{ [(2\alpha)^2 + (x-x')^2] \right.\right.$$

$$\left.\left. [(2\alpha)^2 + (x + x')^2] \right\} + \frac{2}{3}\left(\frac{\pi}{4a}\right)^2 (2\alpha)^2 \right\} \qquad (2.14)$$

The current density $J_{oz,r}$ is approximated by a series of the form

$$J_{oz,r}(x') = \frac{I_o + I_1 x'^2 + I_2 x'^4 + I_3 x'^6}{\sqrt{1 - x'^2}}$$

This form gives $J_{oz,r}$ the required singular behavior at $x = \pm 1$. The coefficients $I_o$, $I_1$, $I_2$, and $I_3$ are solved for to determine the current density $J_{oz,r}$. By substituting $G_1^o$ and $J_{oz,r}$ back into (2.13), the result is

$$-\frac{1}{2\pi}\int_0^1 \left\{\ln\left|x^2 - x'^2\right| - \frac{1}{2}\ln\left\{[(2\alpha)^2 + (x - x')^2][(2\alpha)^2 + (x + x')^2]\right\}\right.$$

$$\left. + \frac{2}{3}\left(\frac{\pi}{4a}\right)^2 (2\alpha)^2 \right\} \left\{ \frac{I_o + I_1 x'^2 + I_2 x'^4 + I_3 x'^6}{\sqrt{1 - x'^2}} \right\} dx' = 1$$

Point matching on the microstrip is used to solve for the four unknown current density coefficients by performing the integrations, sequentially letting $x = \frac{1}{4}$, $\frac{1}{2}$, $\frac{3}{4}$, and 1,

and then using the four equations to solve for the four unknown coefficients. The individual integrals are solved utilizing the implicit transformations:

$$x = \sin\theta$$

$$x' = \sin\theta'$$

$$x^2 - x'^2 = \frac{1}{2}(\cos 2\theta' - \cos 2\theta)$$

$$dx' = \cos\theta' d\theta'$$

$$\ln\left[\frac{1}{2}(\cos\theta' - \cos\theta)\right] = -\sum_{n=1,2..}^{\infty} \frac{2\cos n\theta \cos n\theta'}{n} - \ln 4$$

Thus we find that

$$-\frac{2I_o}{4\pi}\int_0^1 \frac{\ln(x^2 - x'^2)}{\sqrt{1 - x'^2}}\, dx' = \frac{I_o}{2}\ln 2$$

$$-\frac{2I_1}{4}\int_0^1 \frac{x'^2 \ln(x^2 - x'^2)}{\sqrt{1 - x'^2}}\, dx' = \frac{I_1}{8}(2x^2 + \ln 4 - 1)$$

$$-\frac{2I_2}{4\pi}\int_0^1 \frac{x'^4 \ln(x^2 - x'^2)}{\sqrt{1 - x'^2}}\, dx' = \frac{I_2}{8}(x^4 + x^2 + \frac{3}{4}\ln 4 - \frac{7}{8})$$

$$-\frac{2I_3}{4\pi}\int_0^1 \frac{x'^6 \ln(x^2 - x'^2)}{\sqrt{1 - x'^2}}\, dx' =$$

$$\frac{I_3}{64}(\frac{16}{3}x^6 + 4x^4 + 6x^2 - \frac{37}{6} + 51\ln 4)$$

$$\frac{1}{2\pi}\frac{2}{3}\left(\frac{\pi}{4a}\right)^2(2\alpha)^2 I_o \int_0^1 \frac{1}{\sqrt{1-x'^2}}\,dx' = \frac{1}{3}\left(\frac{\pi}{4a}\right)^2(2\alpha)^2 I_o$$

$$\frac{1}{2\pi}\frac{2}{3}\left(\frac{\pi}{4a}\right)^2(2\alpha)^2 I_1 \int_0^1 \frac{x'^2}{\sqrt{1-x'^2}}\,dx' = \frac{1}{6}\left(\frac{\pi}{4a}\right)^2(2\alpha)^2 I_1$$

$$\frac{1}{2\pi}\frac{2}{3}\left(\frac{\pi}{4a}\right)^2(2\alpha)^2 I_2 \int_0^1 \frac{x'^4}{\sqrt{1-x'^2}}\,dx' = \frac{1}{2}\left(\frac{\pi}{8a}\right)^2(2\alpha)^2 I_2$$

$$\frac{1}{2\pi}\frac{2}{3}\left(\frac{\pi}{4a}\right)^2(2\alpha)^2 I_3 \int_0^1 \frac{x'^6}{\sqrt{1-x'^2}}\,dx' = \frac{5}{3}\left(\frac{\pi}{16a}\right)^2(2\alpha)^2 I_3$$

The integral terms

$$\frac{1}{4\pi}\int_0^1 \ln[(2\alpha)^2 + (x-x')^2][(2\alpha)^2 + (x+x')^2] \left[\frac{I_o + I_1 x'^2 + I_2 x'^4 + I_3 x'^6}{\sqrt{1-x'^2}}\right] dx'$$

cannot be solved in a closed form fashion and, thus are numerically evaluated using a Simpson's Rule approximation. The substitution $x' = \sin\theta'$ is employed to avoid a singularity in the calculation at $x' = 1$.

Once the current density coefficients have been solved for, the total current on the microstrip $I_{oT,r}$ is evaluated by using the integral on the following page:

$$I_{oT,r} = 2\int_0^1 J_{oT,r}\, dx'$$

$$= 2\int_0^1 \frac{I_o + I_1 x'^2 + I_2 x'^4 + I_3 x'^6}{\sqrt{1 - x'^2}}\, dx'$$

and the substitution $x' = \sin\theta$. This yields the result:

$$I_{oT,r} = \pi(I_o + \tfrac{1}{2} I_1 + \tfrac{3}{8} I_2 + \tfrac{5}{16} I_3)$$

The charge density $\rho_o$ and subsequent total charge $q_{oT}$ are solved for in a similar manner as $J_{oz,r}$ and $I_{oT,r}$. The evaluation begins with (2.11)

$$2\int_0^1 G_2^o\, \rho_o\, dx' = \varepsilon_o\, \phi_o = 1 \qquad (2.15)$$

$G_2^o$ is simplified by expressing it as a function of $G_1^o$.

$$G_2^o = \sum_{n=1,3..}^{\infty} \frac{\cos\omega_n x' \sinh\omega_n \alpha \cos\omega_n x}{\omega_n a(\sinh\omega_n \alpha + \kappa\cosh\omega_n \alpha)}$$

$$= \frac{2}{\kappa + 1}\left[G_1^o + \sum_{n=1,3..}^{\infty} \frac{1}{n\pi} \cos\omega_n x' \sinh\omega_n \alpha\right.$$

$$\left.\left(\frac{\kappa + 1}{\sinh\omega_n \alpha + \kappa\cosh\omega_n \alpha} - 2\, e^{-\omega_n \alpha}\right)\cos\omega_n x\right]$$

The charge density $\rho_o(x')$ is approximated by the series

$$\rho_o(x') = \frac{q_o + q_1 x'^2 + q_2 x'^4 + q_3 x'^6}{\sqrt{1 - x'^2}}$$

which is similar to that used for the current density. Thus, in the same manner as before, the four unknown charge density coefficients are solved for by substituting the expressions for $\rho_o$ and $G_2^o$ into (2.15), performing the integrations, and solving the four equations obtained by point matching at $x = \frac{1}{4}$, $\frac{1}{2}$, $\frac{3}{4}$, and 1 for the unknown charge density coefficients $q_o$, $q_1$, $q_2$, and $q_3$. The integrals

$$2\int_0^1 \frac{2}{\kappa + 1} G_1^o \rho_o \, dx'$$

are performed in the same way as before using the approximation of $G_1^o$ and the Simpson's Rule approximation. The remaining integrals

$$\int_0^1 \sum_{n=1,3..}^{\infty} \frac{4}{n\pi} \frac{\sinh\omega_n\alpha}{\kappa + 1} \left[ \frac{\kappa + 1}{\sinh\omega_n\alpha + \kappa\cosh\omega_n\alpha} - 2e^{-\omega_n\alpha} \right] \cos\omega_n x$$

$$\cos\omega_n x' \frac{q_o + q_1 x'^2 + q_2 x'^4 + q_3 x'^6}{\sqrt{1 - x'^2}} \, dx'$$

are carried out using a Simpson's Rule approximation and the substitution $x' = \sin\theta'$ to avoid the singularity at $x' = 1$.

The total charge $q_{oT}$ on the microstrip is determined by using the integral:

$$q_{oT} = 2\int_0^1 \rho_o(x')\, dx'$$

and the substitution $x' = \sin\theta'$. This yields

$$q_{oT} = \pi(q_o + \frac{1}{2} q_1 + \frac{3}{8} q_2 + \frac{5}{16} q_3)$$

With the results of $I_{oT,r}$ and $q_{oT}$, the static $Z_{co}$ and $\kappa_{eff,o}$ is determined. At $\omega = 0$, $\beta_o = 0$. Therefore, $\beta_1$ is incorporated into the analysis with the frequency being set equal to zero at the conclusion of the static case. Beginning with the equation

$$\vec{E}_o = -j\omega_1 \vec{A}_o - \nabla\Phi_o$$

$$E_{oz} = -j\omega A_{oz} + j\beta_1 \Phi_o$$

On the strip,

$$E_{oz} = 0 = -j\omega A_{oz} + j\beta_1 \Phi_o = -j\omega L_o I_{oT} + j\beta_1 \frac{q_{oT}}{C_o} \qquad (2.16)$$

In this equation, $L_o = A_{oz}/I_{oT}$ is the static inductance per

unit length of line and $C_o = q_{oT}/\Phi_o$ is the static capacitance per unit length of line. Using (2.8)

$$2\int_0^1 G_1^o \, J_{oz} \, dx' = \frac{A_{oz}}{\mu_o}$$

it is evident that $A_{oz}$ and $J_{oz}$ are directly proportional to $A_{oz,r}$ and $J_{oz,r}$, respectively. Thus, the value of $L_o$ can also be determined from $L_o = A_{oz,r}/I_{oT,r}$. This illustrates why the values of $\beta_1$ and $Z_{co}$, as yet to be determined, are independent of the nominal value of $A_{oz,r}$. The value of $C_o$ is also independent of the level of $\Phi_o$ by the same reasoning. From the continuity equation

$$\nabla \cdot \vec{J} = \frac{\partial J_{ox}}{\partial x} - j\beta_1 J_{oz} = -j\omega_1 \rho_o$$

Integrating over the width of the microstrip yields

$$\beta_1 I_{oT} = \omega_1 q_{oT} \tag{2.17}$$

since $J_{ox} = 0$ across the strip. Combining (2.16) and (2.17) finally results in

$$\beta_1 = \omega_1 \sqrt{L_o C_o} \tag{2.18}$$

This is the value of the propagation constant in the zero

frequency limit and is also used as the approximate value in the 1 level iteration. As can be seen, $\beta_1 = 0$ at $\omega_1 = 0$ which is consistent with all of the previous theory.

A value of $\kappa_{eff,o}$ is determined at $\omega_1 = 0$ by defining it as follows:

$$\kappa_{eff,o} = \frac{\beta_1}{k_{o,1}} = \sqrt{\frac{L_o C_o}{\mu_o \varepsilon_o}} = c\sqrt{L_o C_o} \qquad (2.19)$$

The final parameter to solve for is the characteristic impedance $Z_{co}$ of the stripline. This is easily determined by the following:

$$Z_{co} = \frac{\Phi_o}{I_{oT}} = \frac{\frac{\beta_1 I_{oT}}{\omega_1 C_o}}{I_{oT}} = \sqrt{\frac{L_o}{C_o}} \qquad (2.20)$$

The current and charge density coefficients are now scaled correctly as they are needed, properly scaled, for future calculations. Equation (2.16)

$$\omega A_{oz} = \beta_1 \Phi_o$$

properly relates the levels of the potentials. Let

$$A_{oz} = K A_{oz,r}$$

where K is the constant of proportionality which correctly scales $A_{oz}$. As stated previously,

$$A_{oz,r} = \mu_o$$

$$\phi_o = \frac{1}{\epsilon_o}$$

Thus

$$K = \frac{\beta_1}{\omega\mu_o\epsilon_o}$$

which, from (2.8), is also the constant of proportionality between $J_{oz}$ and $J_{oz,r}$. Therefore, the current density and, furthermore, total current $I_{oT}$ is properly scaled by the relations

$$J_{oz} = c^2\sqrt{L_oC_o}\,J_{oz,r} \qquad (2.21a)$$

$$I_{oT} = c^2\sqrt{L_oC_o}\,I_{oT,r} \qquad (2.21b)$$

## 2.4 Higher Order Solutions

The analysis continues with the calculation of $\beta_2$ and $Z_{c1}$ at a finite frequency $\omega_1$. The value of $\omega_1$ should be low enough to use the static solution as a good first approximation before calculating a better value of $\beta$. The procedure continues with the calculation of the Fourier coefficients of $\rho_o$ and

$J_{oz}$. This is done using

$$\rho_{on} = \frac{2}{a}\int_0^1 \rho_o(x')\cos\omega_n x'\,dx' \qquad (2.22a)$$

$$J_{on} = \frac{2}{a}\int_0^1 J_{oz}(x')\cos\omega_n x'\,dx' \qquad (2.22b)$$

along with the substitution $x' = \sin\theta'$. These integrals are solved numerically using a Simpson's Rule approximation. A sufficient amount of coefficients should be calculated until $\rho_{on}$ and $J_{on}$ are very nearly equal to zero.

The Fourier representation of $A_{oz}$ and $\Phi_o$ are solved for at any point in the cross-section of the stripline. $A_{oz}$ satisfies (2.8)

$$\nabla_t^2 A_{oz} = -\mu_o J_{oz}(x)\delta(y-\alpha)$$

with the boundary conditions

$$A_{oz},\ \frac{\partial A_{oz}}{\partial y} \text{ are continuous at } y = \alpha .$$

$$A_{oz} = 0 \text{ at } y = 0,\infty .$$

$$A_{oz} = 0 \text{ at } x = a, -a .$$

A Fourier representation of $A_{oz}$ is used. Assume

$$A_{oz} = \begin{cases} \sum_{n=1,3..}^{\infty} A_n \sinh\omega_n y \cos\omega_n x & y \leq \alpha \\ \sum_{n=1,3..}^{\infty} B_n e^{-\omega_n y} \cos\omega_n x & y \geq \alpha \end{cases}$$

The coefficients, $A_n$ and $B_n$, are solved for by invoking continuity of $A_{oz}$ at $y = \alpha$ and integrating (2.8) over a small region centered on $y = \alpha$, thus

$$A_n \sinh\omega_n \alpha = B_n e^{-\omega_n \alpha}$$

$$\frac{\partial A_{ozn}}{\partial y}\Bigg|_{\alpha^-}^{\alpha^+} = -\omega_n B_n e^{-\omega_n \alpha} - \omega_n A_n \cosh\omega_n \alpha = -\mu_o J_{on}$$

$$A_n = \frac{\mu_o}{\omega_n} e^{-\omega_n \alpha} J_{on}$$

$$B_n = \frac{\mu_o}{\omega_n} \sinh\omega_n \alpha \, J_{on}$$

Therefore, the Fourier representation of $A_{oz}$ is

$$A_{oz} = \begin{cases} \sum_{n=1,3..}^{\infty} \frac{\mu_o}{\omega_n} e^{-\omega_n \alpha} J_{on} \sinh\omega_n \alpha \cos\omega_n x & y \leq \alpha \\ \sum_{n=1,3..}^{\infty} \frac{\mu_o}{\omega_n} \sinh\omega_n \alpha \, J_{on} e^{-\omega_n y} \cos\omega_n x & y \geq \alpha \end{cases} \qquad (2.23)$$

$\Phi_o$ is found using (2.11)

$$\nabla_t^2 \Phi_o = - \frac{\rho_o}{\epsilon_o} \delta(y-y')$$

with the boundary conditions

$$\Phi_o,\ \kappa(y) \frac{\partial \Phi_o}{\partial y} \quad \text{continuous at} \quad y = \alpha$$

$$\Phi_o \quad \text{continuous at} \quad y = y'$$

$$\Phi_o = 0 \quad \text{at} \quad y = 0, \infty$$

$$\Phi_o = 0 \quad \text{at} \quad y = a, -a$$

Assume

$$\Phi_o = \begin{cases} \sum_{n=1,3..}^{\infty} a_n \sinh\omega_n y \cos\omega_n x & 0 \leq y \leq \alpha \\ \sum_{n=1,3..}^{\infty} (b_n e^{-\omega_n y} + c_n e^{\omega_n y}) \cos\omega_n x & \alpha \leq y \leq y' \\ \sum_{n=1,3..}^{\infty} d_n e^{-\omega_n y} \cos\omega_n x & y' \leq y \end{cases}$$

The equations used to solve for the unknown coefficients emanate from the continuity of $\Phi_o$ at $y = \alpha$, the continuity of $\kappa(y) \frac{\partial \Phi_o}{\partial y}$ at $y = \alpha$, the continuity of $\Phi_o$ at $y = y'$, and the

integration of (2.11) over y. Thus,

$$a_n \sinh\omega_n\alpha = b_n e^{-\omega_n\alpha} + c_n e^{\omega_n\alpha}$$

$$\kappa a_n \omega_n \cos\omega_n\alpha = - b_n\omega_n e^{-\omega_n\alpha} + c_n\omega_n e^{\omega_n\alpha}$$

$$b_n e^{-\omega_n y'} + c_n e^{\omega_n y'} = d_n e^{-\omega_n y'}$$

$$- d_n\omega_n e^{-\omega_n y'} - (- b_n\omega_n e^{-\omega_n y'} + c_n\omega_n e^{\omega_n y'}) = - \frac{\rho_{on}}{\varepsilon_o}$$

After solving the equations for the coefficients and letting the source point $y' = \alpha$, the result becomes

$$\Phi_o = \begin{cases} \displaystyle\sum_{n=1,3..}^{\infty} \frac{\rho_{on} \sinh\omega_n y}{\varepsilon_o\omega_n(\sinh\omega_n\alpha + \kappa\cosh\omega_n\alpha)} \cos\omega_n x & y \leq \alpha \\ \displaystyle\sum_{n=1,3..}^{\infty} \frac{\rho_{on} e^{\omega_n\alpha}\sinh\omega_n\alpha\, e^{-\omega_n y}}{\varepsilon_o\omega_n(\sinh\omega_n\alpha + \kappa\cosh\omega_n\alpha)} \cos\omega_n x & y \geq \alpha \end{cases} \qquad (2.24)$$

The analysis continues with the next iteration of field entities. The frequency is raised to $\omega_1$ and the propagation constant is approximated using the static solution of $\beta_1$. The Green's functions are also redeveloped as they are now chosen to be frequency dependent. All of the following theoretical development will be enumerated as the 1 level iteration. It should be noted that all further iteration processes will be carried out in the exact same format.

In the zero frequency limit $A_{ox}$ and $A_{oy}$ are both zero. At $\omega = \omega_1$ this is no longer true, but nevertheless the first corrections for $A_{1x}$ and $A_{1y}$ are small. It is possible to find both $A_{1x}$ and $A_{1y}$ approximately by using the solutions for $A_{oz}$ and $\Phi_o$. We can then find better approximations to $A_z$ and $\Phi$, which are labelled $A_{1z}$ and $\Phi_1$. We can then iterate again to obtain improved solutions for $A_{2x}$ and $A_{2y}$ and then for $A_{2z}$ and $\Phi_2$. After a few iterations the solutions converge to stable values, at which point the frequency $\omega$ is increased to $\omega_2$. The solutions obtained at $\omega_1$ are used in a similar iteration process to find the converged solution at $\omega = \omega_2$.

$A_{1y}$ is the first field entity to be found. From (2.3b), $A_{1y}$ must satisfy

$$[\nabla_t^2 - (\beta_1^2 - \kappa(y)k_{o,1}^2)]\, A_{1y} = j\omega\mu_o\varepsilon_o\Phi_o \frac{\partial\kappa(y)}{\partial y} \tag{2.25}$$

where

$$\frac{\partial\kappa(y)}{\partial y} = -(\kappa-1)\delta(y-\alpha)$$

Note that the known potential $\Phi_o$ is used on the right hand side. The solution for $A_{1y}$ is

$$A_{1y} = \int_{-a}^{a} G_3^1\, [-j\omega\mu_o\varepsilon_o(\kappa-1)\, \Phi_o(\alpha)]\, dx'$$

The Green's function $G_3^1$ will be chosen to satisfy the equation

$$[\nabla_t^2-(\beta_1^2-\kappa(y)k_{o,1}^2)]\ G_3^1 = -\ \delta(x-x')\ \delta\ (y-y') \qquad (2.26)$$

with the boundary conditions

$G_3^1$, $\frac{\partial G_3^1}{\partial y}$ are continuous at $y = \alpha$

$$\frac{\partial G_3^1}{\partial y} = 0 \quad \text{at} \quad y = 0$$

$$G_3^1 = 0 \quad \text{at} \quad x = a, -a$$

Assume

$$G_3^1 = \begin{cases} \sum_{n=1,3..}^{\infty} A_n \frac{\cos\omega_n x'}{a} \cosh\omega_{2n,1} y \cos\omega_n x & y \leq \alpha \\ \sum_{n=1,3..}^{\infty} B_n \frac{\cos\omega_n x'}{a} e^{-\omega_{1n,1} y} \cos\omega_n x & y \geq \alpha \end{cases}$$

where

$$\omega_{2n,1} = \sqrt{\omega_n^2 - \kappa k_{o,1}^2 + \beta_1^2} \qquad \omega_{1n,1} = \sqrt{\omega_n^2 - k_{o,1}^2 + \beta_1^2}$$

The unknown coefficients are determined by using equations satisfying continuity of $G_3^1$ at $y = \alpha$ and the integral of (2.26) over a small interval along $y$ centered on $y = \alpha$. Thus

$$A_n \cosh\omega_{2n,1} = B_n e^{-\omega_{1n,1}\alpha}$$

$$- \omega_{1n,1} B_n e^{-\omega_{1n,1}\alpha} - \omega_{2n,1} A_n \sinh\omega_{2n,1}\alpha = - 1$$

Hence,

$$A_n = \frac{1}{\omega_{2n,1}\sinh\omega_{2n,1}\alpha + \omega_{1n,1}\cosh\omega_{2n,1}\alpha}$$

$$B_n = \frac{\cosh\omega_{2n,1}\alpha e^{\omega_{1n,1}\alpha}}{\omega_{2n,1}\sinh\omega_{2n,1}\alpha + \omega_{1n,1}\cosh\omega_{2n,1}\alpha}$$

and the solution $G_3^1$ is

$$G_3^1 = \begin{cases} \sum_{n=1,3..}^{\infty} \dfrac{\cos\omega_n x' \cosh\omega_{2n,1} y}{a(\omega_{2n,1}\sinh\omega_{2n,1}\alpha + \omega_{1n,1}\cosh\omega_{2n,1}\alpha)} \cos\omega_n x & y \leq \alpha \\ \sum_{n=1,3..}^{\infty} \dfrac{\cos\omega_n x' \cosh\omega_{2n,1}\alpha \, e^{\omega_{1n,1}\alpha} e^{-\omega_{1n,1} y}}{a(\omega_{2n,1}\sinh\omega_{2n,1}\alpha + \omega_{1n,1}\cosh\omega_{2n,1}\alpha)} \cos\omega_n x & y \geq \alpha \end{cases} \qquad (2.27)$$

where

$$\omega_{1n,1} = \sqrt{\omega_n^2 - k_{o,1}^2 + \beta_1^2} \qquad \omega_{2n,1} = \sqrt{\omega_n^2 - \kappa k_{o,1}^2 + \beta_1^2}$$

The solution for $A_{1y}$ at $y = \alpha$ is

$$A_{1y} = \sum_{n=1,3..}^{\infty} \frac{-j\omega_1\mu_o\varepsilon_o(\kappa-1)\cosh\omega_{2n,1}\alpha\ \phi_{on}(\alpha)}{\omega_{2n,1}\sinh\omega_{2n,1}\alpha + \omega_{1n,1}\cosh\omega_{2n,1}\alpha} \cos\omega_n x \qquad (2.28)$$

The quantity $\left.\frac{\partial A_{1y}}{\partial y}\right|_{y = \alpha^+}$ can now be determined and is

$$\left.\frac{\partial A_{1y}}{\partial y}\right|_{y = \alpha^+} = \sum_{n=1,3..}^{\infty} - \omega_{1n,1}A_{1yn}(\alpha)\cos\omega_n x$$

$$= \sum_{n=1,3..}^{\infty} \frac{j\omega_1\mu_o\varepsilon_o\omega_{1n,1}(\kappa-1)\cosh\omega_{2n,1}\alpha\ \phi_{on}(\alpha)}{\omega_{2n,1}\sinh\omega_{2n,1}\alpha + \omega_{1n,1}\cosh\omega_{2n,1}\alpha} \cos\omega_n x \qquad (2.29)$$

The quantity $\phi_1(x,\alpha^+)$ is determined in terms of $A_{1x}$. On the microstrip, $E_{1x} = 0$. Thus,

$$E_{1x} = -j\omega_1 A_{1x} - \frac{\partial\phi_1}{\partial x} = 0$$

Integrating over x yields

$$\phi_1(x,\alpha^+) = -j\omega_1\int_0^x A_{1x}dx' + \phi_1(0,\alpha)$$

$$= -j\omega_1\int_0^x\int_0^{x'} \frac{\partial A_{1x}}{\partial x''}\,dx''\,dx' + \phi_1(0,\alpha) \qquad (2.30)$$

The term $\phi_1(0,\alpha)$ represents the D.C. value of $\phi_1$ which is maintained at $\frac{1}{\varepsilon_o}$, as used in the static solution, for this and all other

iterations. The function $\frac{\partial A_{1x}}{\partial x}$ is found using the Lorentz condition:

$$\nabla \cdot \vec{A} = \frac{\partial A_x}{\partial x} + \frac{\partial A_y}{\partial y} + \frac{\partial A_z}{\partial z} = \frac{\partial A_x}{\partial x} + \frac{\partial A_y}{\partial y} - j\beta A_z = -j\omega\mu_o\varepsilon_o\kappa(y)\Phi$$

At $y = a^+$, the solution for $\frac{\partial A_{1x}}{\partial x}$ becomes

$$\frac{\partial A_{1x}}{\partial x} = j\beta_1 A_{oz} - \frac{\partial A_{1y}}{\partial y} - j\omega_1\mu_o\varepsilon_o\Phi_o(x,a^+) \tag{2.31}$$

After representing (2.31) as a Fourier series, substituting it into (2.30), and performing the integrations, $\Phi_1$ is expressed as

$$\Phi_1(x,a^+) = \sum_{n=1,3..}^{\infty} \frac{j\omega_1}{\omega_n^2}\left(j\beta_1 A_{ozn} - \frac{\partial A_{1yn}}{\partial y} - j\omega_1\mu_o\varepsilon_o\Phi_{on}\right)$$

$$(\cos\omega_n x - 1) + \frac{1}{\varepsilon_o} \tag{2.32}$$

The next step is to solve for the new charge density $\rho_1$. An equation must first be developed to accomodate this task.

Consider a Green's function $G_2^1$ satisfying

$$[\nabla_t^2 - (\beta_1^2 - \kappa(y)k_{o,1}^2)]\, G_2^1 = -\delta(x-x')\delta(y-y') \tag{2.33}$$

with boundary conditions

$G_2^1$ , $\kappa(y)\frac{\partial G_2^1}{\partial y}$ are continuous at $y = a$

$G_2^1$ is continuous at $y = y'$

$G_2^1 = 0$ at $y = 0, \infty$

$G_2^1 = 0$ at $x = a, -a$

Assume

$$G_2^1 = \begin{cases} \sum_{n=1,3..}^{\infty} A_n \frac{\cos\omega_n x'}{a} \sinh\omega_{2n,1} y \cos\omega_n x & 0 \leq y \leq \alpha \\ \sum_{n=1,3..}^{\infty} (B_n e^{-\omega_{1n,1} y} + C_n e^{\omega_{1n,1} y}) \frac{\cos\omega_n x'}{a} \cos\omega_n x & \alpha \leq y \leq y' \\ \sum_{n=1,3..}^{\infty} D_n \frac{\cos\omega_n x'}{a} e^{-\omega_{1n,1} y} \cos\omega_n x & y' \leq y \end{cases}$$

where

$$\omega_{1n,1} = \sqrt{\omega_n^2 \quad _{o,1} + \beta_1^2} \qquad \omega_{2n,1} = \sqrt{\omega_n^2 - \kappa k_{o,1}^2 + \beta_1^2}$$

The equations employed to solve for the unknown coefficients use the boundary condition that $G_2^1$ is continuous at $y = \alpha$, the boundary condition that $\kappa(r) \frac{\partial G_2^1}{\partial y}$ is continuous at $y = \alpha$, the boundary condition that $G_2^1$ is continuous at $y = y'$, and the integral of (2.33) over y. Thus, the equations are

$$A_n \sinh\omega_{2n,1}\alpha = B_n e^{-\omega_{1n,1}\alpha} + C_n e^{\omega_{1n,1}\alpha}$$

$$\kappa\omega_{2n,1} A_n \cosh\omega_{2n,1}\alpha = -\omega_{1n,1} B_n e^{-\omega_{1n,1}\alpha} + \omega_{1n,1} C_n e^{\omega_{1n,1}\alpha}$$

$$B_n e^{-\omega_{1n,1}y'} + C_n e^{\omega_{1n,1}y'} = D_n e^{-\omega_{1n,1}y'}$$

$$-\omega_{1n,1} D_n e^{-\omega_{1n,1}y'} - (-\omega_{1n,1} B_n e^{-\omega_{1n,1}y'} + \omega_{1n,1} C_n e^{\omega_{1n,1}y'}) = -1$$

After solving for the coefficients and letting the source point $y' = \alpha$, the solution for $G_2^1$ becomes

$$G_2^1 = \begin{cases} \displaystyle\sum_{n=1,3..}^{\infty} \frac{\cos\omega_n x' \sinh\omega_{2n,1} y}{a(\omega_{1n,1}\sinh\omega_{2n,1}\alpha + \kappa\,\omega_{2n,1}\cosh\omega_{2n,1}\alpha)} \cos\omega_n x & \alpha \geq y \\ \displaystyle\sum_{n=1,3..}^{\infty} \frac{\cos\omega_n x' \sinh\omega_{2n,1}\alpha e^{\omega_{1n,1}\alpha} e^{-\omega_{1n,1}y}}{a(\omega_{1n,1}\sinh\omega_{2n,1}\alpha + \kappa\,\omega_{2n,1}\cosh\omega_{2n,1}\alpha)} \cos\omega_n x & \alpha \leq y \end{cases} \tag{2.34}$$

Next consider the following:

$$\Phi_{1n}\left[\frac{\partial^2}{\partial y^2} - (\omega_n^2 - \kappa(y)k_{o,1}^2 + \beta_1^2)\right] G_{2n}^1 -$$

$$G_{2n}^1\left[\frac{\partial^2}{\partial y^2} - (\omega_n^2 - \kappa(y)k_{o,1}^2 + \beta_1^2)\right] \Phi_{2n}^1$$

$$= \frac{d}{dy}\left[\Phi_{1n}\frac{\partial G_{2n}^1}{\partial y} - G_{2n}^1\frac{\partial \Phi_{1n}}{\partial y}\right] = -\Phi_{1n}\delta(y-\alpha^+) + G_{2n}^1\frac{\rho_{1n}}{\varepsilon_o}\delta(y-\alpha^+)$$

Integrating over y yields

$$\Phi_{1n} \frac{\partial G^1_{2n}}{\partial y} - G^1_{2n} \frac{\partial \Phi_{1n}}{\partial y} \Bigg|_{\alpha^+}^{\infty} = - \Phi_{1n}(\alpha^+) + G^1_{2n}(\alpha^+) \frac{\rho_{1n}}{\varepsilon_o} \tag{2.35}$$

$$\Phi_{1n} \frac{\partial G^1_{2n}}{\partial y} - G^1_{2n} \frac{\partial \Phi_{1n}}{\partial y} \Bigg|_{0}^{\alpha^-} = 0 \tag{2.36}$$

Multiplying (2.36) by $\kappa$ and adding to (2.35) gives

$$G^1_{2n}\, \kappa(y) \frac{\partial \Phi_{1n}}{\partial y} \Bigg|_{\alpha^-}^{\alpha^+} = - \Phi_{1n}(\alpha^+) + G^1_{2n}(\alpha^+) \frac{\rho_{1n}}{\varepsilon_o}$$

Using (2.4)

$$G^1_{2n}(\alpha^+) \frac{\rho_{1n}}{\varepsilon_o} = \Phi_{1n}(\alpha^+) - j\omega_1(1-\kappa) G^1_{2n}\, A_{1yn}(\alpha^+) \tag{2.37}$$

Summing the Fourier components (2.37) results in ($y = \alpha^+$)

$$\sum_{n=1,3..}^{\infty} G^1_{2n} \frac{\rho_{1n}}{\varepsilon_o} \cos\omega_n x = \sum_{n=1,3..}^{\infty} \left[\Phi_{1n} - j\omega_1(1-\kappa) G^1_{2n}\, A_{1yn}\right] \cos\omega_n x \tag{2.38}$$

Equation (2.38) is thus equivalent to

$$2\int_0^1 G^1_2 \frac{\rho_1}{\varepsilon_o}\, dx' = \Phi_1 - j\omega_1(1-\kappa) \sum_{n=1,3..}^{\infty} G^1_{2n}\, A_{1yn} \cos\omega_n x \tag{2.39}$$

Equation (2.39) is used to solve for the charge density $\rho_1$.

The procedure in carrying out this assignment begins by substituting

(2.32) for $\Phi_1$. $A_{1yn}$ is substituted by the equivalent Fourier component in (2.28). $G^1_{2n}$ is substituted, letting $y = \alpha$, by

$$G^1_{2n} = \frac{\sinh\omega_{2n,1}\alpha}{\omega_{1n,1}\sinh\omega_{2n,1}\alpha + \kappa\omega_{2n,1}\cosh\omega_{2n,1}\alpha}$$

As done previously, $\rho_1$ is represented by the form

$$\rho_1(x') = \frac{q_o + q_1x'^2 + q_2x'^4 + q_3x'^6}{\sqrt{1 - x'^2}}$$

The integral on the left side of (2.39) is carried out by making a substitution for $G^1_2$. This substitution allows a rapid and accurate convergence of the integral. The substitution is as follows:

$$\begin{aligned}
2\int_0^1 G^1_2\rho_1 dx' &= 2\int_0^1 G^o_2\rho_1 dx' + 2\int_0^1 (G^1_2 - G^o_2)\rho_1 dx' \\
&= 2\int_0^1 G^o_2\rho_1 dx' + 2\int_0^1 \sum_{n=1,3..}^{\infty} (G^1_{2n} - G^o_{2n})\rho_1 dx' \cos\omega_n x \\
&= 2\int_0^1 G^o_2\rho_1 dx' + \\
&\quad 2\int_0^1 \sum_{n=1,3..}^{\infty} \left[\frac{\cos\omega_n x' \sinh\omega_{2n,1}\alpha}{a(\omega_{1n,1}\sinh\omega_{2n,1}\alpha + \kappa\omega_{2n,1}\cosh\omega_{2n,1}\alpha)} - \right. \\
&\quad \left. \frac{\cos\omega_n x' \sinh\omega_n\alpha}{a\omega_n(\sinh\omega_n\alpha + \kappa\cosh\omega_n\alpha)}\right] \rho_1 dx' \cos\omega_n x \\
&= 2\int_0^1 G^o_2\rho_1 dx' + 2\sum_{n=1,3..}^{\infty} C_n \int_0^1 \rho_1 \cos\omega_n x' dx' \cos\omega_n x \qquad (2.40)
\end{aligned}$$

The integrals involved in solving for $2\int_0^1 G_2^o \rho_1 dx'$ are identical as the closed form approximation previously solved for in the static solution. As n gets large, the value of $C_n$ quickly approaches zero which facilitates a rapid convergence of the Fourier series summation. The integrals involved in the summation are evaluated using a Simpson's Rule approximation.

The charge density coefficients are determined using (2.40) in conjunction with (2.39), point matching at $x = \frac{1}{4}$, $\frac{1}{2}$, $\frac{3}{4}$, and 1, and solving the four resulting equations for the coefficients.

The current density $J_{1z}$ is determined by first solving for a relative current density $J_{1z,r}$ and then properly scaling it to give $J_{1z}$. $J_{1z,r}$ has the familiar form

$$J_{1z,r}(x') = \frac{I_o + I_1 x'^2 + I_2 x'^4 + I_3 x'^6}{\sqrt{1 - x'^2}}$$

From (2.3),

$$[\nabla_t^2 - (\beta_1^2 - \kappa(y) k_{o,1}^2)] A_{1z,r} = - \mu_o J_{1z,r}$$

where $A_{1z,r}$ is the relative value of $A_{1z}$ which is also correctly scaled at a later point. Therefore, the solution of $J_{1z,r}$ satisfies the equation

$$2\int_0^1 G_1^1 J_{1z,r} dx' = \frac{A_{1z,r}}{\mu_o} \qquad (2.41)$$

The Green's function $G_1^1$ is next solved for. $G_1^1$ must satisfy the equation

$$[\nabla_t^2 - (\beta_1^2 - \kappa(y)k_{o,1}^2)]\, G_1^1 = -\,\delta(x-x')\delta(y-y') \qquad (2.42)$$

with boundary conditions

$G_1^1$ and $\dfrac{\partial G_1^1}{\partial y}$ are continuous at $y = \alpha$

$G_1^1$ is continuous at $y = y'$

$G_1^1 = 0$ at $y = 0, \infty$

$G_1^1 = 0$ at $x = a, -a$

Assume that $(y' = \alpha)$

$$G_1^1 = \begin{cases} \displaystyle\sum_{n=1,3..}^{\infty} A_n \frac{\cos\omega_n x'}{a} \sinh\omega_{2n,1} y \cos\omega_n x & y \leq \alpha \\ \displaystyle\sum_{n=1,3..}^{\infty} B_n \frac{\cos\omega_n x'}{a} e^{-\omega_{1n,1} y} \cos\omega_n x & y \geq \alpha \end{cases}$$

where

$$\omega_{1n,1} = \sqrt{\omega_n^2 - k_{o,1}^2 + \beta_1^2} \qquad \omega_{2n,1} = \sqrt{\omega_n^2 - \kappa k_{o,1}^2 + \beta_1^2}$$

The unknown coefficients, $A_n$ and $B_n$, are found using equations satisfying the boundary condition that $G_1^1$ is continuous at $y = \alpha$ and the integral of (2.42) over y. Thus,

$$A_n \sinh\omega_{2n,1}\alpha = B_n e^{-\omega_{1n,1}\alpha}$$

$$- \omega_{1n,1} B_n e^{-\omega_{1n,1}\alpha} - \omega_{2n,1} A_n \cosh\omega_{2n,1}\alpha = -1$$

The coefficients are readily found to be

$$A_n = \frac{1}{\omega_{1n,1}\sinh\omega_{2n,1}\alpha + \omega_{2n,1}\cosh\omega_{2n,1}\alpha}$$

$$B_n = \frac{\sinh\omega_{2n,1}\, e^{\omega_{1n,1}\alpha}}{\omega_{1n,1}\sinh\omega_{2n,1}\alpha + \omega_{2n,1}\cosh\omega_{2n,1}\alpha}$$

Therefore, $G_1^1$ is expressed completely as follows:

$$G_1^1 = \begin{cases} \sum_{n=1,3..}^{\infty} \dfrac{\cos\omega_n x' \sinh\omega_{2n,1} y}{a(\omega_{1n,1}\sinh\omega_{2n,1}\alpha + \omega_{2n,1}\cosh\omega_{2n,1}\alpha)} \cos\omega_n x & y \leq \alpha \\ \sum_{n=1,3..}^{\infty} \dfrac{\cos\omega_n x' \sinh\omega_{2n,1}\alpha e^{\omega_{1n,1}\alpha} e^{-\omega_{1n,1}}}{a(\omega_{1n,1}\sinh\omega_{2n,1}\alpha + \omega_{2n,1}\cosh\omega_{2n,1}\alpha)} \cos\omega_n x & y \geq \alpha \end{cases} \tag{2.43}$$

In (2.43) we let $y = \alpha$ and substitute this into (2.41). The integral $2\int_0^1 G_1^1 J_{1z,r}\, dx'$ is carried out by making a substitution for $G_1^1$ that gives a simpler evaluation. This substitution is as follows:

$$2\int_0^1 G_1^1 J_{1z,r}\,dx' = 2\int_0^1 G_1^o J_{1z,r}\,dx' + 2\int_0^1 (G_1^1 - G_1^o) J_{1z,r}\,dx'$$

$$= 2\int_0^1 G_1^o J_{1z,r}\,dx' + 2\sum_{n=1,3..}^{\infty} \int_0^1 (G_{1n}^1 - G_{1n}^o) J_{1z,r}\,dx' \cos\omega_n x$$

$$= 2\int_0^1 G_1^o J_{1z,r}\,dx' +$$

$$2\sum_{n=1,3..}^{\infty} \int_0^1 \left[ \frac{\sinh\omega_{2n,1}\alpha}{a(\omega_{1n,1}\sinh\omega_{2n,1}\alpha + \omega_{2n,1}\cosh\omega_{2n,1}\alpha)} - \frac{\sinh\omega_n\alpha e^{-\omega_n\alpha}}{a\omega_n} \right] J_{1z,r}\cos\omega_n x'\,dx'\cos\omega_n x$$

$$= 2\int_0^1 G_1^o J_{1z,r}\,dx' + 2\sum_{n=1,3..}^{\infty} \int_0^1 D_n J_{1z,r}\cos\omega_n x'\,dx'\cos\omega_n x$$

The integrals involved in solving $2\int_0^1 G_1^o J_{1z,r}\,dx'$ are identical as the closed form approximation previously solved for in the static solution. As n gets large, the value of $D_n$ quickly approaches zero which enhances the rapid convergence of the Fourier series summation. The integrals involved in the summation are solved by using a Simpson's Rule approximation.

The value of $A_{1z,r}$ is chosen to equal $\Phi_1$ displayed in (2.32). This selection of $A_{1z,r}$ accomodates a simple solution to $J_{1z,r}$ and is shown to be a completely arbitrary specification.

The solution of $J_{1z,r}$ is carried out by performing the aforementioned substitutions, creating four equations by point matching at $x = \frac{1}{4}$ , $\frac{1}{2}$ , $\frac{3}{4}$ , and 1, and and finally solving these equations

for the four unknown coefficients. Thus, $J_{1z,r}$ is now determined.

The new and more accurate propagation constant $\beta_2$ and characteristic impedance $Z_{c1}$ are next determined. The first step in accomplishing this is to calculate the total charge $q_{1T}$ and total relative current $I_{1T,r}$ on the microstrip. These tasks are carried out using the integrals

$$q_{1T} = 2\int_0^1 \rho_1(x')dx' = \pi(q_o + \frac{1}{2}\, q_1 + \frac{3}{8}\, q_2 + \frac{5}{16}\, q_3)$$

$$I_{1T,r} = 2\int_0^1 J_{1z,r}(x')dx' = \pi(I_o + \frac{1}{2}\, I_1 + \frac{3}{8}\, I_2 + \frac{5}{16}\, I_3)$$

in conjunction with the substitution $x' = \sin\theta'$. On the stripline,

$$E_{1z} = -j\omega_1 A_{1z} + j\beta_2 \Phi_1 = 0 \tag{2.44}$$

As has been previously defined,

$$A_{1z} = KA_{1z,r} \tag{2.45}$$

where K is the scaling factor. By virtue of (2.41), it is seen that

$$J_{1z} = KJ_{1z,r} \tag{2.46}$$

Combining (2.44) with (2.45) yields

$$\omega_1 K A_{1z,r} = \beta_2 \Phi_1 \tag{2.47}$$

Using the previously chosen value

$$A_{1z,r} = \Phi_1$$

(2.47) becomes

$$K = \frac{\beta_2}{\omega_1} \tag{2.48}$$

In the same fashion as (2.17), upon integrating the continuity equation over x, it is required that

$$\beta_2 I_{1T} = \omega_1 q_{1T} \tag{2.49}$$

Substituting (2.46) and (2.48) into (2.49) finally results in

$$\beta_2 = \omega_1 \sqrt{\frac{q_{1T}}{I_{1T,r}}} \tag{2.50}$$

This is the new and more accurate value of the propagation constant. Using $\beta_2$, a value of $\kappa_{eff,1}$ is solved:

$$\kappa_{eff,1} = \left(\frac{\beta_2}{k_{o,1}}\right)^2$$

The final entity calculated is $Z_{c1}$ at the given frequency $\omega_1$.

$Z_{cl}$ is defined as the ratio of the line integral of $E_{1y}$ along $x = 0$, from 0 to $\alpha$ along y, divided by the total z directed current $I_{1T}$ on the microstrip. This line integral, which is the total potential difference between the ground plane and the microstrip, is found from

$$V_{1T} = \int_0^{\alpha} \vec{E} \cdot d\vec{y} = -\int_0^{\alpha} (-j\omega_1 \vec{A}_1 - \nabla\Phi_1) \cdot d\vec{y}$$

$$= \int_0^{\alpha} (j\omega_1 A_{1y} + \frac{\partial \Phi_1}{\partial y}) dy = \Phi_1(\alpha) + j\omega_1 \int_0^{\alpha} A_{1y} dy$$

The total current is solved using the previously determined $\beta_2$ and $I_{1T,r}$.

$$I_{1T} = KI_{1T,r} = \frac{\beta_2}{\omega_1} I_{1T,r}$$

Thus,

$$Z_{cl} = \frac{V_{1T}}{I_{1T}} = \frac{\omega_1(\Phi_1(\alpha) + j\omega_1 \int_0^{\alpha} A_{1y} dy)}{\beta_2 I_{1T,r}} \qquad (2.51)$$

The expression for $\int_0^{\alpha} A_{1y} dy$ is easily evaluated using the equation for $A_{1y}$ and letting $0 \leq y \leq \alpha$.

A property that should be noted is the independence of the final results of $\beta_2$ and $Z_{cl}$ on the assigned value to $A_{1z,r}$. This independence is evidenced in (2.47) where any assigned value of $A_{1z,r}$ would just adjust the value of K. The chosen value of $\Phi_1$

obviously simplifies the subsequent calculations. Once the value of $\beta_2$ is determined, the scaling constant K can then be easily calculated.

Before the next iteration process begins for calculations of new values of $\beta$ and $Z_c$ at a new or same frequency, certain procedures are taken. The values of the current density coefficients are properly scaled by using (2.46) and (2.48). This yields

$$J_{1z} = \frac{\beta_2}{\omega_1} J_{1z,r}$$

The Fourier coefficients of $J_{1z}$ and $\rho_1$ are calculated using the equations

$$J_{1zn} = \frac{2}{a}\int_0^1 J_{1z}(x')\cos\omega_n x' dx'$$

$$\rho_{1n} = \frac{2}{a}\int_0^1 \rho_1(x')\cos\omega_n x' dx'$$

along with the substitution $x' = \sin\theta'$ and a Simpson's Rule approximation. An adequate quantity of these coefficients should be calculated for proper convergence of future calculations using them.

An equation for $A_{1z}$ is determined using the properly scaled version of (2.41). We begin with

$$A_{1z} = 2\mu_o\int_0^1 G_1^1 J_{1z} dx' = \sum_{n=1,3..}^{\infty} \mu_o G_{1n}^1 J_{1n}\cos\omega_n x$$

Therefore, at $y = \alpha$,

$$A_{1z}(x,\alpha) = \sum_{n=1,3..}^{\infty} \frac{\mu_o J_{1n} \sinh\omega_{2n,1}}{\omega_{1n,1}\sinh\omega_{2n,1}\alpha + \omega_{2n,1}\cosh\omega_{2n,1}\alpha} \cos\omega_n x \qquad (2.52)$$

where

$$\omega_{1n,1} = \sqrt{\omega_n^2 - k_{o,1}^2 + \beta_1^2} \qquad \omega_{2n,1} = \sqrt{\omega_n^2 - \kappa k_{o,1}^2 + \beta_1^2}$$

The Fourier series of $\Phi_1$ is next determined. Stating (2.39) in complete Fourier series notation,

$$\Phi_1(x,\alpha) = \frac{1}{\varepsilon_o} \sum_{n=1,3..}^{\infty} G_{2n}^1 \rho_{1n} \cos\omega_n x - j\omega_1(\kappa-1) \sum_{n=1,3..}^{\infty} G_{2n}^1 A_{1yn} \cos\omega_n x \qquad (2.53)$$

Upon substituting the previously solved Fourier coefficients into (2.53), the final result is

$$\Phi_1(x,\alpha) = \sum_{n=1,3..}^{\infty} \frac{(\rho_{1n} - j\omega_1\varepsilon_o(\kappa-1)A_{1yn})}{\varepsilon_o(\omega_{1n,1}\sinh\omega_{2n,1}\alpha + \kappa\omega_{2n,1}\cosh\omega_{2n,1}\alpha)} \cos\omega_n x \qquad (2.54)$$

At this point in the analysis, the 1 level iteration has been completed. All entities which are required for the next iteration have been solved for. The next iteration may fulfill one of two tasks: it may improve the values of $\beta$ and $Z_c$ by solving all of the equations again with $\beta_2$ replacing $\beta_1$ and keeping the frequency constant at $\omega_1$ or it may solve for new values of $\beta$ and $Z_c$ by increasing the frequency to a higher $\omega_2$ and using the approximate $\beta_2$ at this

new frequency. The iteration repeats at the location of the solution of $A_{1y}$ with all enumerated iteration levels increased by 1 and continues until the Fourier solution of the new $\Phi_2$ function is found. This iteration process may continue infinitely with the frequency continuously increasing. Figure 2.2 summarizes and depicts the order of solution of the field entities in the Perturbation-Iteration Theory.

This is the conclusion of the Perturbation-Iteration Method. Chapter 3 presents data of various entities calculated from applying the theory to different structures. It also compares certain data to established theoretical and experimental data to exhibit the validity and accuracy of this technique.

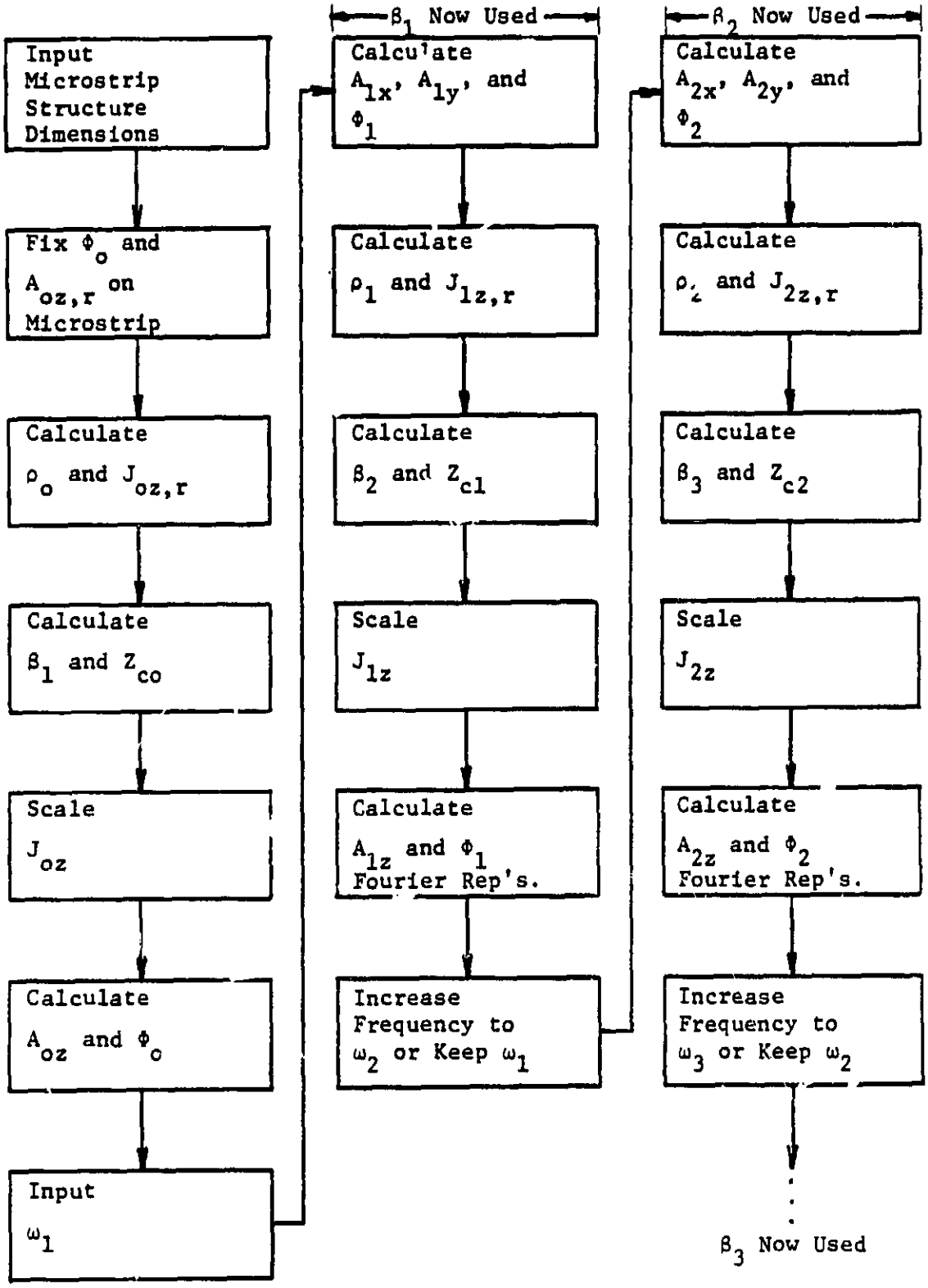


Figure 2.2 Block Diagram of Perturbation-Iteration Method.

## CHAPTER 3

## CALCULATIONS AND RESULTS

The Perturbation-Iteration Method was used to find the effective dielectric constant and characteristic impedance for various combinations of $\kappa$ and dimension ratios $\frac{W}{H}$ over a range of frequencies. In each instance, the dimension A equals 10W or 10H, whichever is larger and H = 1mm. This gives validity to the assumption of using the side ground walls. The data is organized on the following in tables which list the computed values of $\kappa_{eff}$ and $Z_c$. Each table represents a specified combination of $\kappa$ and $\frac{W}{H}$ ratios of the stripline structure over a range of frequencies. Graphs of $\kappa_{eff}$ and $Z_c$ are displayed to interpolate data between calculated points and are organized with all combinations of the $\frac{W}{H}$ ratios at each value of $\kappa$ shown on each graph. These graphs are labelled as Fig's. 2.3 - 2.14.

The evaluation of the accuracy of the numerical procedure used in this thesis is difficult because of the lack of good data to compare the results with. Kuester and Chang have noted that there are large variations in computed values for the effective dielectric constant as presented by different authors [18]. This lack of data has thus limited the verification of the accuracy of the numerical procedure used to that of a few special cases.

Figure 2.15 illustrates a graph which compares data calculated from the Perturbation-Iteration Method with data taken from the

following sources: a fullwave analysis by T. Itoh and R. Mittra [14]. a dispersion model analysis by W. J. Getsinger [10], an improved analysis of [10] by T. C. Edwards and R. P. Owens [19], and experimental data [19]. The Perturbation-Iteration Method compares very favorably with all of this previous work for the special case of $\kappa = 10.15$ and three values of $\frac{W}{H}$. In the Table accompanying the figure 2W and H are given in millimeters. In Fig. 2.11 the results are compared with computations made by Jansen for $\kappa = 9.9$. Jansen's results were read from the graphical data presented and multiplied by 1.01 to make the results equivalent to those obtained for $\kappa = 10$ using the Perturbation-Iteration Method. The two sets of results compare very well for $\frac{W}{H} = 1$. For $\frac{W}{H} = 0.5$ and 0.25 Jansen's results appear to be approximately 1% higher (this conclusion is subject to the error in reading data from the curves and may not be correct). The effective dielectric constant at zero frequency, as obtained from Wheeler's approximate theory, is also shown for $\frac{W}{H} = 0.5$ and 0.25 in Fig. 2.11. These values lie below those calculated using the Perturbation-Iteration Method and seem to suggest that the latter are most likely very accurate.

Examination of the tabulated data shows that for wide strips and large dielectric constants at higher frequencies the numerical procedure used converges to a value for the effective dielectric constant that is larger than that of the substrate. This is a clear indication that a 4 term expansion of the charge and current distribution along with point matching at 4 points on the strip

in the interval 0 to 1 is inadequate for wide strips and large dielectric constants. The region where the results become inaccurate are mostly in regions outside of those of practical interest. For example with a substrate having $\kappa = 10$ a substrate thickness of 0.25mm would be appropriate in which case the 5 Ghz data in Fig. 2.11 becomes 20 Ghz data (the frequency scale must be multiplied by 4 because of the reduced height).

It can be seen that some of the dispersion curves for the larger values of $\frac{W}{H}$ in Fig's. 2.5, 2.7, 2.9, 2.11, and 2.14 show a second inflection point. This marks the region where the numerical solution begins to become inaccurate. The boundary of this region has been marked by a broken curve in these figures. The data beyond these boundaries is not believed to be accurate.

The limitations noted above are not due to any failure of the Perturbation-Iteration Method but is due to the over simplified numerical procedure adopted to solve the integral equations. By using Galerkin's method or the method of least squares along with additional terms in the expansions for the charge and current distributions results that are valid over a wider range of parameter values could be obtained.

In the region where the results become inaccurate the calculated current and charge distributions no longer have the expected behavior. This is seen in Fig's. 2.16 - 2.19 where graphs of the charge and current are displayed for sufficiently accurate and inaccurate expansions. The graphs only indicate one-half of the micro-

strip as the entities are symmetric around the origin. The Perturbation-Iteration Method is generally valid for values of $\kappa_{eff}$ up to approximately $.9\kappa$. The range of frequencies where $\kappa_{eff}$ is valid also contains valid values of $Z_c$.

TABLE 1

$\kappa = 2$ $\quad H = 1mm \quad$ $\frac{W}{H} = .25$

| f(GHz) | 0 | 1 | 2 | 4 | 8 | 12 | 15 | 20 | 30 | | | |
|---|---|---|---|---|---|---|---|---|---|---|---|---|
| $\kappa_{eff}$ | 1.60 | 1.60 | 1.60 | 1.61 | 1.61 | 1.62 | 1.63 | 1.65 | 1.67 | | | |
| $Z_c$ | 130.3 | 130.3 | 130.4 | 130.8 | 132.2 | 134.3 | 136.3 | 140.0 | 147.3 | | | |

TABLE 2

$\kappa = 2$ $\quad H = 1mm \quad$ $\frac{W}{H} = .5$

| f(GHz) | 0 | 1 | 2 | 4 | 8 | 12 | 15 | 20 | 30 | | | |
|---|---|---|---|---|---|---|---|---|---|---|---|---|
| $\kappa_{eff}$ | 1.63 | 1.63 | 1.63 | 1.64 | 1.64 | 1.65 | 1.67 | 1.69 | 1.73 | | | |
| $Z_c$ | 97.5 | 97.5 | 97.6 | 98.0 | 99.5 | 101.8 | 103.8 | 107.7 | 116.2 | | | |

TABLE 3

$\kappa = 2$ $\quad H = 1mm \quad$ $\frac{W}{H} = 1$

| f(GHz) | 0 | 1 | 2 | 4 | 8 | 12 | 15 | 20 | 30 | | | |
|---|---|---|---|---|---|---|---|---|---|---|---|---|
| $\kappa_{eff}$ | 1.69 | 1.69 | 1.69 | 1.70 | 1.71 | 1.73 | 1.75 | 1.76 | 1.80 | | | |
| $Z_c$ | 68.1 | 68.2 | 68.3 | 68.9 | 70.8 | 73.4 | 75.8 | 79.9 | 90.6 | | | |

TABLE 4

$\kappa = 2$ $\quad H = 1mm \quad$ $\frac{W}{H} = 2$

| f(GHz) | 0 | 1 | 2 | 4 | 8 | 12 | 15 | 20 | 30 | | | |
|---|---|---|---|---|---|---|---|---|---|---|---|---|
| $\kappa_{eff}$ | 1.76 | 1.76 | 1.76 | 1.77 | 1.79 | 1.81 | 1.83 | 1.87 | 2.01 | | | |
| $Z_c$ | 43.4 | 43.5 | 43.7 | 44.5 | 47.1 | 50.8 | 54.6 | 63.0 | 93.6 | | | |

TABLE 5

$\kappa = 2$ $\quad H = 1mm \quad$ $\frac{W}{H} = 3$

| f(GHz) | 0 | 1 | 2 | 4 | 8 | 12 | 15 | 20 | | | | |
|---|---|---|---|---|---|---|---|---|---|---|---|---|
| $\kappa_{eff}$ | 1.80 | 1.80 | 1.81 | 1.82 | 1.84 | 1.84 | 1.91 | 2.00 | | | | |
| $Z_c$ | 32.2 | 32.3 | 32.5 | 33.5 | 36.9 | 42.7 | 49.3 | 67.6 | | | | |

TABLE 6

$\kappa = 2$ $\quad H = 1mm \quad$ $\frac{W}{H} = 4$

| f(GHz) | 0 | 1 | 2 | 4 | 8 | 12 | 15 | 17 | 19 | 20 | | |
|---|---|---|---|---|---|---|---|---|---|---|---|---|
| $\kappa_{eff}$ | 1.83 | 1.83 | 1.83 | 1.85 | 1.88 | 1.93 | 2.00 | 2.07 | 2.20 | 2.30 | | |
| $Z_c$ | 25.6 | 25.8 | 26.1 | 27.3 | 31.8 | 40.7 | 52.9 | 66.0 | 86.6 | 101.6 | | |

TABLE 7

$\kappa = 2$ $H = 1mm$ $\frac{W}{H} = 5$

| f(GHz) | 0 | 1 | 2 | 4 | 8 | 12 | 15 | | | | | |
|---|---|---|---|---|---|---|---|---|---|---|---|---|
| $\kappa_{eff}$ | 1.85 | 1.85 | 1.85 | 1.87 | 1.91 | 2.00 | 2.16 | | | | | |
| $Z_c$ | 21.4 | 21.5 | 21.9 | 23.3 | 29.3 | 43.5 | 68.9 | | | | | |

TABLE 8

$\kappa = 6$ $H = 1mm$ $\frac{W}{H} = .25$

| f(GHz) | 0 | 1 | 2 | 4 | 8 | 12 | 15 | 20 | 30 | | | |
|---|---|---|---|---|---|---|---|---|---|---|---|---|
| $\kappa_{eff}$ | 2.79 | 2.79 | 2.79 | 2.81 | 2.85 | 2.91 | 2.95 | 2.98 | 3.03 | | | |
| $Z_c$ | 98.8 | 98.8 | 99.0 | 99.6 | 101.9 | 104.9 | 107.3 | 110.6 | 118.8 | | | |

TABLE 9

$\kappa = 4$ $H = 1$ mm $\frac{W}{H} = .5$

| f(GHz) | 0 | 1 | 2 | 4 | 8 | 12 | 15 | 20 | 30 | | | |
|---|---|---|---|---|---|---|---|---|---|---|---|---|
| $\kappa_{eff}$ | 2.88 | 2.88 | 2.89 | 2.91 | 2.97 | 3.04 | 3.10 | 3.15 | 3.24 | | | |
| $Z_c$ | 73.4 | 73.4 | 73.6 | 74.3 | 76.6 | 79.7 | 82.3 | 86.0 | 94.7 | | | |

TABLE 10

$\kappa = 4$ $H = 1$ mm $\frac{W}{H} = 1$

| f(GHz) | 0 | 1 | 2 | 4 | 8 | 12 | 15 | 20 | 30 | | | |
|---|---|---|---|---|---|---|---|---|---|---|---|---|
| $\kappa_{eff}$ | 3.06 | 3.06 | 3.07 | 3.10 | 3.19 | 3.25 | 3.31 | 3.41 | 3.68 | | | |
| $Z_c$ | 50.7 | 50.8 | 51.0 | 51.8 | 54.4 | 57.4 | 60.1 | 65.5 | 79.7 | | | |

TABLE 11

$\kappa = 4$ $H = 1\,mm$ $\frac{W}{H} = 2$

| f(GHz) | 0 | 1 | 2 | 4 | 8 | 12 | 15 | 20 | 25 | 27.5 | | |
|---|---|---|---|---|---|---|---|---|---|---|---|---|
| $\kappa_{eff}$ | 3.26 | 3.27 | 3.29 | 3.33 | 3.44 | 3.57 | 3.69 | 4.00 | 4.51 | 4.94 | | |
| $Z_c$ | 31.9 | 32.0 | 32.4 | 33.4 | 36.7 | 41.9 | 47.3 | 60.7 | 82.0 | 97.1 | | |

TABLE 12

$\kappa = 4$ $H = 1\,mm$ $\frac{W}{H} = 3$

| f(GHz) | 0 | 1 | 2 | 4 | 8 | 12 | 15 | 17.5 | 19 | 20 | | |
|---|---|---|---|---|---|---|---|---|---|---|---|---|
| $\kappa_{eff}$ | 3.38 | 3.40 | 3.42 | 3.48 | 3.62 | 3.86 | 4.17 | 4.61 | 5.06 | 5.48 | | |
| $Z_c$ | 23.5 | 23.6 | 24.0 | 25.3 | 30.1 | 39.2 | 51.2 | 67.4 | 81.3 | 92.8 | | |

**TABLE 13**

$\kappa = 4$ $\quad H = 1\,mm$ $\quad \frac{W}{H} = 4$

| f(GHz) | 0 | 1 | 2 | 4 | 8 | 12 | 13.5 | 15 | | | | |
|---|---|---|---|---|---|---|---|---|---|---|---|---|
| $\kappa_{eff}$ | 3.47 | 3.48 | 3.51 | 3.58 | 3.79 | 4.27 | 4.66 | 5.37 | | | | |
| $Z_c$ | 18.6 | 18.8 | 19.2 | 20.8 | 27.7 | 45.0 | 57.7 | 77.1 | | | | |

**TABLE 14**

$\kappa = 4$ $\quad H = 1mm$ $\quad \frac{W}{H} = 5$

| f(GHz) | 0 | 1 | 2 | 4 | 6 | 8 | 10 | 12 | | | | |
|---|---|---|---|---|---|---|---|---|---|---|---|---|
| $\kappa_{eff}$ | 3.53 | 3.55 | 3.58 | 3.65 | 3.78 | 3.98 | 4.34 | 5.26 | | | | |
| $Z_c$ | 15.5 | 15.7 | 16.2 | 18.1 | 21.8 | 28.2 | 40.3 | 65.8 | | | | |

TABLE 15

$\kappa = 6$ $H = 1mm$ $\frac{W}{H} = .25$

| f(GHz) | 0 | 1 | 2 | 4 | 8 | 12 | 15 | 20 | 30 | | | |
|---|---|---|---|---|---|---|---|---|---|---|---|---|
| $\kappa_{eff}$ | 3.97 | 3.97 | 3.98 | 4.02 | 4.12 | 4.23 | 4.27 | 4.32 | 4.45 | | | |
| $Z_c$ | 82.8 | 82.8 | 83.0 | 83.8 | 86.4 | 89.5 | 91.5 | 95.3 | 105.9 | | | |

TABLE 16

$\kappa = 6$ $H = 1mm$ $\frac{W}{H} = .5$

| f(GHz) | 0 | 1 | 2 | 4 | 8 | 12 | 15 | 20 | 30 | | | |
|---|---|---|---|---|---|---|---|---|---|---|---|---|
| $\kappa_{eff}$ | 4.12 | 4.13 | 4.14 | 4.19 | 4.33 | 4.49 | 4.55 | 4.64 | 4.87 | | | |
| $Z_c$ | 61.3 | 61.4 | 61.6 | 62.5 | 65.1 | 68.4 | 70.6 | 74.7 | 85.0 | | | |

TABLE 17

$\kappa = 6$ $H = 1mm$ $\frac{W}{H} = .1$

| f(GHz) | 0 | 1 | 2 | 4 | 8 | 12 | 15 | 20 | 25 | 27.5 | | |
|---|---|---|---|---|---|---|---|---|---|---|---|---|
| $\kappa_{eff}$ | 4.42 | 4.43 | 4.45 | 4.53 | 4.69 | 4.83 | 4.9( | 5.21 | 5.53 | 5.73 | | |
| $Z_c$ | 42.2 | 42.3 | 42.6 | 43.5 | 46.2 | 49.6 | 52.7 | 58.9 | 66.4 | 70.6 | | |

TABLE 18

$\kappa = 6$ $H = 1mm$ $\frac{W}{H} = .2$

| f(GHz) | 0 | 1 | 2 | 4 | 8 | 12 | 15 | 20 | 22.5 | | | |
|---|---|---|---|---|---|---|---|---|---|---|---|---|
| $\kappa_{eff}$ | 4.76 | 4.78 | 4.82 | 4.92 | 5.16 | 5.48 | 5.84 | 6.78 | 7.59 | | | |
| $Z_c$ | 26.4 | 26.6 | 26.9 | 28.1 | 32.0 | 38.4 | 45.5 | 63.8 | 77.3 | | | |

TABLE 19

$\kappa = 6$ $H = 1\,mm$ $\frac{W}{H} = .3$

| f(GHz) | 0 | 1 | 2 | 4 | 8 | 12 | 15 | | | | | |
|---|---|---|---|---|---|---|---|---|---|---|---|---|
| $\kappa_{eff}$ | 4.96 | 4.99 | 5.04 | 5.17 | 5.54 | 6.25 | 7.44 | | | | | |
| $Z_c$ | 19.4 | 19.6 | 20.0 | 21.5 | 27.5 | 40.4 | 59.7 | | | | | |

TABLE 20

$\kappa = 6$ $H = 1mm$ $\frac{W}{H} = .4$

| f(GHz) | 0 | 1 | 2 | 4 | 6 | 8 | 10 | 12 | | | | |
|---|---|---|---|---|---|---|---|---|---|---|---|---|
| $\kappa_{eff}$ | 5.10 | 5.14 | 5.20 | 5.36 | 5.59 | 5.94 | 6.57 | 7.98 | | | | |
| $Z_c$ | 15.4 | 15.6 | 16.1 | 18.0 | 21.5 | 27.4 | 37.3 | 57.3 | | | | |

TABLE 21

$\kappa = 6$ $H = 1mm$ $\frac{W}{H} = .5$

| f(GHz) | 0 | 1 | 2 | 4 | 6 | 8 | | | | | | |
|---|---|---|---|---|---|---|---|---|---|---|---|---|
| $\kappa_{eff}$ | 5.21 | 5.25 | 5.32 | 5.51 | 5.85 | 6.51 | | | | | | |
| $Z_c$ | 12.7 | 13.0 | 13.6 | 16.0 | 21.0 | 31.3 | | | | | | |

TABLE 22

$\kappa = 8$ $H = 1mm$ $\frac{W}{H} = .05$

| f(GHz) | 0 | 1 | 2 | 4 | 8 | 12 | 15 | 20 | 25 | | | |
|---|---|---|---|---|---|---|---|---|---|---|---|---|
| $\kappa_{eff}$ | 4.89 | 4.90 | 4.91 | 4.95 | 5.06 | 5.12 | 5.15 | 5.20 | 5.2534 | | | |
| $Z_c$ | 118.0 | 118.1 | 118.3 | 119.1 | 122.0 | 124.7 | 127.0 | 131.9 | 138.8 | | | |

TABLE 23

$\kappa = 8$ $H = 1$ mm $\frac{W}{H} = .125$

| f(GHz) | 0 | 1 | 2 | 4 | 8 | 12 | 15 | 17.5 | 20 | 22.5 | 25 | |
|---|---|---|---|---|---|---|---|---|---|---|---|---|
| $\kappa_{eff}$ | 5.01 | 5.01 | 5.03 | 5.08 | 5.22 | 5.31 | 5.35 | 5.38 | 5.42 | 5.45 | 5.49 | |
| $Z_c$ | 92.1 | 92.2 | 92.4 | 93.3 | 96.0 | 98.8 | 101.1 | 103.2 | 105.7 | 108.6 | 112.0 | |

TABLE 24

$\kappa = 8$ $H = 1$ mm $\frac{W}{H} = .25$

| f(GHz) | 0 | 1 | 2 | 4 | 8 | 12 | 15 | 20 | 25 | | | |
|---|---|---|---|---|---|---|---|---|---|---|---|---|
| $\kappa_{eff}$ | 5.15 | 5.15 | 5.17 | 5.24 | 5.42 | 5.54 | 5.60 | 5.69 | 5.80 | | | |
| $Z_c$ | 72.7 | 72.7 | 73.0 | 73.9 | 76.7 | 79.5 | 81.7 | 86.1 | 91.6 | | | |

TABLE 25

$\kappa = 8$ $H = 1mm$ $\frac{W}{H} = .5$

| f(GHz) | 0 | 1 | 2 | 4 | 8 | 12 | 15 | 20 | 30 | | | |
|---|---|---|---|---|---|---|---|---|---|---|---|---|
| $\kappa_{eff}$ | 5.36 | 5.37 | 5.40 | 5.49 | 5.73 | 5.93 | 6.01 | 6.17 | 6.63 | | | |
| $Z_c$ | 53.8 | 53.9 | 54.1 | 55.0 | 57.9 | 61.0 | 63.3 | 67.9 | 79.0 | | | |

TABLE 26

$\kappa = 8$ $H = 1mm$ $\frac{W}{H} = 1$

| f(GHz) | 0 | 1 | 2 | 4 | 8 | 12 | 15 | 20 | 25 | | | |
|---|---|---|---|---|---|---|---|---|---|---|---|---|
| $\kappa_{eff}$ | 5.77 | 5.79 | 5.84 | 5.97 | 6.22 | 6.47 | 6.70 | 7.18 | 7.84 | | | |
| $Z_c$ | 36.9 | 37.0 | 37.3 | 38.4 | 41.2 | 44.9 | 48.3 | 55.1 | 63.3 | | | |

TABLE 27

$\kappa = 8$ $\quad H = 1mm$ $\quad \frac{W}{H} = 2$

| f(GHz) | 0 | 1 | 2 | 4 | 8 | 12 | 15 | 17.5 | | | | |
|---|---|---|---|---|---|---|---|---|---|---|---|---|
| $\kappa_{eff}$ | 6.25 | 6.29 | 6.36 | 6.53 | 6.94 | 7.57 | 8.31 | 9.20 | | | | |
| $Z_c$ | 23.1 | 23.2 | 23.6 | 24.9 | 29.3 | 36.9 | 45.7 | 55.7 | | | | |

TABLE 28

$\kappa = 8$ $\quad H = 1mm$ $\quad \frac{W}{H} = 3$

| f(GHz) | 0 | 1 | 2 | 4 | 8 | 12 | 13.5 | | | | | |
|---|---|---|---|---|---|---|---|---|---|---|---|---|
| $\kappa_{eff}$ | 6.54 | 6.59 | 6.68 | 6.90 | 7.60 | 9.23 | 10.57 | | | | | |
| $Z_c$ | 16.9 | 17.1 | 17.6 | 19.3 | 26.4 | 43.8 | 55.6 | | | | | |

TABLE 29

$\kappa = 10$ $H = 1mm$ $\frac{W}{H} = .05$

| f(GHz) | 0 | 1 | 2 | 4 | 8 | 12 | 15 | 20 | | | | |
|---|---|---|---|---|---|---|---|---|---|---|---|---|
| $\kappa_{eff}$ | 6.00 | 6.01 | 6.02 | 6.08 | 6.24 | 6.30 | 6.35 | 6.42 | | | | |
| $Z_c$ | 106.5 | 106.6 | 106.9 | 107.9 | 110.8 | 113.5 | 116.0 | 121.8 | | | | |

TABLE 30

$\kappa = 10$ $H = 1mm$ $\frac{W}{H} = .125$

| f(GHz) | 0 | 1 | 2 | 4 | 8 | 12 | 15 | 20 | 22.5 | | | |
|---|---|---|---|---|---|---|---|---|---|---|---|---|
| $\kappa_{eff}$ | 6.15 | 6.16 | 6.18 | 6.26 | 6.46 | 6.55 | 6.61 | 6.72 | 6.78 | | | |
| $Z_c$ | 83.1 | 83.2 | 83.5 | 84.5 | 87.4 | 90.0 | 92.5 | 97.8 | 101.4 | | | |

TABLE 31

$\kappa$ = 10 H = 1mm $\frac{W}{H}$ = .25

| f(GHz) | 0 | 1 | 2 | 4 | 8 | 12 | 15 | 20 | | | | |
|---|---|---|---|---|---|---|---|---|---|---|---|---|
| $\kappa_{eff}$ | 6.33 | 6.34 | 6.37 | 6.47 | 6.73 | 6.86 | 6.95 | 7.10 | | | | |
| $Z_c$ | 65.5 | 65.6 | 65.9 | 66.9 | 69.8 | 72.5 | 74.9 | 80.0 | | | | |

TABLE 32

$\kappa$ = 10 H = 1mm $\frac{W}{H}$ = .5

| f(GHz) | 0 | 1 | 2 | 4 | 8 | 12 | 15 | 20 | 25 | | | |
|---|---|---|---|---|---|---|---|---|---|---|---|---|
| $\kappa_{eff}$ | 6.61 | 6.62 | 6.66 | 6.80 | 7.16 | 7.38 | 7.51 | 7.77 | 8.10 | | | |
| $Z_c$ | 48.5 | 48.6 | 48.8 | 49.9 | 52.8 | 55.8 | 58.3 | 63.3 | 69.0 | | | |

TABLE 33

$\kappa = 10$ H + 1 mm $\frac{W}{H} = 1$

| f(GHz) | 0 | 1 | 2 | 4 | 8 | 12 | 15 | 20 | | | | |
|---|---|---|---|---|---|---|---|---|---|---|---|---|
| $\kappa_{eff}$ | 7.13 | 7.16 | 7.23 | 7.43 | 7.78 | 8.17 | 8.53 | 9.33 | | | | |
| $Z_c$ | 33.2 | 33.3 | 33.7 | 34.8 | 37.7 | 41.7 | 45.4 | 52.8 | | | | |

TABLE 34

$\kappa = 10$ H = 1 mm $\frac{W}{H} = 2$

| f(GHz) | 0 | 1 | 2 | 4 | 8 | 12 | 15 | | | | | |
|---|---|---|---|---|---|---|---|---|---|---|---|---|
| $\kappa_{eff}$ | 7.75 | 7.80 | 7.92 | 8.17 | 8.81 | 9.89 | 11.18 | | | | | |
| $Z_c$ | 20.7 | 20.9 | 21.3 | 22.7 | 27.6 | 36.4 | 46.8 | | | | | |

TABLE 35

$\kappa = 10$ $H = 1$ mm $\frac{W}{H} = 3$

| f(GHz) | 0 | 1 | 2 | 4 | 8 | 10 | 12 | | | | | |
|---|---|---|---|---|---|---|---|---|---|---|---|---|
| $\kappa_{eff}$ | 8.12 | 8.20 | 8.34 | 8.67 | 9.83 | 10.97 | 13.20 | | | | | |
| $Z_c$ | 15.2 | 15.4 | 15.3 | 17.8 | 26.2 | 34.7 | 48.6 | | | | | |

TABLE 36

$\kappa = 12$ $H = 1$ mm $\frac{W}{H} = .05$

| f(GHz) | 0 | 1 | 2 | 4 | 8 | 12 | 15 | 20 | | | | |
|---|---|---|---|---|---|---|---|---|---|---|---|---|
| $\kappa_{eff}$ | 7.11 | 7.12 | 7.14 | 7.23 | 7.41 | 7.50 | 7.56 | 7.66 | | | | |
| $Z_c$ | 97.9 | 98.0 | 98.3 | 99.3 | 102.1 | 105.0 | 107.9 | 114.6 | | | | |

TABLE 37

$\kappa = 12$ $H = 1\,mm$ $\frac{W}{H} = .125$

| f(GHz) | 0 | 1 | 2 | 4 | 8 | 12 | 15 | 17.5 | 20 | | | |
|---|---|---|---|---|---|---|---|---|---|---|---|---|
| $\kappa_{eff}$ | 7.29 | 7.30 | 7.33 | 7.44 | 7.69 | 7.81 | 7.89 | 7.96 | 8.04 | | | |
| $Z_c$ | 76.4 | 76.5 | 76.7 | 77.8 | 80.6 | 83.4 | 86.1 | 88.9 | 92.3 | | | |

TABLE 38

$\kappa = 12$ $H = 1mm$ $\frac{W}{H} = .25$

| f(GHz) | 0 | 1 | 2 | 4 | 8 | 12 | 15 | 17.5 | 20 | | | |
|---|---|---|---|---|---|---|---|---|---|---|---|---|
| $\kappa_{eff}$ | 7.50 | 7.52 | 7.56 | 7.71 | 8.04 | 8.20 | 8.31 | 8.41 | 8.52 | | | |
| $Z_c$ | 60.2 | 60.3 | 60.6 | 61.6 | 64.5 | 67.3 | 69.9 | 72.5 | 75.6 | | | |

TABLE 39

$\kappa = 12$ $H = 1mm$ $\frac{W}{H} = .5$

| f(GHz) | 0 | 1 | 2 | 4 | 8 | 10 | 12 | 13.5 | 15 | 17.5 | 20 | 22.5 |
|---|---|---|---|---|---|---|---|---|---|---|---|---|
| $\kappa_{eff}$ | 7.85 | 7.87 | 7.93 | 8.13 | 8.61 | 8.73 | 8.85 | 8.94 | 9.03 | 9.21 | 9.42 | 9.65 |
| $Z_c$ | 44.5 | 44.6 | 44.9 | 46.0 | 49.0 | 50.5 | 52.0 | 53.3 | 54.7 | 57.2 | 60.0 | 62.9 |

TABLE 40

$\kappa = 12$ $H = 1mm$ $\frac{W}{H} = 1$

| f(GHz) | 0 | 1 | 2 | 4 | 8 | 12 | 15 | 17.5 | 20 | | | |
|---|---|---|---|---|---|---|---|---|---|---|---|---|
| $\kappa_{eff}$ | 8.48 | 8.53 | 8.63 | 8.90 | 9.37 | 9.92 | 10.45 | 11.01 | 11.69 | | | |
| $Z_c$ | 30.4 | 30.6 | 30.9 | 32.1 | 35.2 | 39.4 | 43.4 | 47.1 | 51.0 | | | |

TABLE 41

$\kappa = 12$ $H = 1$mm $\frac{W}{H} = 2$

| f(GHz) | 0 | 1 | 2 | 4 | 8 | 12 | 15 | | | | | |
|---|---|---|---|---|---|---|---|---|---|---|---|---|
| $\kappa_{eff}$ | 9.24 | 9.32 | 9.48 | 9.82 | 10.74 | 12.39 | 14.57 | | | | | |
| $Z_c$ | 19.0 | 19.2 | 19.6 | 21.0 | 26.4 | 36.4 | 48.5 | | | | | |

TABLE 42

$\kappa = 12$ $H = 1$mm $\frac{W}{H} = 3$

| f(GHz) | 0 | 1 | 2 | 4 | 8 | 10 | | | | | | |
|---|---|---|---|---|---|---|---|---|---|---|---|---|
| $\kappa_{eff}$ | 9.70 | 9.81 | 10.00 | 10.47 | 12.25 | 14.26 | | | | | | |
| $Z_c$ | 13.9 | 14.1 | 14.7 | 16.7 | 26.4 | 36.8 | | | | | | |

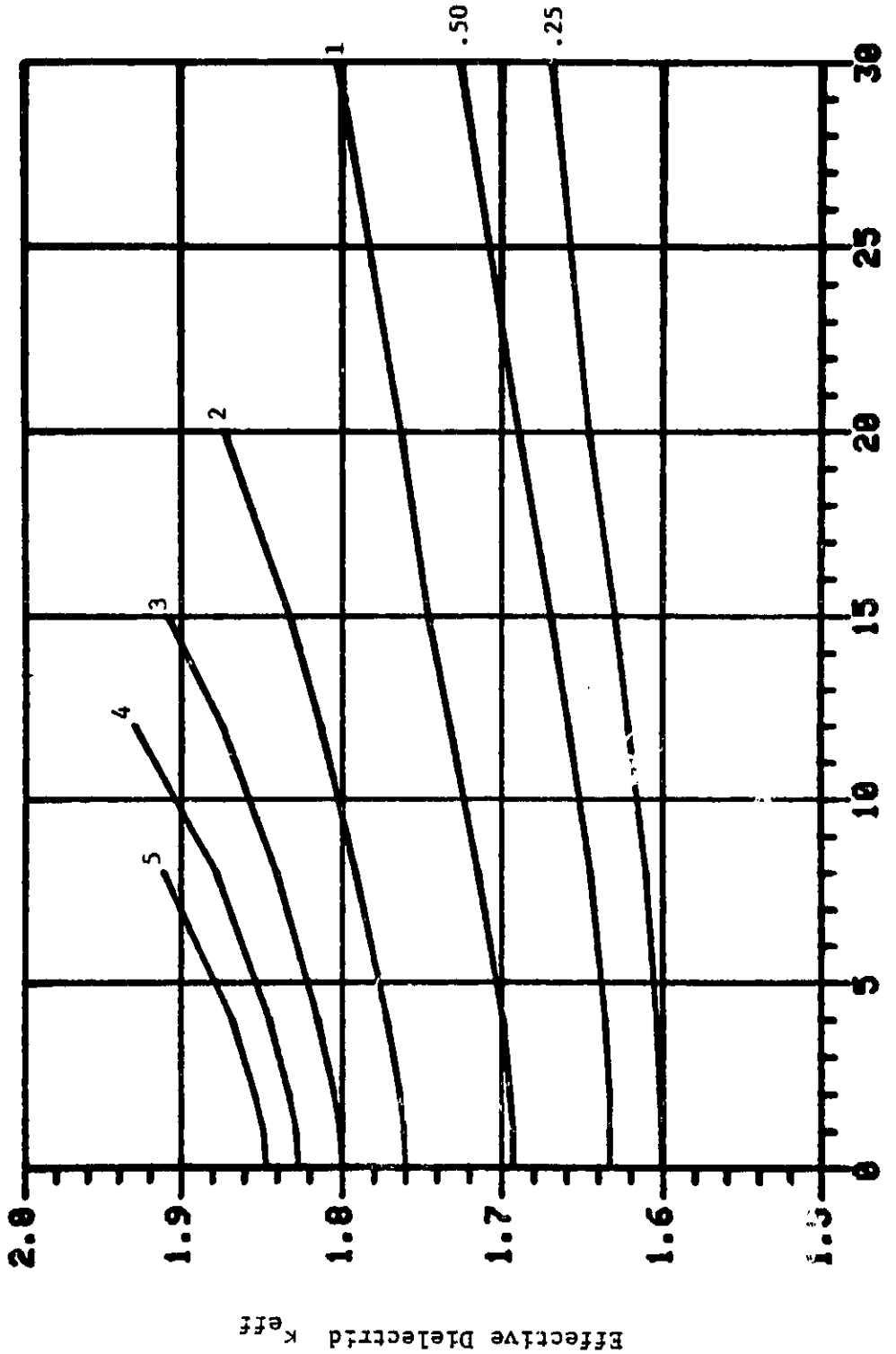


Figure 2.3 Effective dielectric $\kappa_{eff}$ vs. frequency for $\kappa = 2.$ $\frac{W}{H}$ ratios indicated on graph. H = 1mm.

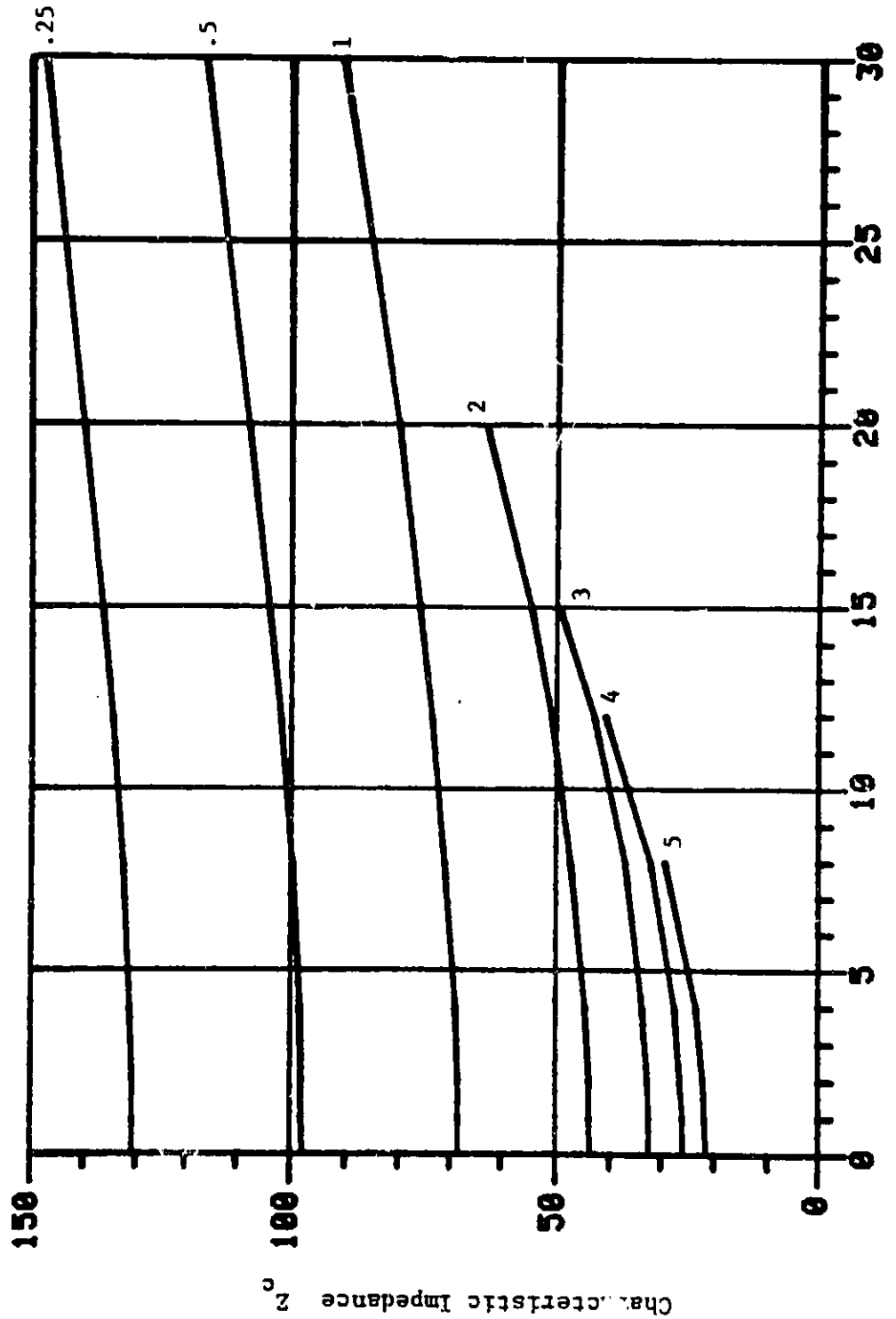


Figure 2.4 Characteristic impedance $Z_c$ vs. frequency for $\kappa = 2$. $\frac{W}{H}$ ratios indicated on graph. H = 1mm.

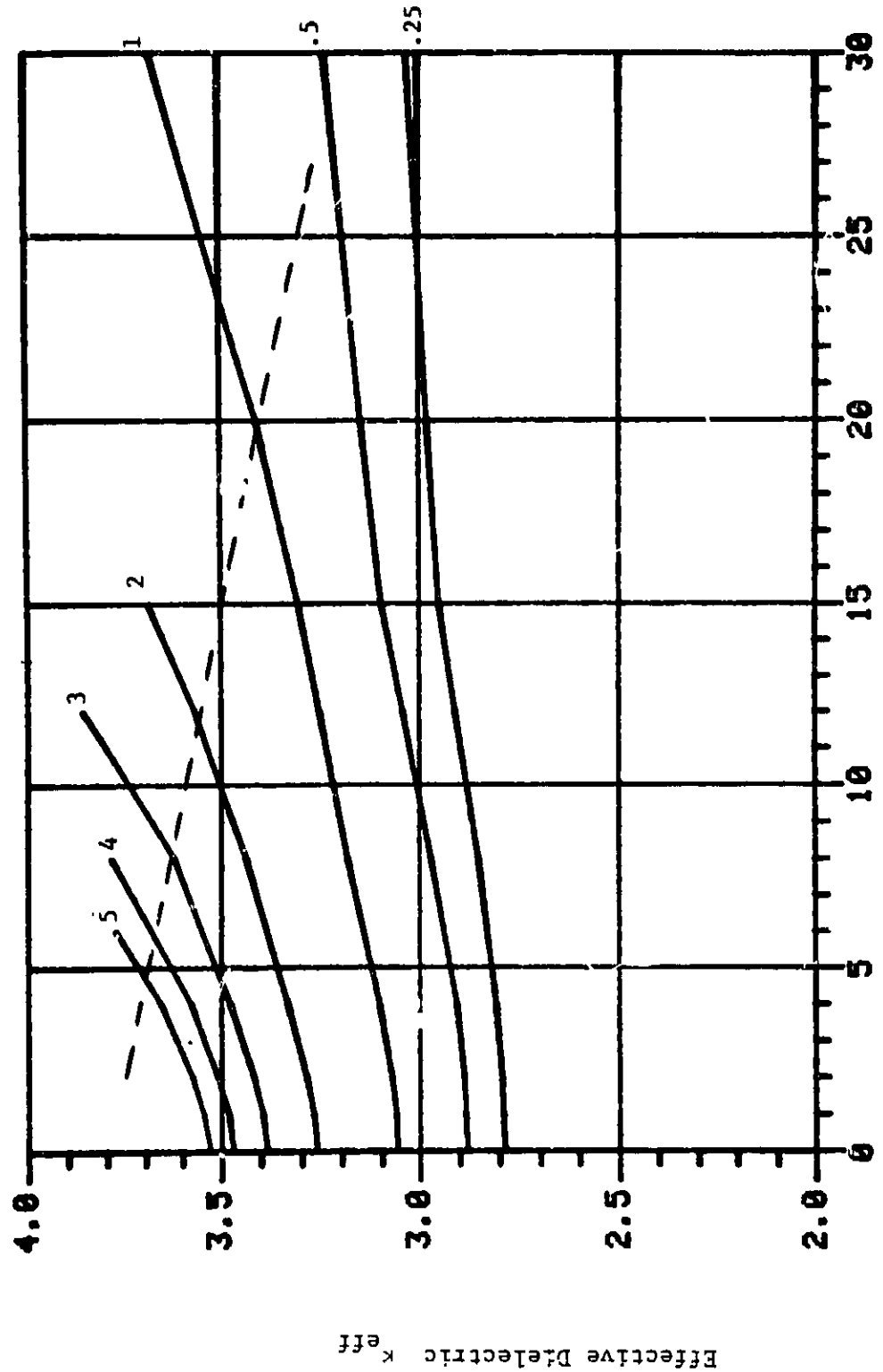


Figure 2.5 Effective dielectric $\kappa_{eff}$ vs. frequency for $\kappa = 4$. $\frac{W}{H}$ ratios indicated on graph. H = 1mm.

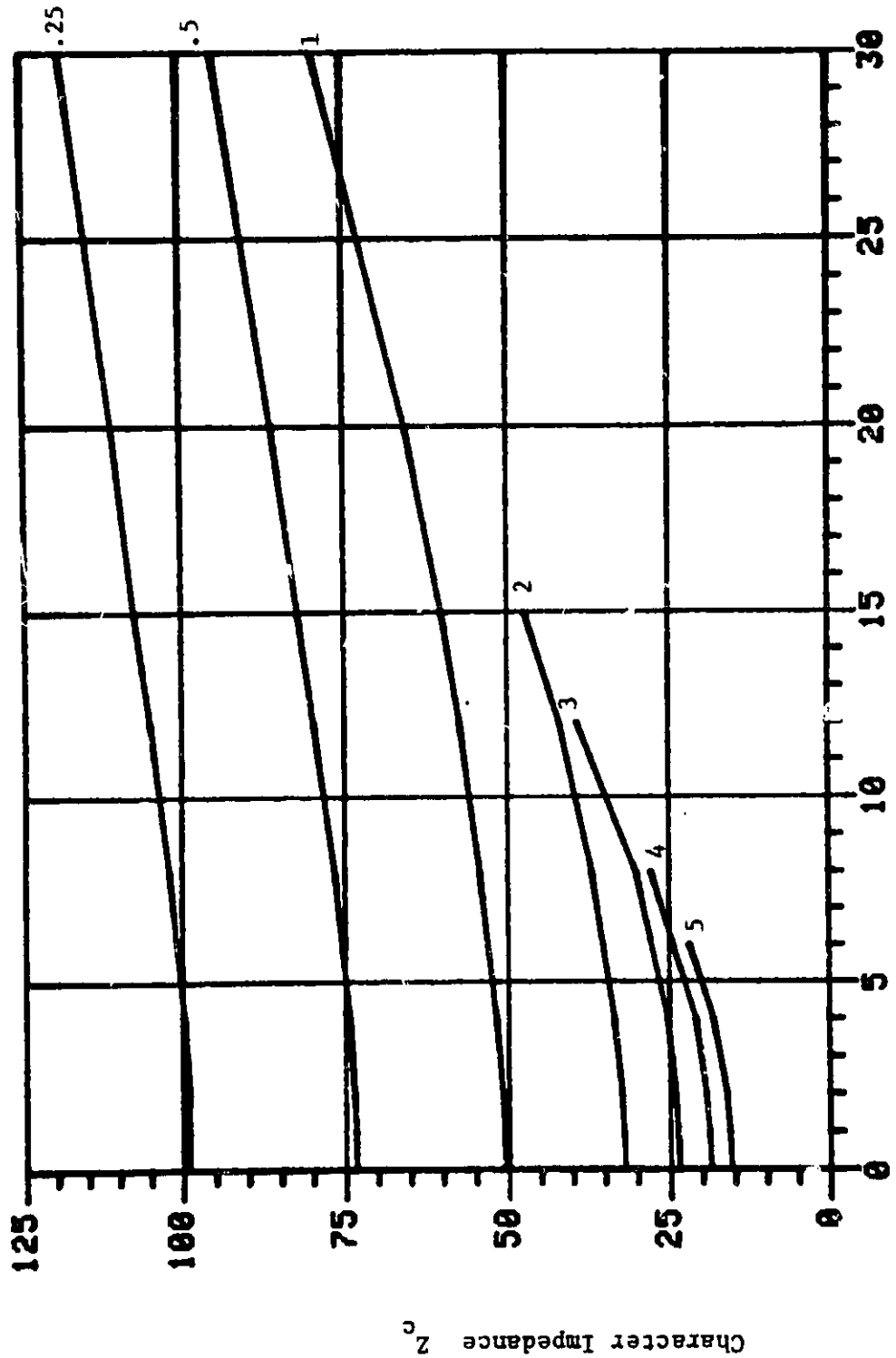


Figure 2.6 Characteristic impedance $Z_c$ vs. frequency for $\kappa = 4$. $\frac{W}{H}$ ratios indicated on graph. H = 1mm.

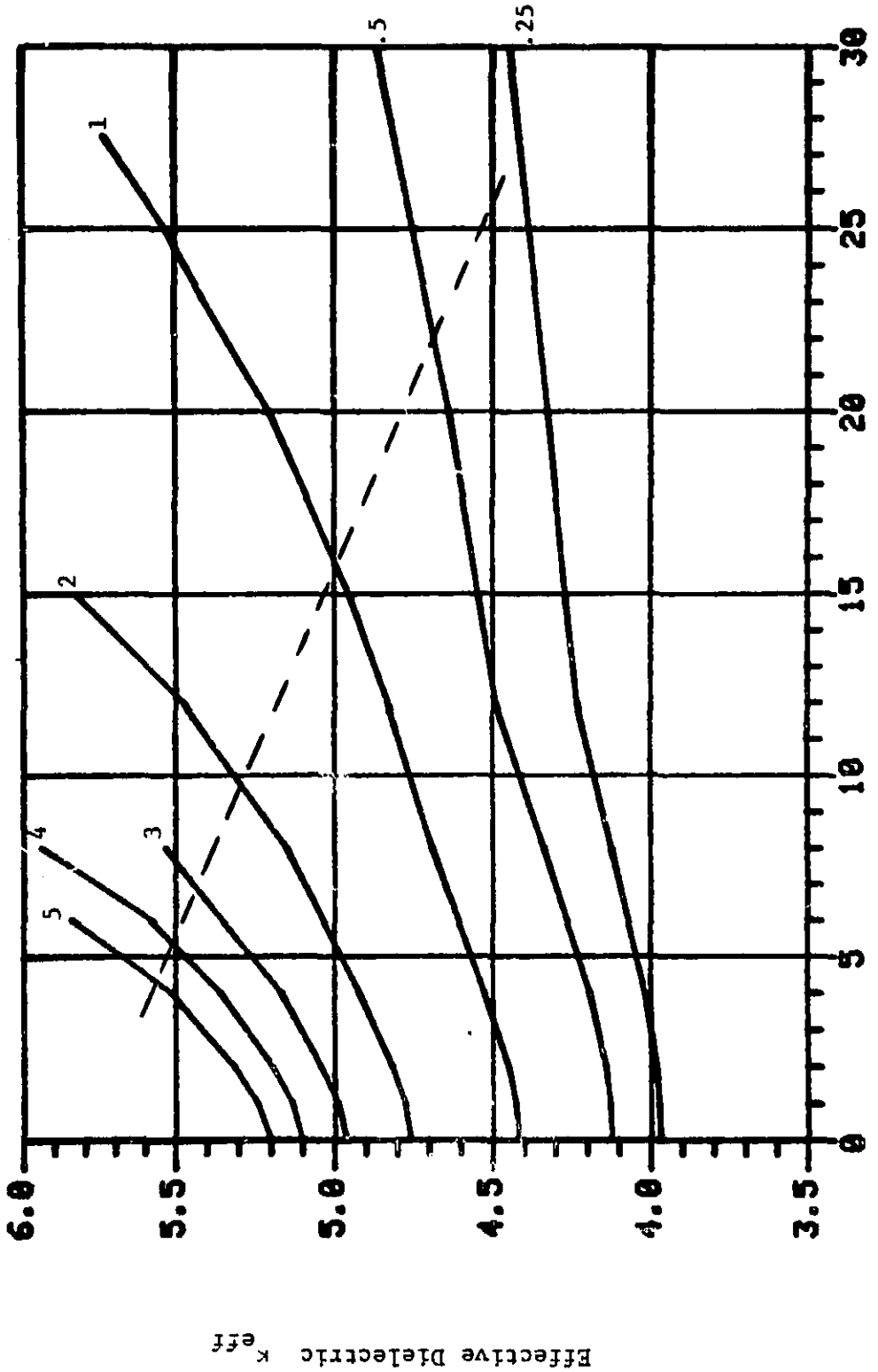


Figure 2.7 Effective dielectric $\kappa_{eff}$ vs. frequency for $\kappa = 6$. $\frac{W}{H}$ ratios indicated on graph. H = 1mm.

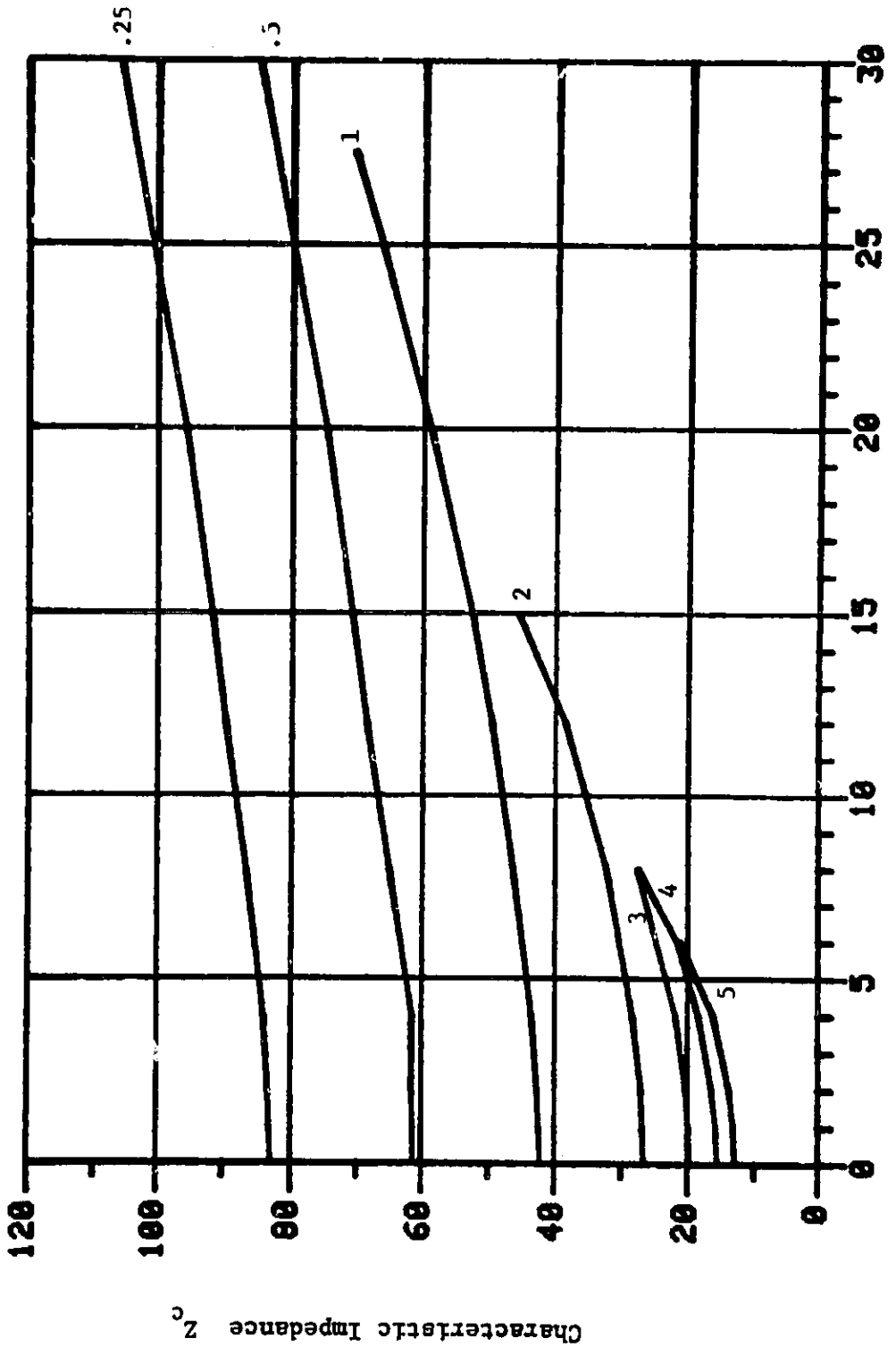


Figure 2.8 Characteristic impedance vs. frequency for $\kappa = 6$. $\frac{W}{H}$ ratios indicated on graph. H = 1mm.

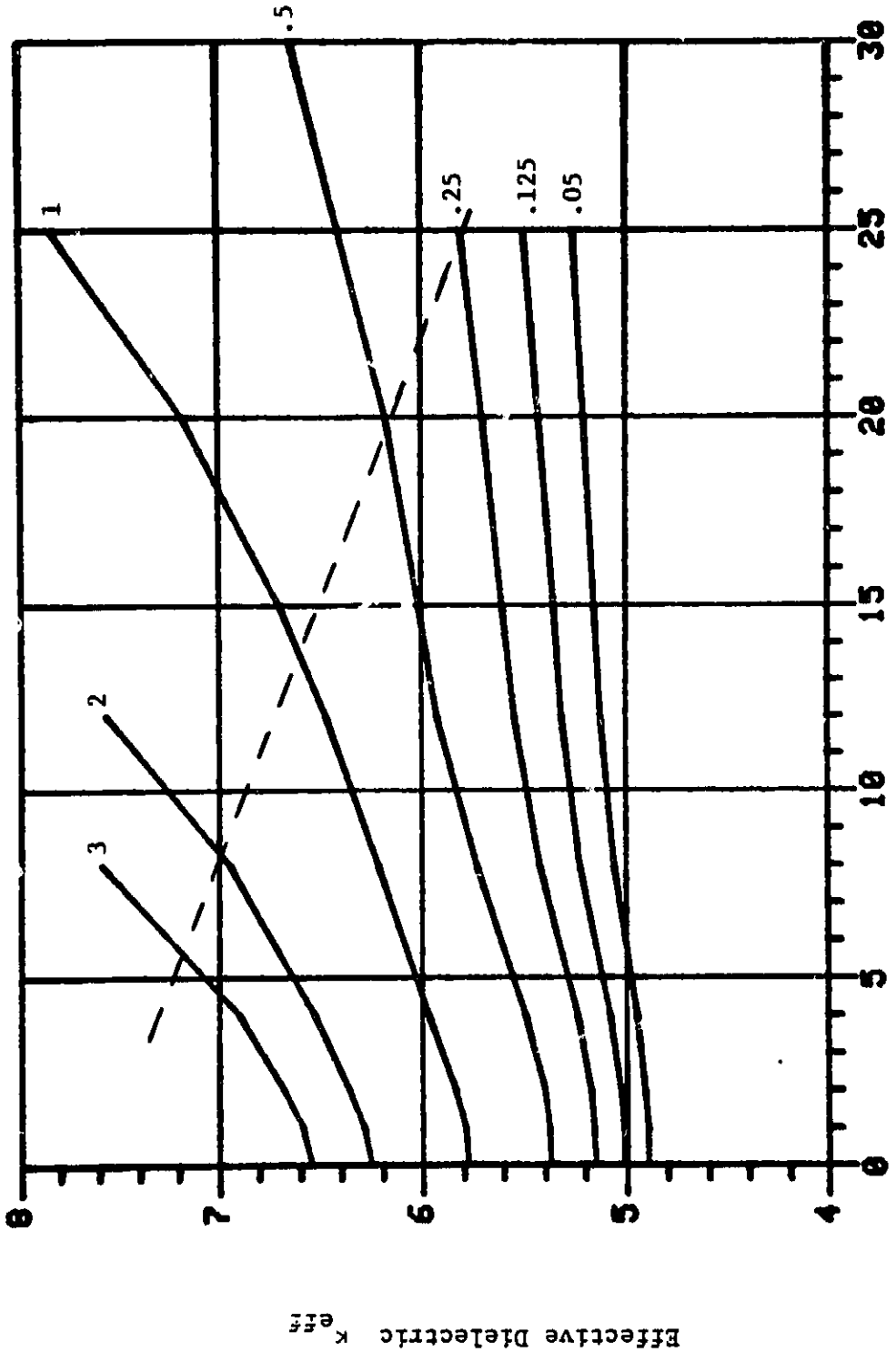


Figure 2.9 Effective dielectric $\kappa_{eff}$ vs. frequency for $\kappa = 8$. $\frac{W}{H}$ ratios indicated on graph. H = 1mm.

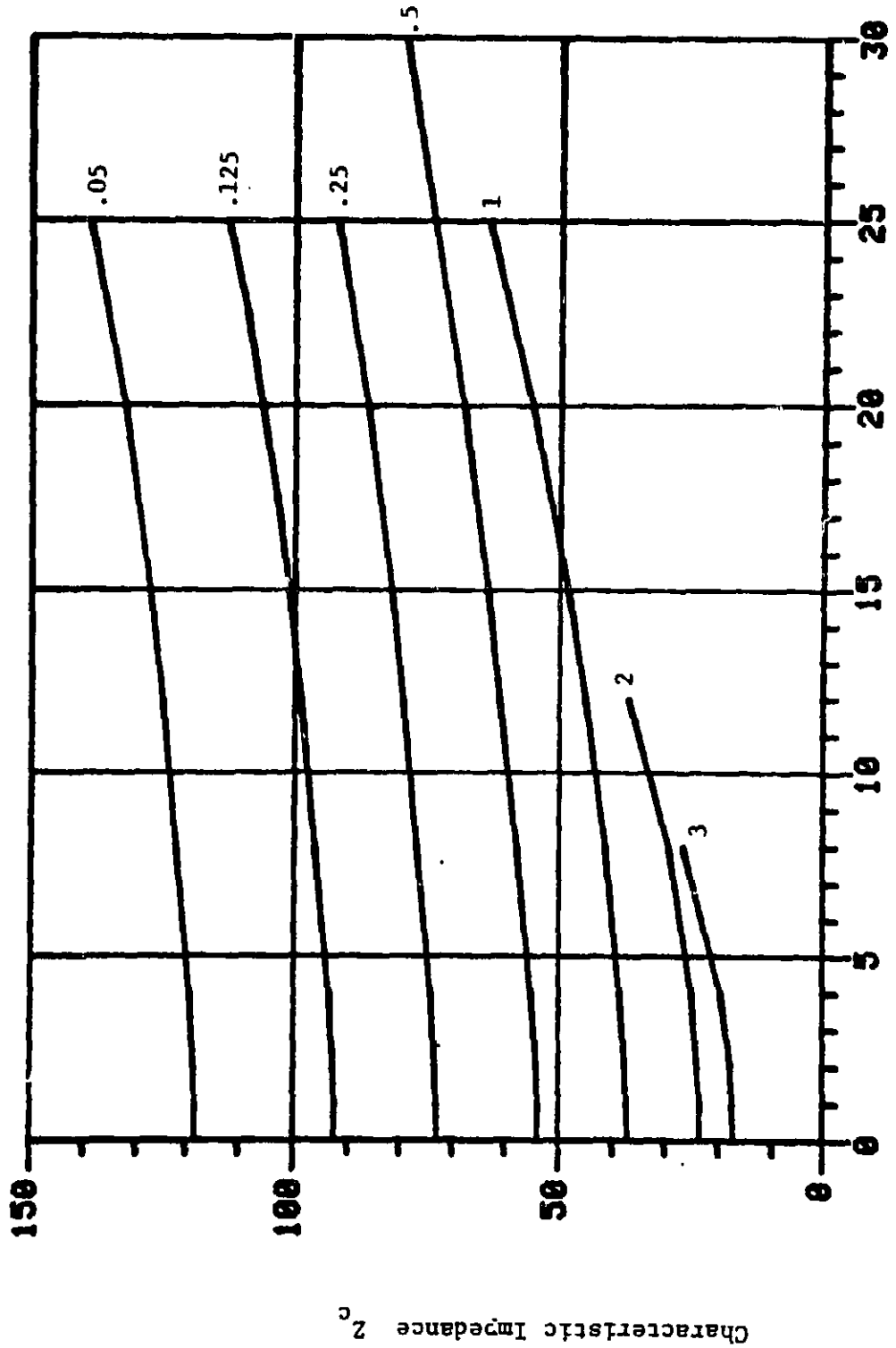


Figure 2.10 Characteristic impedance vs. frequency for $\kappa = 8$. $\frac{W}{H}$ ratios indicated on graph. H = 1mm.

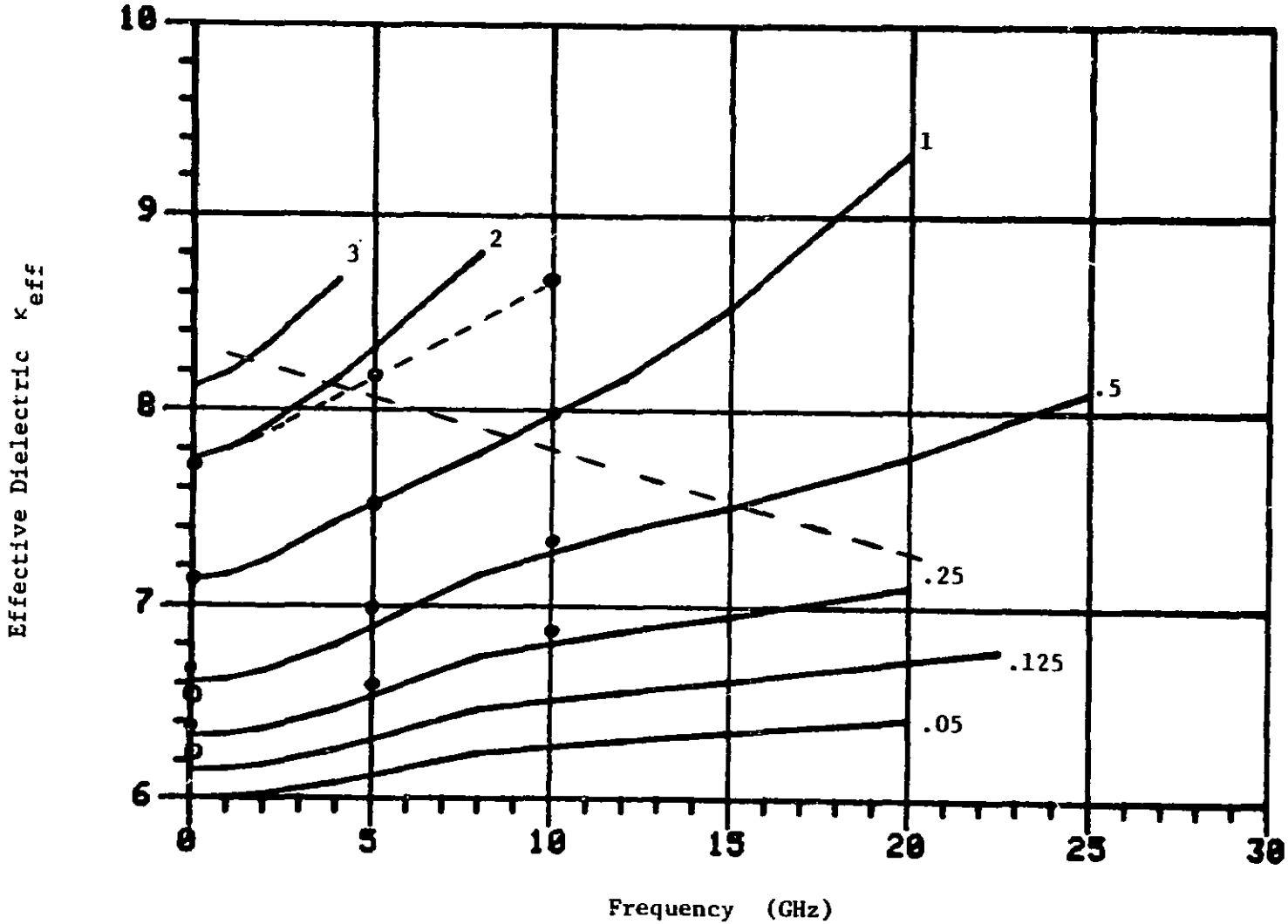


Figure 2.11 Effective dielectric $\kappa_{eff}$ vs. frequency for $\kappa = 10$. $\frac{W}{H}$ ratios indicated on graph. H = 1mm. • From Jansen [16], ◦ From Wheeler [3]

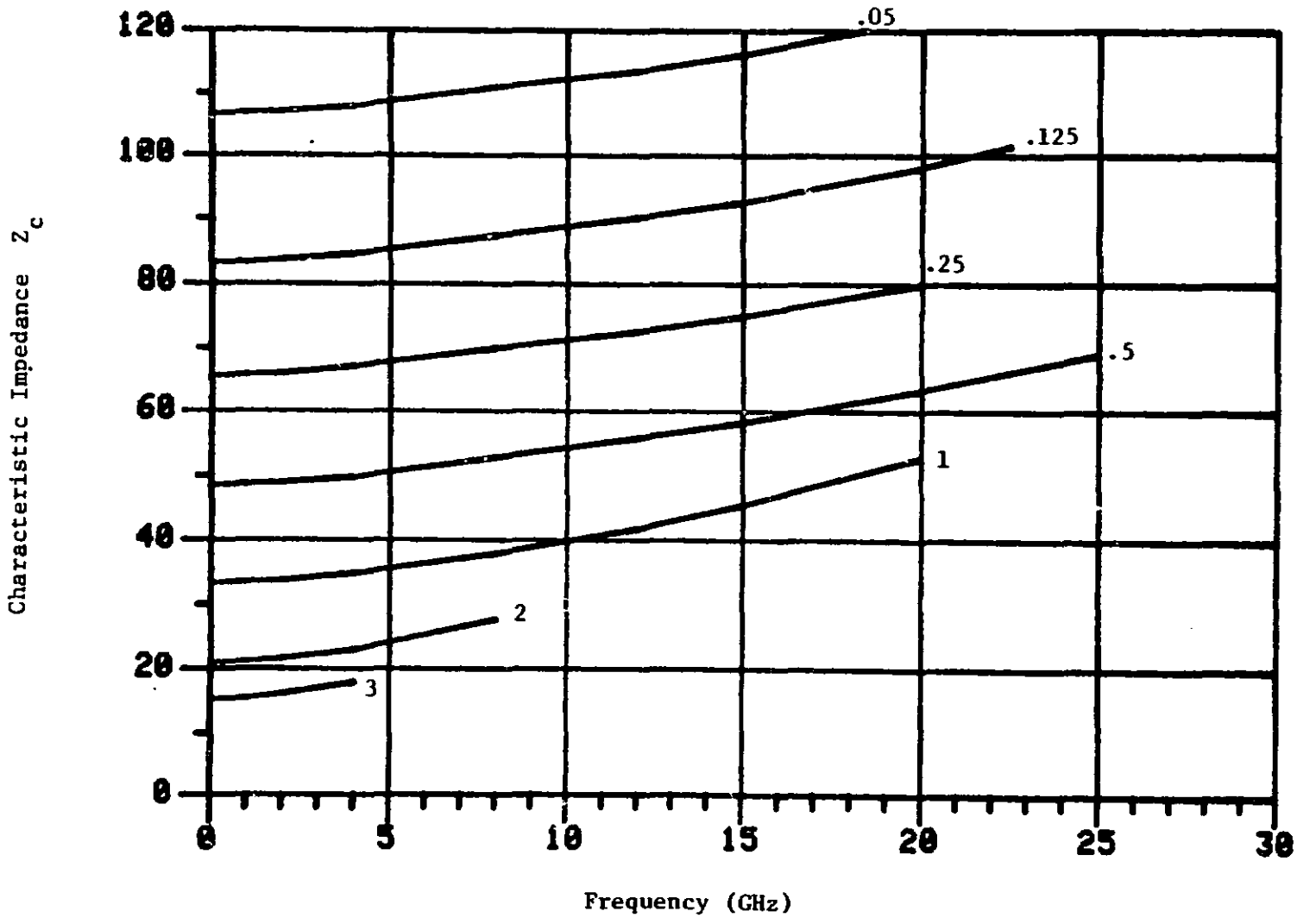


Figure 2.12 Characteristic impedance $Z_c$ vs. frequency for $\varepsilon_r$ = 10. $\frac{W}{H}$ ratios indicated on graph. H = 1mm.

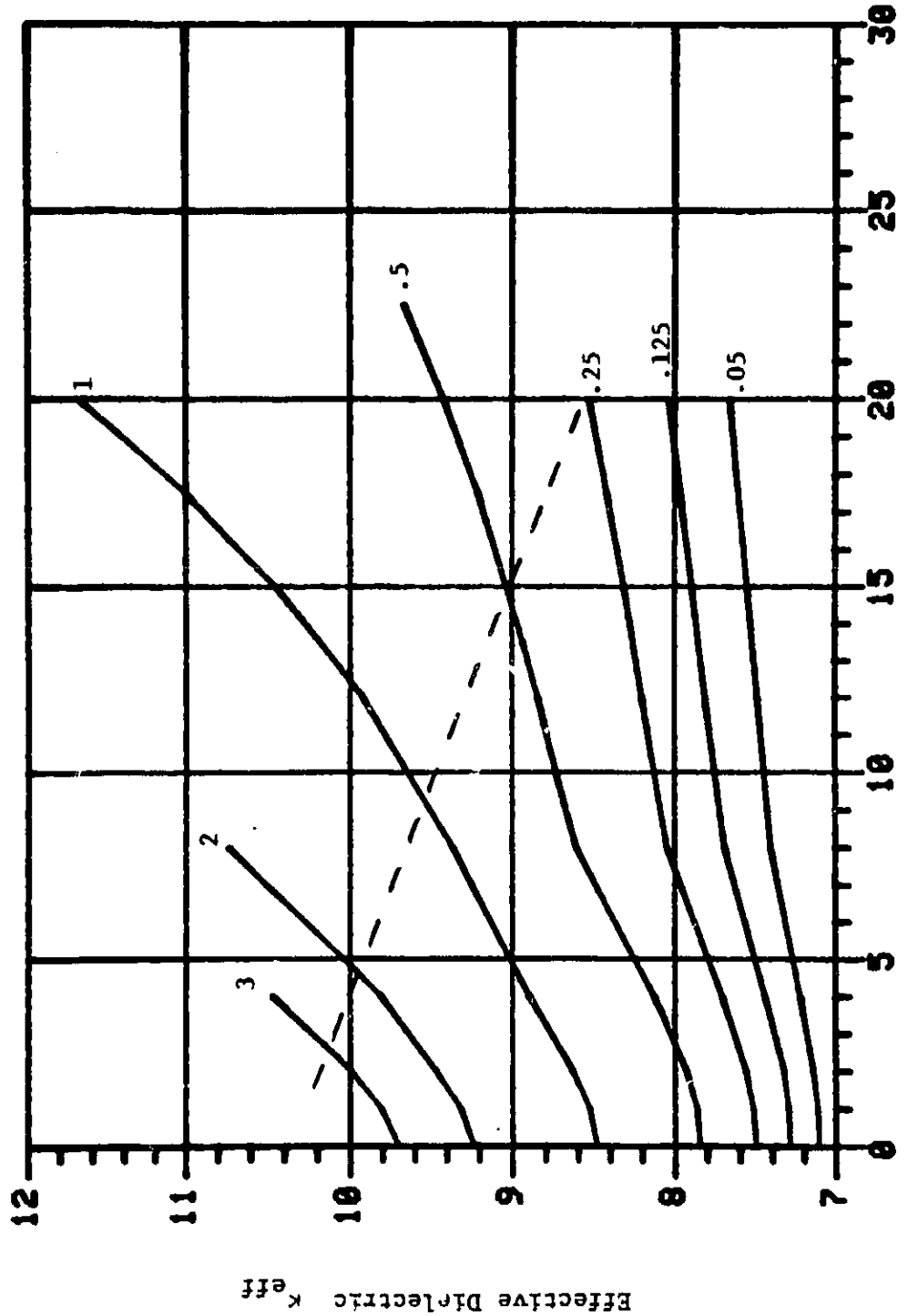


Figure 2.13 Effective dielectric $\kappa_{eff}$ vs. frequency for $\kappa$ = 12. $\frac{W}{H}$ ratios indicated on graph. H = 1mm.

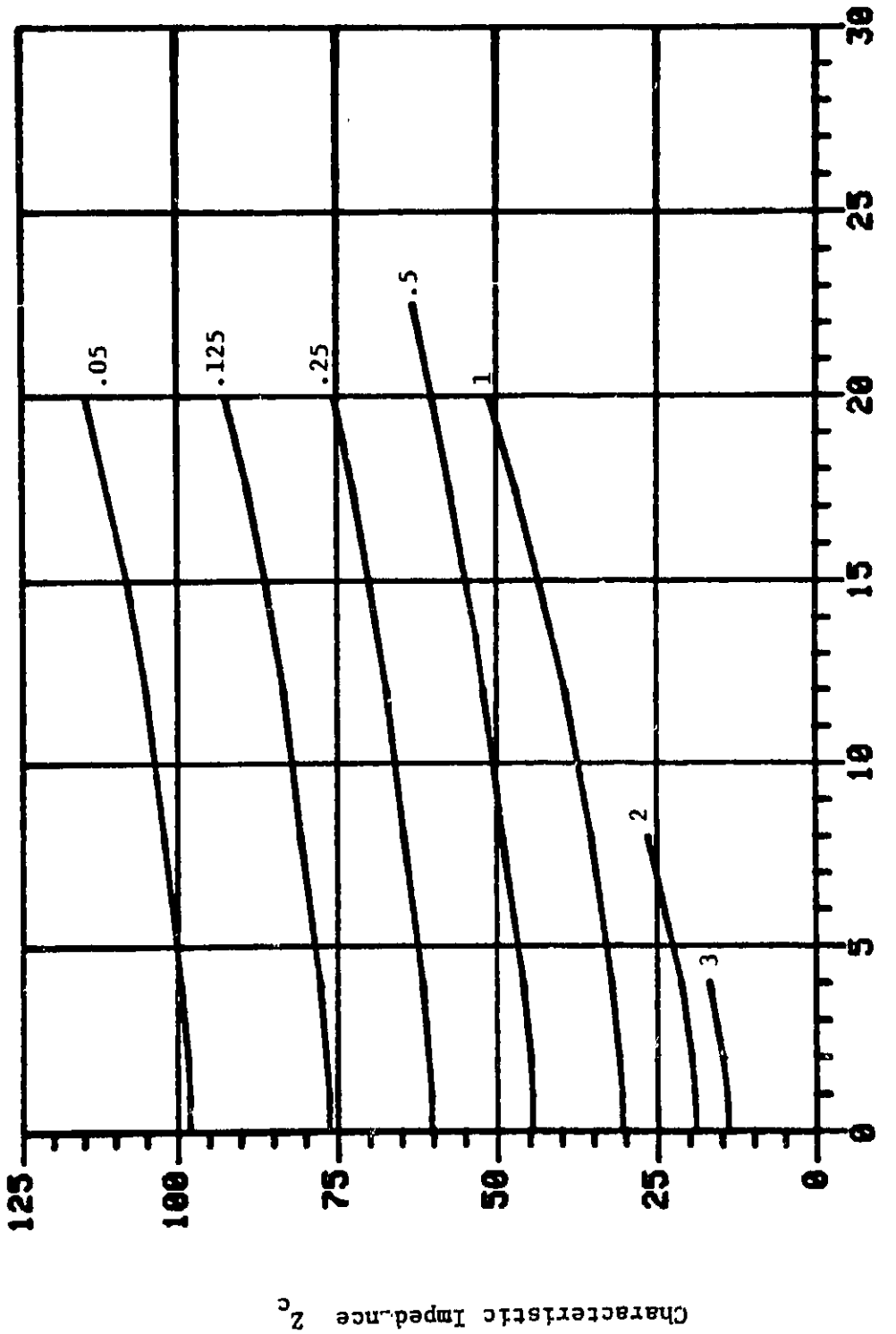


Figure 2.14 Characteristic impedance $Z_c$ vs. frequency for $\kappa = 12.$ $\frac{W}{H}$ ratios indicated on graph. H = 1mm.

| line number | κ | 2W | H |
|---|---|---|---|
| 1 | 10.15 | 1.5 | .65 |
| 2 | 10.15 | .585 | .65 |
| 3 | 10.15 | .260 | .65 |

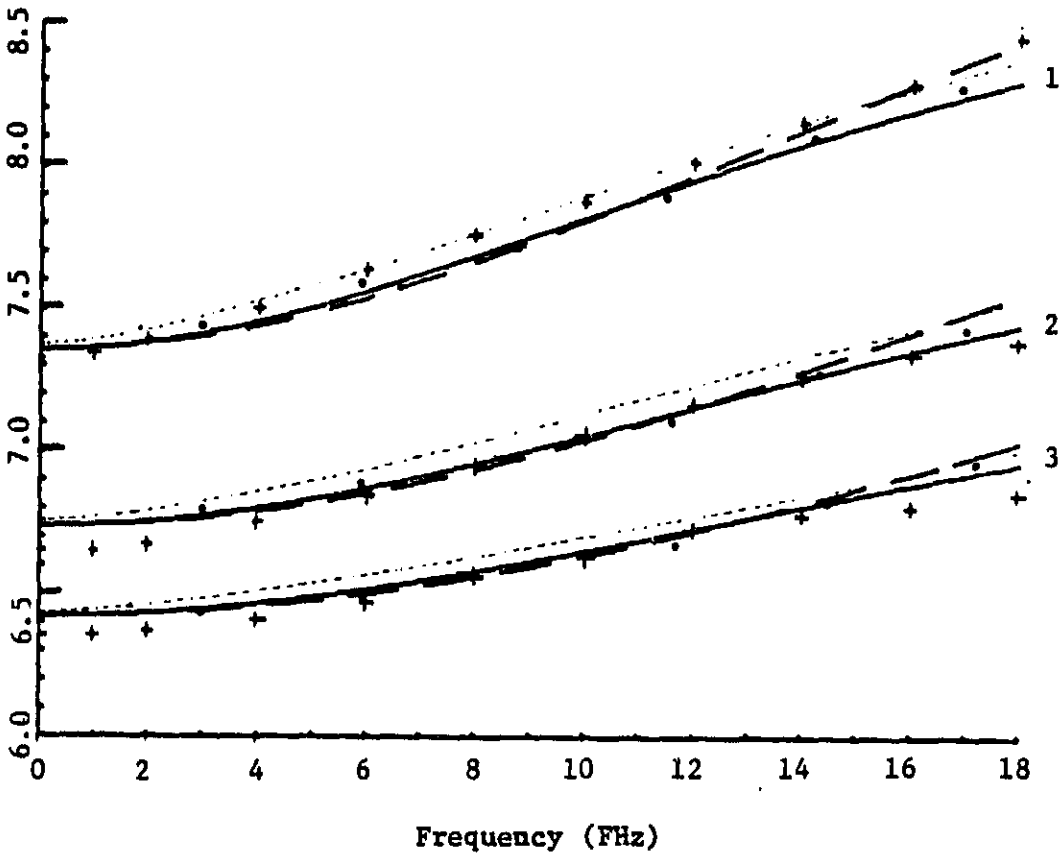


Figure 2.15 Comparison of $\kappa_{eff}$ vs. frequency plots.

- · Experimental results
- — — Dispersion model analysis [ ]
- --- Fullwave analysis [ ]
- —— Improved dispersion model analysis [ ]
- \+ Perterbation-Iteration Method

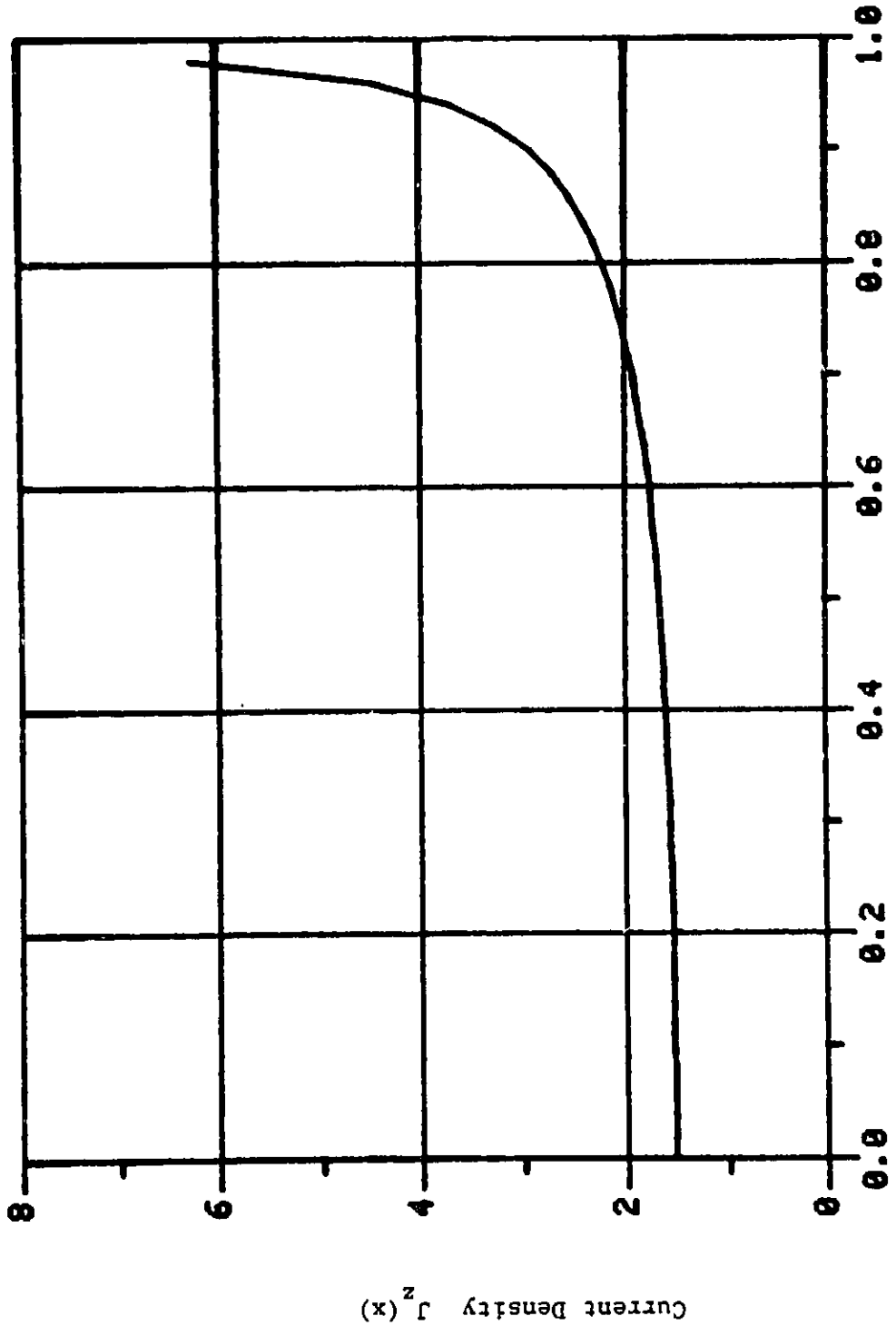


Figure 2.16 Accurate current density $J_z(x)$ vs. microstrip units for $\kappa = 10$, $\frac{W}{H} = 2$, and $f = 4$ GHz.

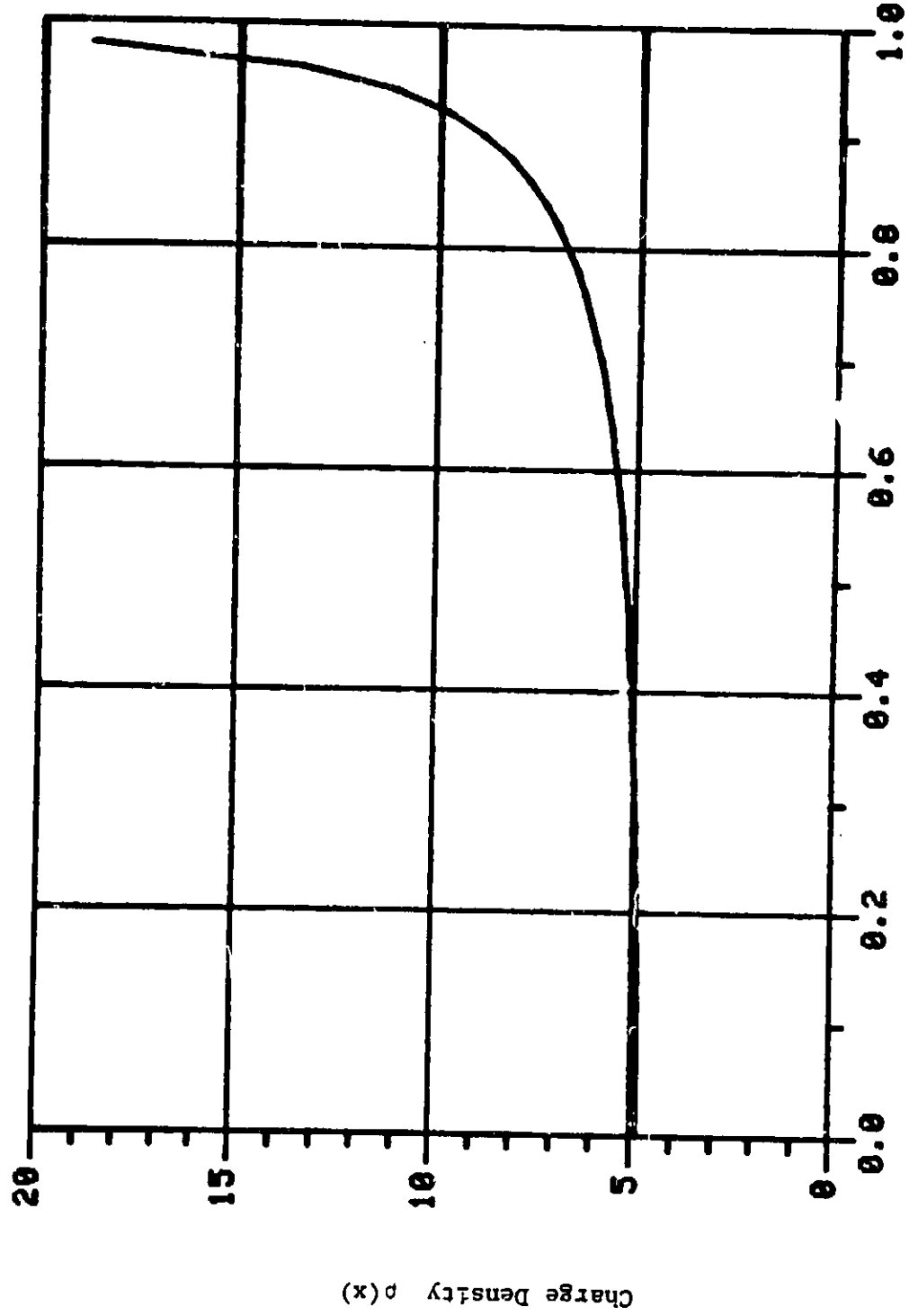


Figure 2.17 Accurate charge density $\rho(x)$ vs. Microstrip units for $\kappa = 4$, $\frac{W}{H} = 1$, and $f = 4$GHz.

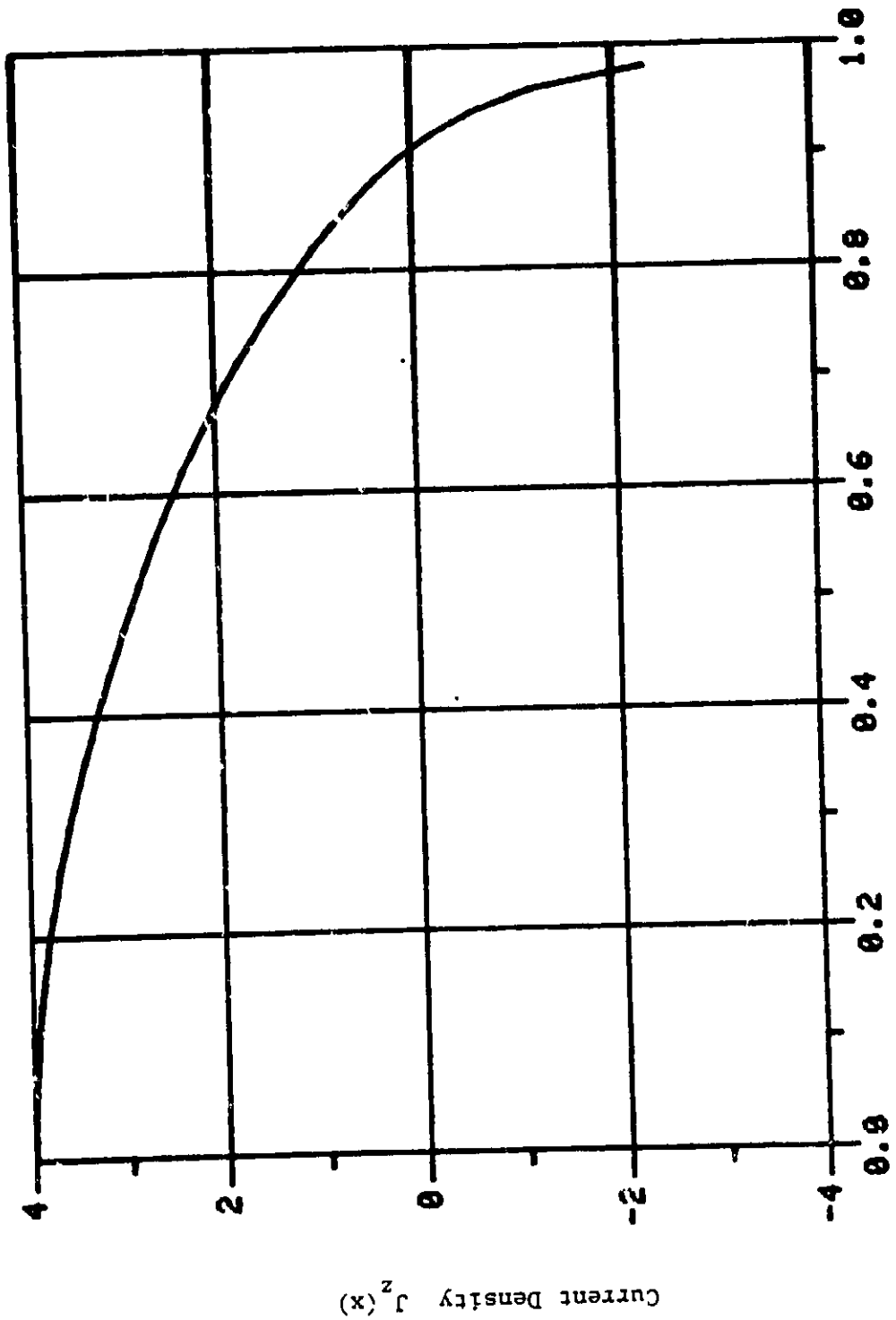


Figure 2.18 Inaccurate current density $J_z(x)$ vs. microstrip units for $\kappa = 10$, $\frac{W}{H} = 2$, and $f = 12\text{GHz}$.

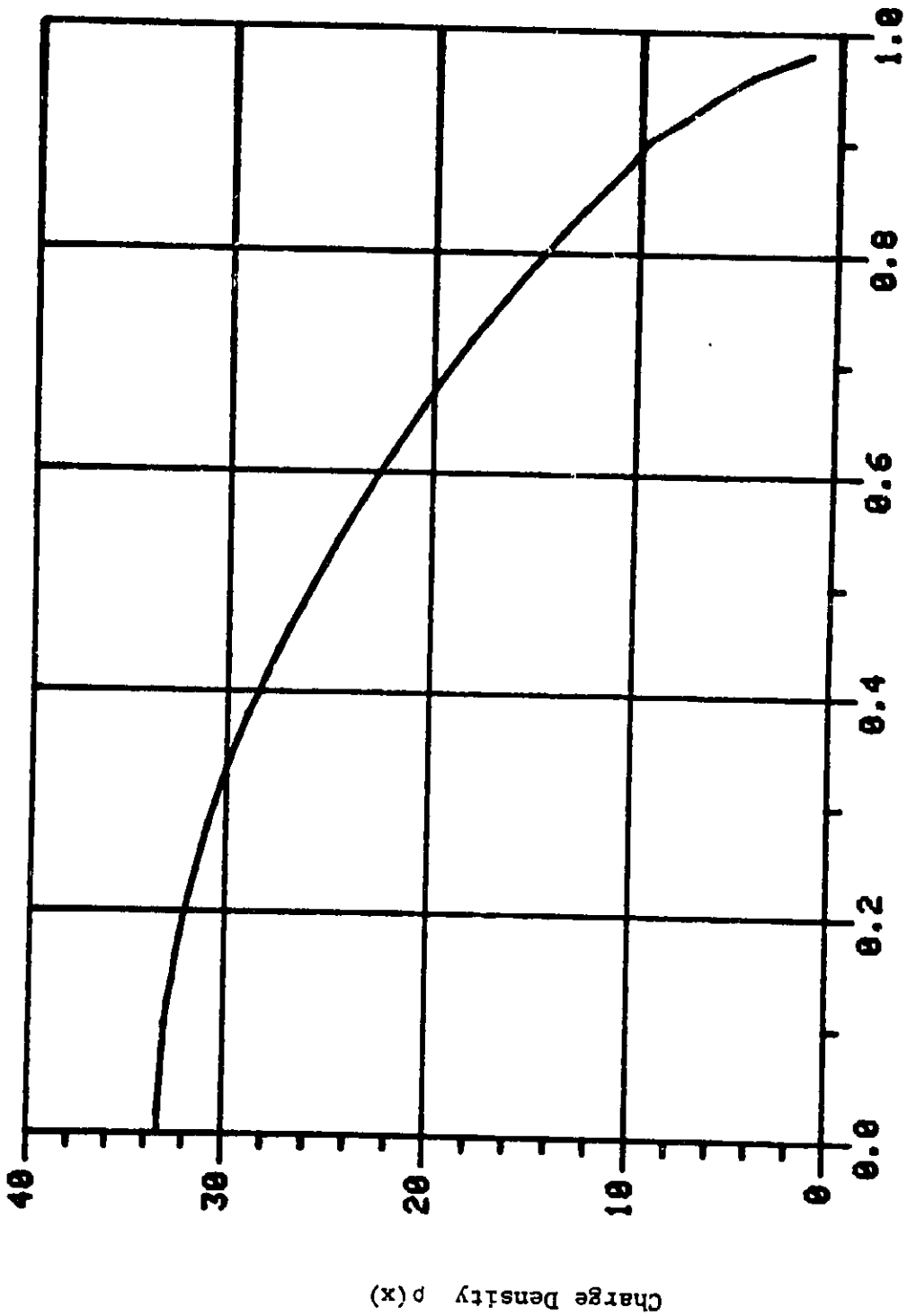


Figure 2.19 Inaccurate charge density $\rho(x)$ vs microstrip units for $\kappa = 10$, $\frac{W}{H} = 2$, and $f = 12$GHz.

# CHAPTER 4

## CONCLUSIONS

This thesis has developed a Perturbation-Iteration Method for analyzing microwave striplines. The theory began with the static analysis being developed followed by the higher order analysis. The static analysis was developed by using two static Green's functions. The higher order analysis was developed using three frequency dependent Green's functions and satisfying the frequency dependent wave equations. Extensive tables and graphs of computed values of $\kappa_{eff}$ and $Z_c$ over a range of frequencies was presented for different structures. Data was also presented which compared the method with previously developed methods and experimental data. The comparison showed that the results were accurate to at least 1% over most of the parameter range of practical interest.

The Perturbation-Iteration Method is a relatively easy method to use as it contains no transcentental dispersion equations that must be solved. Rather, it employs a set of equations which, when solved simultaneously, produce answers for $\beta$ and $Z_c$ directly and which satisfy the field requirements of the structure. The ease of using this method is also enhanced by the fact that it calculates values based on ratios of the stripline dimensions. Therefore, once one set of dimensions are used for computations, other structures with the same dimension ratios can be directly analyzed by employing a frequency scaling. An example of this feature is a structure with microstrip width of 2 units, height above the ground plane of 1 unit

and frequency of 1 GHz has the same characteristics as a structure of microstrip width 1 unit, height above the ground plane of 0.5 units, and frequency 2 GHz. This scaling feature enhances the value of the method greatly.

Over the course of developing the method, another method was developed which proved inadequate. It used a perturbation series which expanded $\beta$ in odd powers of frequency. It initially solved for a higher order solution. The static solution was identical as used in the Perturbation-Iteration Method. The higher order solution used the same static Green's functions as the static case along with frequency dependent sources. The method proved to be unsuitable as the computed values of $\beta$ and $Z_c$ did not converge to any exact values because they were dependent on the dimension a. This dependence led to the abandonment of the metnod in favor of the Perturbation-Iteration Method.

The validity of the numerical procedure used, holds over a broad range of frequencies but, becomes less accurate as the frequency is raised to high values. As the width of the microstrip is increased, the range of frequencies where the method is accurate decreases. However, the range of frequencies where the method becomes less reliable is also the same range where higher order modes propagate down the stripline. These ranges of frequencies are not actually practical for use and thus are not a serious limitation to the effectiveness of the procedure for practical stripline structures.

The Perturbation-Iteration Method is a very practical method and can be applied in related areas. The theory can be modified to accomodate different structures such as slotlines and coplanar waveguides. The accuracy can be enhanced by adding extra cief-ficients to the charge and current density expansions which will make the theory valid over a broader range of frequencies. The Theory could be extended to separate and then solve for each mode of frequencies where multiple modes propagate. The method could also be reformulated to solve for $\beta$ and $Z_c$ in the Fourier transform domain in a similar fashion as the fullwave analysis referred to in Chap. 1. It is believed that the loss in accuracy at very high frequencies is due to the use of a four term expansion of the charge nd current distribution on the strip along with point matching at four points along the strip. Other numerical procedures can be used to remove this limitation. Never the less, the simple procedure used is adequate for striplines of the type normally used in practice.

## BIBLIOGRAPHY


1. Schneider, M.V., Microstrip Lines for Microwave Integraced Circuits, B. S. T. J., Vol. 48, 1969, pp. 1421-1444.

2. Wheeler, H.A., Transmission Line Properties of Parallel Wide Strip by Conformal Mapping Approximation, IEEE Trans, Vol. MTT-12, 1964, pp. 280-289.

3. Wheeler, H.A., Transmission Line Properties of Parallel Strips Separated by a Dielectric, IEEE Trans., Vol MTT-13, 1965, pp. 172-185.

4. Yamashita, E. and R. Mittra, Variational Method for the Analysis of Microstrip Lines, IEEE Trans., Vol, MTT-16, 1968, pp. 251-256.

5. Yamashita, E., Variational Method for the Analysis of Microstrip-Like Transmission Lines, IEEE Trans., Vol. MTT- 16, 1968, pp. 529-535.

6. Green, H.E., The Numerical Solution of Some Important Transmission Line Problems, IEEE Trans., Vol. MTT-13, 1965, pp. 676-692.

7. Silvester, P., TEM Properties of Microstrip Transmission Lines, Proc. IEE, Vol. 115, 1968, pp. 43-49.

8. Jain, O.P. et al., Coupled Mode Model of Dispersion in Microstrip, Electron. Lett., Vol. 7, 1971, pp. 405-407.

9. Schneider, M.V., Microstrip Dispersion, Proc. IEEE, Vol. 60, 1972. pp. 144-146.

10. Getsinger, W.J., Microstrip Dispersion Model, IEEE Trans. Vol. MTT-21, 1973, pp. 34-39.

11. Kompa, G. and R. Mehran, Planar Waveguide Model for Calculating Microstrip Components, Electron. Lett., Vol. 11, 1975, pp. 459-460.

12. Carlin, H.J., A Simplified Circuit Model for Microstrip, IEEE Trans., Vol. MTT-21, 1973, pp. 589-591.

13. Denlinger, E.J., A Frequency Dependent Solution for Microstrip Transmission Lines, IEEE Trans., Vol. MTT-19, 1971, pp. 30-39.

14. Itoh, T., and R. Mittra, Spectral-Domain Approach for Calculating Dispersion Characteristics of Microstrip Lines, IEEE Trans., Vol. MTT-21, 1973, pp. 496-498.

15. Knorr, J.B., and A. Tufekcioglu, Spectral Domain Calculation of Microstrip Characteristic Impedance, IEEE Trans., Vol. MTT-23, 1975, pp. 725-728.

16. Jansen, R.H., High Speed Computation of Single and Coupled Microstrip Parameters Including Dispersion, High-Order Modes, Loss and Finite Strip Thickness, IEEE Trans., Vol. MTT-26, 1978, pp. 75-82.

17. Yamashita, E., and K. Atsuki, Analysis of Microstrip-like Transmission Lines by Nonuniform Discretization of Integral Equations, IEEE Trans., Vol. MTT-24, 1976, pp. 195-200.

18. Kuester, E.F., and D.C. Chang, An Appraisal of Methods for Computation of the Dispersion Characteristics of Open Microstrip. IEEE Trans., Vol. MTT-27, 1979, pp. 691-694.

19. Edwards, T.C., and R.P. Owens, 2-18 Ghz Dispersion Measurements on 10-100 Ohm Microstrip Lines on Sapphire, IEEE Trans. Vol. MTT-24, 1976, pp. 506-513.

## APPENDIX

## COMPUTER PROGRAM

```
TYPE GORSU.FOR
C       THE FOLLOWING PROGRAM WILL DETERMINE THE PROPAGATION CONSTANT
C       BETA AND CHARACTERISTIC IMPEDANCE Z SUB C USING THE PERTURBA-
C       TION-ITERATION METHOD AS DEVELOPED BY DR. ROBERT E. COLLIN
C       AND BRIAN E. KRETCH FOR THE LATTER'S MASTER DEGREE THESIS
C       AS PRESENTED ON AUGUST 30, 1965.VARIOUS COMMENTS AND INSTRUC-
C       TIONS WILL BE INCLUDED IN THIS PROGRAM TO ASSIST THE USER OF
C       THIS PROGRAM.
C
C       ***************************************************************
C
        INTEGER N,M,P,R,INT,FOUR,FLAG,FLAG2
        REAL HEIGHT,SWIDTH,DWIDTH,KAPPA
        REAL*8 H,XPRIME,V1,V2,V3,V4,V5,V6,W1,DD(0:3,0:3)
        REAL*8 V7,V8,CONSTANT,PHISAV,ASUBO,CURR2P,HERE
        REAL*8 A,K1,K2,K3,TEMP1,TEMP2,TEMP3,TEST,XX(0:3)
        REAL*8 S1,S2,S3,S4,S5,S6,S7,GSUBC(0:3),CHARGE(0:3)
        REAL*8 AA1,AA2,AA3,AA4,AA5,AA6,AA7,MEGAN,EPSEFF
        REAL*8 BB1,BB2,BB3,ETA,GC,GC1,BETA1,THETA
        REAL*8 X,D3A,D3B,PI,ALPHA,D2A,T1,T2,T3,T4,T5
        REAL*8 OMEGA,FREQ,C,BETASQ,KSUBO,FF(0:3,0:3)
        REAL*8 CC0,CC1,CC2,CC3,CURR,PERM,IND,CAP,IMP
        REAL*8 D(0:3),E(0:3),L(0:3),CHAR,EPS,BETA,CONST
        REAL*8 Y(0:3),Z(0:3,0:3),AMAT(0:3),I(0:3)
        REAL*8 JFOUR,CFOUR,EE(0:3,0:3),ZPR(0:3,0:3)
        REAL*8 QSUBN(0:3),CHARGE2(0:3),I2(0:3),ZSBO
        REAL*8 CURR2,CHAR2,ZSUBC,ZSUBO,ZZ1,INCR,MEG2
        REAL*8 ZZ9(0:3),AA8,BB4,I2PR(0:3),HERINC
        REAL*8 MEGAN1,MEGAN2,QQ(0:3),PHINEW,ASUBY
        REAL*8 ASUBY(1:500),PHIOLD(1:500),NEWBET
        REAL*8 ASUBZ(1:500),YY(0:3,0:3),AMAT1(0:3)
C
```

```
C
C     THE INPUT PARAMETERS OF THE MICROSTRIP STRUCTURE TO
C     EXAMINED ARE INPUT AT THIS POINT.ALL DIMENSIONS ARE
C     TO BE INPUT IN MILLIMETERS SINCE THE PROGRAM INTERNALLY
C     MUST CONVERT THE INPUT FREQUENCY TO UNITS RELATING
C     TO THE WIDTH OF THE MICROSTRIP. THE SUBSTRATE HEIGHT
C     IS THE HEIGHT BETWEEN THE GROUND PLANE AND THE MICRO-
C     STRIP. THE SUBSTRATE WIDTH IS THE TOTAL DISTANCE
C     BETWEEN THE SIDE GROUND WALLS 2B. THE MICROSTRIP WIDTH
C     IS THE TOTAL WIDTH OF THE MICROSTRIP 2W. RAPPO IS THE
C     VALUE OF THE DIELECTRIC CONTANT OF THE DIELECTRIC.
C     THE FIRST FREQUENCY INTERVAL THE FIRST FREQUENCY WHICH THE
C     METHOD MEASURES FOR BETA AND Z SUB C. THIS INPUT IS IN
C     GIGOHERTZ. SINCE A SIMPSON'S RULE IS USED THROUGHOUT
C     THE PROGRAM FOR VARIOUS INTEGRATIONS, AN INTERVAL MUST
C     BE INPUT WHICH IS THE NUMBER OF DIVISIONS IN WHICH THE
C     INTEGRATION INTERVAL IS DIVIDED INTO. FOR MOST CALCU-
C     LATIONS, THE INTERVAL OF 10 IS MORE THAN SUFFICIENT TO YIELD
C     ACCURATE RESULTS. THE GREEN'S FUNCTION SUB Z (LEVEL 0) HAS A
C     FOURIER SERIES WHICH IS SUMMED UP IN PERFORMING THE INTEGRATION
C     FOR THE CHARGE DENSITY. THE GREEN'S FUNCTION SUB C ITERATION
C     NUMBER IS THE TERM NUMBER (NOT THE NUMBER OF TERMS -- THE SERIES
C     IS SUMMED OVER THE ODD COMPONENTS ONLY. THEREFORE, IF N=2, THE
C     SERIES USES TERMS NUMBER 1,3,5,7 AND NOT THE FIRST 2 TERMS) IS
C     THE NUMBER OF TERMS USED IN THE INTEGRATION. THE FOURIER SERIES
C     NUMBER IS THE TERM NUMBER(NOT NUMBER OF TERMS--SAME AS BEFORE)
C     WHICH THE PROGRAM USES UP TO OF THE FOURIER SERIES OF THE CHARGE
C     DENSITY. CURRENT DENSITY AND POTENTIALS. THE GREEN'S FUNCTION
C     SUB C ITERATION NUMBER HAS USED 150 WHICH IS FAR MORE THAN AMPLE
C     AND THE FOURIER SERIES NUMBER HAS USED 100 WHICH IS AGAIN
C     MUCH MORE THAN NEEDED. THE FOURIER SERIES NUMBER DOES NOT EXCEED
C     100 BY THE WAY THE PROGRAM IS DESIGNED. IT IS DOUBTFUL THAT ANY
C     VALUE NEAR THIS WOULD EVER BE NEEDED THOUGH.
```

```
C     ********************************************************************
C
      TYPE*,' INPUT ALL DIMENSIONS IN MILLIMETERS'
      TYPE*,' INPUT SUBSTRATE HEIGHT?'
      ACCEPT*,HEIGHT
      TYPE*,' INPUT SUBSTRATE WIDTH?'
      ACCEPT*,DWIDTH
      TYPE*,' INPUT MICROSTRIP WIDTH?
      ACCEPT*,SWIDTH
      TYPE*,' INPUT KAPPA?'
      ACCEPT*,KAPPA
      TYPE*,' INPUT FIRST FREQUENCY INTERVAL IN HERTZ?
      ACCEPT*,FREQ
      TYPE*,' INPUT SIMPSONS RULE INTERVAL NUMBER?'
      ACCEPT*,INT
      TYPE*,' INPUT GREENS FUNCTION SUB C ITERATION NUMBER?'
      ACCEPT*,ITER
      TYPE*,' INPUT FOURIER COEFFICIENT NUMBER?'
      ACCEPT*,FOUR
      PI=3.141592654
      C=3E+08
      ALPHA=(2*HEIGHT)/SWIDTH
      EPS=(1./(PI*(36E+09)))
      PERM=(PI*(4E-07))
      A=DWIDTH/SWIDTH
      HERT=(FREQ*SWIDTH)/2000
      OMEGA=2.*PI*HERT
      KSUB0=OMEGA/C
      ETA=(KAPPA-1)/(KAPPA+1)
      K1=(2./3.)*((PI/(4.*A))**2)*((2.*ALPHA)**2)
      K2=-(1./(4.*PI))
C
```

```
C     ****************************************************************
C
C     THIS BEGINS THE CALCULATION PROCESS OF THE PERTURBATION-ITERATION
C     METHOD. THE FIRST STAGE IS TO CALCULATE THE STATIC VALUES OF BETA
C     AND Z SUB C. TO ACCOMPLISH THIS, A MATRIX MUST BE DEVELOPED FOR
C     EACH OF THE GREEN'S FUNCTION SUB 1-CURRENT DENSITY AND GREEN'S FUNCTION
C     SUB 2-CHARGE DENSITY INTEGRALS WHICH WILL ULTIMATELY BE INVERTED TO
C     FIND THE CURRENT DENSITY COEFFICIENTS AND CHARGE DENSITY COEFFICIENTS.
C     THE GREEN'S FUNCTION SUB 1-CURRENT DENSITY INTEGRAL MATRIX IS DEVELOPED
C     FIRST. THIS IS CALCULATED IN THE FOLLOWING.
C
C     ****************************************************************
C
      DO 10 N=0,3
            X=((1./4.)*N)+(1./4.)
            B(0)=(1./2.)*(LOG(2.0))
            B(1)=(1./8.)*((2*(X**2))*LOG(4.0)-1.)
            B2N=(X**4)+(X**2)
            B(2)=(1./8.)*(B2N+((3./4.)*LOG(4.0))-(7./6.))
            B3N=(-6*(X**2))+(37./6.)-(5*LOG(4.0))
            B3B=((-16./3.)*(X**6))-(4*(X**4))
            B(3)=(-1./64.)*(B3N+B3B)
            E(0)=(N1*N2*PI)
            E(1)=(N1*N2*(PI/2))
            E(2)=(N1*N2*PI*(3./8.))
            E(3)=(N1*N2*PI*(5./16.))
            DO 20 M=0,3
                  C(M)=0
20          CONTINUE
            DO 30 M=0,INT
                  ARGINE=(1.*M)/(1.*INT)
```

```
                IF (M.EQ.INT) GO TO 70
                IF ((MOD(M,2)).EQ.1) TEST=4
                IF ((MOD(M,2)).EQ.0) TEST=2
                IF (M.EQ.0) TEST=1
                V1=((X-XPRIME)**2)+((2*ALPHA)**2)
                V2=((X+XPRIME)**2)+((2*ALPHA)**2)
                T1=((X-1)**2)+((2*ALPHA)**2)
                T2=((X+1)**2)+((2*ALPHA)**2)
                T4=LOG(V1*V2)
                T5=LOG(T1*T2)
                V3=(K2*(-1./2.))*T4
                V4=(K2*(-1./2.))*T5
                W1=(1/(SQRT(1-(XPRIME**2))))
                DO 50 P=0,5
                        IF (P.EQ.0) GO TO 40
                        V5=2*W1*TEST
                        V6=V3*(XPRIME**(2*P))
                        T(P)=V5*(V6-V4)
                        GO TO 50
40                      T(P)=2*W1*TEST*(V3-V4)
50              CONTINUE
                DO 60 P=0,5
                        L(P)=L(P)+T(P)
60              CONTINUE
                GO TO 30
70              T3=(1./2.)**2*K2*(PI/2.)
                T(0)=T3*(LOG(T1*T2))
                DO 80 P=0,5
                        L(P)=((1./(3.*INT))*L(P))+T(0)
80              CONTINUE
30      CONTINUE
        DO 90 M=0,5
```

```
                    Z(N,M)=B(M)*E(M)+L(M)
                    BB(N,M)=Z(N,M)
 90             CONTINUE
                AMAT(N)=1
 10     CONTINUE
 100    FORMAT (/)
C
C      THE CURRENT DENSITY COEFFICIENTS ARE SOLVED FOR USING THE SUBROUTINE
C      'MATRIX' WHICH SOLVES FOR THE FOUR UNKNOWN COEFFICIENTS.
C
       PRINT 100
       CALL MATRIX(Z,AMAT,I)
       CC0=PI*I(0)
       CC1=(PI*I(1))/2.
       CC2=(3.*PI*I(2))/8.
       CC3=(5.*PI*I(3))/16
C
C      THE TOTAL 0 LEVEL CURRENT ON THE MICROSTRIP IS CALCULATED ON THE
C      MICROSTRIP BY INTEGRATING THE CURRENT DENSITY ACROSS THE MICROSTRIP.
C
       CURR=CC0+CC1+CC2+CC3
C
C      THE 0 LEVEL INDUCTANCE IS CALCULATED ON THE MICROSTRIP.
C
       IND=PERM/CURR
       K3=1./CURR
C
C      THE GREEN'S FUNCTION SUB 2-CHARGE DENSITY INTEGRAL MATRIX IS DEVELOPED
C      USING THE PREVIOUSLY CALCULATED MATRIX ON ADDING THE GREEN'S FUNCTION
C      SERIES TO IT WHICH EMPLOYS THE GREEN'S FUNCTION SUB C ITERATION
C      NUMBER. THE GREEN'S FUNCTION SUB C SERIES IS INTEGRATED USING THE
C      SIMPSON'S RULE APPROXIMATION.
```

```
C
      DO 200 N=0,3
             X=((1./4.)*N)+(1./4.)
             DO 210 M=0,3
                    GSUBC(M)=0
210          CONTINUE
             DO 220 M=1,ITER,2
                    MEGAN=(PI*(1.*M))/(2.*A)
                    S1=EXP(-2*MEGAN*ALPHA)
                    S2=EXP(-4*MEGAN*ALPHA)
                    S3=ETA*(S1-S2)
                    S4=1+(ETA*S1)
                    S5=(COS(MEGAN*X))/(M*PI)
                    S6=-(S3*S5)/S4
                    DO 230 P=0,INT
                           THETA=((1.*P)*PI)/(2.*INT)
                           IF ((MOD(P,2)).EQ.1) TEST=4
                           IF ((MOD(P,2)).EQ.0) TEST=2
                           IF ((P.EQ.0).OR.(P.EQ.INT)) TEST=1
                           BB1=MEGAN*(SIN(THETA))
                           BB2=S6*(COS(BB1))
                           DO 240 K=0,3
                                  IF (K.EQ.0) GO TO 250
                                  BB3=(SIN(THETA))**(2*K)
                                  XX(K)=(2.*PI*TEST*BB2*BB3)/(6.*INT)
                                  GO TO 260
250                               XX(K)=(2.*PI*TEST*BB2)/(6.*INT)
260                               GSUBC(K)=GSUBC(K)+XX(K)
240                        CONTINUE
230                 CONTINUE
220          CONTINUE
             DO 270 M=0,3
```

```
                Z(N,M)=(DD(N,M)+GSUBC(M))*(2/(KAPPA+1))
                EE(N,M)=Z(N,M)
270           CONTINUE
              AMAT(N)=1
200     CONTINUE
C
C       THE CHARGE DENSITY COEFFICIENTS ARE SOLVED FOR USING 'MATRIX',
C
        CALL MATRIX(Z,AMAT,CHARGE)
        CC0=PI*CHARGE(0)
        CC1=(PI*CHARGE(1))/2.
        CC2=(3.*PI*CHARGE(2))/8.
        CC3=(5.*PI*CHARGE(3))/16.
C
C       THE TOTAL 0 LEVEL CHARGE IS CALCULATED ON THE MICROSTRIP BY INTE-
C       GRATING THE CHARGE DENSITY ACROSS THE MICROSTRIP.
C
        CHAR=CC0+CC1+CC2+CC3
C
C       THE 0 LEVEL CAPACITANCE IS CALCULATED ON THE MICROSTRIP.
C
        CAP=EPS*CHAR
C
C       THE 0 LEVEL EFFECTIVE PERMITTIVITY AND 0 LEVEL CHARACTERISTIC
C       IMPEDANCE ARE CALCULATED ON THE MICROSTRIP USING THE 0 LEVEL
C       CAPACITANCE AND INDUCTANCE AND PRINTED OUT.
C
        EPSEFF=(C**2)*(IND*CAP)
520     FORMAT(' EFFECTIVE PERMITTIVITY     ',E25.16)
        IMP=SQRT(IND/CAP)
530     FORMAT(' CHARACTERISTIC IMPEDANCE AT ZERO FREQUENCY - ',E25.16)
        PRINT 530,IMP
        PRINT 520,EPSEFF
```

```
C       THE HIGHER ORDER SOLUTION OF THE PERTURBATION-ITERATION METHOD IS
C       NOW BEGUN. THE FIRST TASK IS TO APPROXIMATE BETA USING THE STATIC
C       FREQUENCY DEPENDENT SOLUTION FOR BETA ALONG WITH THE GIVEN INPUT
C       FREQUENCY INTERVAL.
C
        BETA1=OMEGA*(SQRT(IND*CAP))
C
C       THE FOLLOWING LOOP SOLVES FOR THE FOURIER SERIES COMPONENTS OF THE
C       STATIC POTENTIALS PHI SUB 0 AND THE Z COMPONENT OF A SUB Z. THIS IS
C       USING THE SUBROUTINE 'FOURCO' WHICH SOLVES FOR THE FOURIER SERIES
C       COEFFICIENTS OF THE CHARGE AND CURRENT DENSITY SOLUTIONS. THESE
C       COEFFICIENTS ARE SOLVED FOR TWO AT A TIME -- ONE FOR CHARGE DENSITY
C       AND ONE FOR THE CURRENT DENSITY.
C
        DO 370 M=1,FOUR,2
                MEGAN=(PI*(1.*M))/(2.*A)
                CALL FOURCO(CHARGE,1,MEGAN,INT,A,JFOUR,CFOUR)
                JFOUR=JFOUR*(SQRT(IND*CAP))*(C**2)
                AA0=EXP(-MEGAN*ALPHA)
                AA1=SINH(MEGAN*ALPHA)
                AA2=COSH(MEGAN*ALPHA)
                AA3=EPS*MEGAN*(AA1+(KAPPA*AA2))
                PHIOLD(M)=(CFOUR*(AA1))/AA3
                ASUBZ(M)=(PERM*JFOUR*AA1*AA0)/MEGAN
370     CONTINUE
800     DO 450 P=0,3
                B(P)=0
                E(P)=0
                ZZ1=0
450     CONTINUE
```

```
C
C       THE FOLLOWING LOOP SOLVES FOR THE N LEVEL POTENTIAL PHI BY
C       SOLVING FOR A SUB Y - LEVEL N AND THE DERIVATIVE OF IT.THE
C       N-1 LEVEL POTENTIALS ARE ALSO USED IN THIS CALCULATION.
C
        DO 440 M=1,FOUR,2
                MEGAN=(PI*(1.*M))/(2.*H)
                MEGAN1=SQRT((MEGAN**2)+((EPSEFF-1)*(KSUB0**2)))
                MEG2=((MEGAN**2)+((EPSEFF-KAPPA)*(KSUB0**2)))
                IF (MEG2.LT.0) THEN
                        MEG2=-MEG2
                        MEGAN2=SQRT(MEG2)
                        AA0=SIN(MEGAN2*ALPHA)
                        AA1=COS(MEGAN2*ALPHA)
                ELSE
                        MEGAN2=SQRT(MEG2)
                        AA0=SINH(MEGAN2*ALPHA)
                        AA1=COSH(MEGAN2*ALPHA)
                ENDIF
                AA2=(MEGAN2*AA0)+(MEGAN1*AA1)
                AA3=-OMEGA*PERM*EPS*(KAPPA-1)*AA1
                ASUB1(M)=(AA3*PHIOLD(M))/AA2
                BASUB1=-MEGAN1*ASUB1(M)
                AA4=(SQRT(EPSEFF))*KSUB0*ASUB2(M)
                AA5=-OMEGA*PERM*EPS*PHIOLD(M)
                PHINEW=(-OMEGA*(AA4-BASUB1-AA3))/(MEGAN**2)
                AA6=(MEGAN1*AA0)+(MEGAN2*KAPPA*AA1)
                AA7=(-EPS*OMEGA*(1-KAPPA)*ASUB1(M)*AA0)/AA6
                Z21=Z21+((PHIOLD(M)*AA0)/(MEGAN2*AA2))
                DO 440 P=0,3
                        X=((1.*P)/4.)+(1./4.)
                        D(P)=D(P)+(EPS*PHINEW*((COS(MEGAN*X))-1))
                        E(P)=E(P)+(AA/(COS(MEGAN*X)))
440             CONTINUE
```

```
400     CONTINUE
        ZZ1=ZZ1*(KAPPA-1)*EPS*(KSUB0**2)
        DO 540 N=0,3
                DO 510 M=0,3
                        Z(N,M)=0
                        YY(N,M)=0
510             CONTINUE
540     CONTINUE
C
C       THE FREQUENCY DEPENDENT GREEN'S FUNCTION INTEGRALS FOR THE HIGHER
C       ORDER LEVEL CHARGE AND CURRENT DENSITY INTEGRALS ARE DETERMINED
C       USING THE 0 LEVEL CLOSED FORM CALCULATIONS OUTLINED IN THE THESIS.
C       THE FOLLOWING LOOP CALCULATES THE DIFFERENCE INTEGRALS OF THE
C       GREEN'S FUNCTION INTEGRALS BY SUBTRACTING THE 0 LEVEL FOURIER SERIES
C       REPRESENTATION GREEN' FUNCTION FROM THE HIGHER ORDER FOURIER SERIES
C       REPRESENTATION. THIS ALLOWS FOR A QUICK CONVERGENCE OF THE SUMMATION.
C
        DO 300 R=1,FOUR,2
                MEGAN=((1.*R)*PI)/(2.*H)
                MEGAN1=SQRT((MEGAN**2)+((EPSEFF-1)*(KSUB0**2)))
                MEG2=((MEGAN**2)+((EPSEFF-KAPPA)*(KSUB0**2)))
                DO 640 M=0,3
                        QQ(M)=0
640             CONTINUE
                DO 310 M=0,INT
                        THETA=((1.*M)*PI)/(2.*INT)
                        IF ((MOD(M,2)).EQ.1) TEST=4
                        IF ((MOD(M,2)).EQ.0) TEST=2
                        IF ((M.EQ.0).OR.(M.EQ.INT)) TEST=1
                        S1=SIN(THETA)
                        S2=COS(MEGAN*S1)
                        DO 320 P=0,3
```

```
                                IF (P.EQ.0) GO TO 330
                                QQ(P)=QQ(P)+((2.*PI*TEST*(S1**P)*S2)/(6.*INT))
                                GO TO 320
330                             QQ(0)=QQ(0)+((2.*PI*TEST*S2)/(6.*INT))
320                     CONTINUE
310             CONTINUE
                AA0=EXP(-MEGAN*ALPHA)
                AA1=SINH(MEGAN*ALPHA)
                AA2=COSH(MEGAN*ALPHA)
C
C       THE FOLLOWING IS AN EXAMPLE USED THROUGH THE PROGRAM OF A PROTECTION
C       DEVICE TO PREVENT THE SQUARE ROOT OF A NEGATIVE NUMBER. THIS OCCUR-
C       IS POSSIBLE IN THE CALCULATION OF OMEGA SUB 2N,N AND ONLY EFFECT IS
C       CHANGING SOME HYPERBOLIC FUNCTIONS TO TRIGONOMETRIC FUNCTIONS.
C
                IF (MEG2.LT.0) THEN
                        MEG2=-MEG2
                        MEGAN2=SQRT(MEG2)
                        AA3=SIN(MEGAN2*ALPHA)
                        AA4=COS(MEGAN2*ALPHA)
                ELSE
                        MEGAN2=SQRT(MEG2)
                        AA3=SINH(MEGAN2*ALPHA)
                        AA4=COSH(MEGAN2*ALPHA)
                ENDIF
                AA5=(MEGAN1*AA3)+(RAPPA*MEGAN2*AA4)
                AA6=MEGAN*((AA1+(RAPPA*AA2))
                AA7=((AA3/AA5)-(AA1/AA6))/A
                BB1=(MEGAN1*AA3)+(MEGAN2*AA4)
                BB2=AA3/BB1
                BB3=((AA6*AA1)/MEGAN
                BB4=(BB2-BB3)/A
```

```
                DO 340 N=0,3
                        X=((1.*N)/4.)*(1./4.)
                        DO 380 M=0,3
                                Z(N,M)=Z(N,M)+(QQ(M)*AA7*COS(MEGAN*X))
                                YY(N,M)=YY(N,M)+(QQ(M)*BB4*COS(MEGAN*X))
380                     CONTINUE
340             CONTINUE
300     CONTINUE
C
C       THE SOURCE MATRICES FOR THE CHARGE AND CURRENT DENSITY INTEGRALS ARE
C       CALCULATED USING THE PREVIOUSLY CALCULATED PHI AND A SUB Y. THE TOTAL
C       GREEN'S FUNCTION INTEGRALS ARE ALSO DETERMINED BY ADDING THE CLOSED
C       FORM EXPRESSIONS TO THE JUST CALCULATED DIFFERENCE INTEGRALS.
C
        DO 350 N=0,3
                DO 360 M=0,3
                        Z(N,M)=Z(N,M)+EE(N,M)
                        YY(N,M)=YY(N,M)+DD(N,M)
360             CONTINUE
350     CONTINUE
        DO 460 N=0,3
                AMAT(N)=B(N)-E(N)+1
                AMAT1(N)=B(N)+1
460     CONTINUE
C
C       THE HIGHER ORDER CHARGE DENSITY AND TOTAL CHARGE ARE DETERMINED USING
C       'MATRIX' AND THE CLOSED FORM EXPRESSION WITH JUST DETERMINED CHARGE
C       DENSITY COEFFICIENTS, RESPECTIVELY.
C
        CALL MATRIX(Z,AMAT,CHARGE2)
        CC0=PI*CHARGE2(0)
        CC1=(PI*CHARGE2(1))/2.
```

```
      CC2=(3.*PI*CHARGE2(2))/8.
      CC3=(5.*PI*CHARGE2(3))/16.
      CHAR2=CC0+CC1+CC2+CC3
C
C     THE HIGHER ORDER CURRENT DENSITY AND TOTAL CURRENT ARE DETERMINED USING
C     'MATRIX' AND THE CLOSED FORM EXPRESSION WITH JUST DETERMINED CURRENT
C     DENSITY COEFFICIENTS, RESPECTIVELY.
C
      CALL MATRIX(YY,AMAT1,I2PR)
      CC0=PI*I2PR(0)
      CC1=(PI*I2PR(1))/2.
      CC2=(3.*PI*I2PR(2))/8.
      CC3=(5.*PI*I2PR(3))/16.
      CURR2P=CC0+CC1+CC2+CC3
      PRINT 100
C
C     THE NEW AND MORE ACCURATE VALUES OF BETA AND Z SUB C ARE COMPUTED AT THE
C     GIVEN FREQUENCY. THE CURRENT DENSITY COEFFICIENTS ARE THEN SUBSEQUENTLY
C     CORRECTLY SCALED.
C
      NEWBET=KSUB0*(SQRT(CHAR2/CURR2P))
      ZSB0=SQRT(PERM/EPS)
      ZSUBC=((KSUB0*ZSB0)/(NEWBET*CURR2P))*(1+ZZ1)
      DO 610 N=0,3
            I2(N)=(I2PR(N)*NEWBET)/(OMEGA*PERM*EPS)
610   CONTINUE
C
C     THE FOURIER SERIES OF THE POTENTIALS AT LEVEL A ARE CALCULATED.
C     THIS IS DONE USING THE FOURIER SERIES CALCULATION OF THE CHARGE
C     AND CURRENT DENSITY COEFFICIENTS. THESE CALCULATIONS ARE REQUIRED
C     FOR THE NEXT ITERATION PROCESS.
```

```
C
      DO 620 M=1,FOUR,2
            MEGAN=(PI*(1.*M))/(2.*A)
            MEGAN1=SQRT((MEGAN**2)+((EPSEFF-1.)*(KSUB0**2)))
            MEG2=((MEGAN**2)+((EPSEFF-KAPPA)*(KSUB0**2)))
            CALL FOURCO(CHARGE2,I2PR,MEGAN,INT,A,JFOUR,CFOUR)
            IF (MEG2.LT.0) THEN
                  MEG2=-MEG2
                  MEGAN2=SQRT(MEG2)
                  AA1=SIN(MEGAN2*ALPHA)
                  AA2=COS(MEGAN2*ALPHA)
            ELSE
                  MEGAN2=SQRT(MEG2)
                  AA1=SINH(MEGAN2*ALPHA)
                  AA2=COSH(MEGAN2*ALPHA)
            ENDIF
            AA3=(MEGAN1*AA1)+(MEGAN2*AA2)
            AA4=(MEGAN1*AA1)+(KAPPA*MEGAN2*AA2)
            AA5=(CFOUR*AA1)/(AA4*EPS)
            AA6=(-OMEGA*(KAPPA-1.)*AA1*ASUBT(M))/AA4
            BSUBZ(M)=(PERM*JFOUR*AA1)/AA3
            PHIOLD(M)=(AA5-AA6)
620   CONTINUE
C
C     THE NEW VALUE OF BETA FOR THE NEXT ITERATION IS SUBSTITUTED USING
C     THE JUST CALCULATED VALUE.
C
      BETA1=NEWBET
C
C     BETA, EFFECTIVE DIELECTRIC CONSTANT, AND Z SUB C ARE ALL PRINTED
C     OUT. THE EFFECTIVE DIELECTRIC CONSTANT IS ALSO CALCULATED AT
C     THIS POINT.
C
```

```
600   FORMAT(' PROPAGATION CONSTANT BETA = ',E25.16)
550   FORMAT(' CHARACTERISTIC IMPEDANCE AT FREQ ',E12.6,' = ',E25.16)
      EPSEFF=(BETA1/KSUB0)**2
      PRINT 550,FREQ,ZSUBL
      PRINT 600,BETA1
570   FORMAT(' EFFECTIVE PERMITTIVITY = ',E25.16)
      PRINT 570,EPSEFF
      PRINT 100
C
C     THE PRESENT ITERATION IS NOW COMPLETED. THE ITERATION PROCESS MAY
C     CONTINUE BY REPEATING THE ITERATION PROCEDURE AND KEEPING THE
C     FREQUENCY CONSTANT, REPEATING THE ITERATION PROCEDURE AND IN-
C     CREASING THE FREQUENCY (THE INPUT FREQUENCY INTERVAL IS INPUT
C     IN GIGOHERTZ AND IS THE FREQUENCY INTERVAL WHICH IS ADDED TO THE
C     PRESENT VALUE OF THE FREQUENCY), BEGINNING THE WHOLE PROCESS
C     OVER AGAIN BY ANALYZING A NEW STRUCTURE, OR BY ENDING THE PROGRAM.
C
      TYPE*,'REPEAT ITERATION?'
      TYPE*,'TYPE "0" FOR YES OR "1" FOR NO'
      ACCEPT*,FLAG
      IF (FLAG.EQ.0) GO TO 800
      TYPE*,'INCREMENT FREQUENCY?'
      TYPE*,'TYPE "0" FOR YES OR "1" FOR NO'
      ACCEPT*,FLAG
      IF (FLAG.EQ.1) GO TO 810
      TYPE*,'INPUT FREQUENCY INCREMENT IN HERTZ'
      ACCEPT*,INCR
      FREQ=FREQ+INCR
      HERINC=(INCR*SWIDTH)/2000
      OMEGA=OMEGA+(2.*PI*HERINC)
      KSUB0=OMEGA/C
```

```
      GO TO 800
810   TYPE*,'CONTINUE WITH NEW ANALYSIS OR QUIT?'
      TYPE*,'TYPE "0" TO CONTINUE OR "1" TO QUIT'
      ACCEPT*,FLAG
      IF (FLAG.EQ.0) GO TO 1
      STOP
      END
C
C     SUBROUTINE "MATRIX" CALCULATES THE CHARGE OR CURRENT DENSITY
C     COEFFICIENTS BY USING A SUCCESSIVE MULTIPLY AND SUBTRACT
C     PROCEDURE.
C
      SUBROUTINE MATRIX (Z,AMAT,I)
      INTEGER N,M,R,P
      REAL*8 Z(0:3,0:3),AMAT(0:3),I(0:3),TEMP1,TEMP2,TEMP3
      DO 110 R=0,2
            DO 120 M=R,2
                  TEMP1=Z(M+1,R)
                  DO 130 P=R,3
                        TEMP2=Z(R,P)*TEMP1
                        Z(M+1,P)=(-Z(R,R)*Z(M+1,P))
                       .Z(M+1,P)=Z(M+1,P)+TEMP2
130                 CONTINUE
                  AMAT(M+1)=(-Z(R,R)*AMAT(M+1))
                  AMAT(M+1)=AMAT(M+1)+(TEMP1*AMAT(R))
120           CONTINUE
110   CONTINUE
      DO 140 N=0,3
            IF (N.EQ.0) GO TO 160
            DO 150 P=0,N-1
                  TEMP3=I(3-P)*Z(3-R,3-P)
                  AMAT(3-N)=AMAT(3-N)-TEMP3
```

```
      CONTINUE
      I(3-N)=AMAT(3-N)/Z(3-N,3-N)
130
140   CONTINUE
      RETURN
      END

C
C     THE SUBROUTINE 'FOURCO' CALCULATES ONE FOURIER COEFFICIENT
C     EACH FOR THE CHARGE AND CURRENT DENSITY SERIES BY INPUTTING
C     THE VALUE OF N (FOURIER SERIES NUMBER) AND THE DENSITY
C     COEFFICIENTS.
C

      SUBROUTINE FOURCO(CHARGE,I,MEGAN,INT,A,JFOUR,CFOUR)
      INTEGER INT,N
      REAL*8 CHARGE(0:3),I(0:3),JFOUR,CFOUR,MEGAN,PI,A
      REAL*8 S1,S2,S3,S4,S5,T1,T2,T3,BB1,BB2,THETA,TEST
      PI=3.141592654
      JFOUR=0
      CFOUR=0
      DO 630 N 0,INT
            THETA=(1.*N)*PI/(2.*INT)
            IF ((MOD(N,2)).EQ.1) TEST=1
            IF ((MOD(N,2)).EQ.0) TEST=2
            IF ((N.EQ.0).OR.(N.EQ.INT)) TEST=1
            S1=SIN(THETA)
            S2=COS(MEGAN*S1)
            S3=(S1**3)
            S4=(S1**4)
            S5=(S1**2)
            T1=CHARGE(3)*(S1**3)
            T2=CHARGE(2)*(S1**4)
            T3=CHARGE(1)*(S1**2)
```

```
                BB1=(S3+S4+S5+I(0))*S2
                BB2=(T1+T2+T3+CHARGE(0))*S2
                JFOUR=JFOUR+((2.*PI*TEST*BB1)/(6.*INT*N))
                CFOUR=CFOUR+((2.*PI*TEST*BB2)/(6.*INT*N))
630     CONTINUE
        RETURN
        END
*
*
```